REPORT 78

GOVERNMENT OF WESTERN AUSTRALIA

EAST YILGARN GEOSCIENCE DATABASE 1:100 000 GEOLOGY MENZIES TO NORSEMAN — AN EXPLANATORY NOTE

by P. B. Groenewald, M. G. M. Painter, F. I. Roberts, M. McCabe, and A. Fox

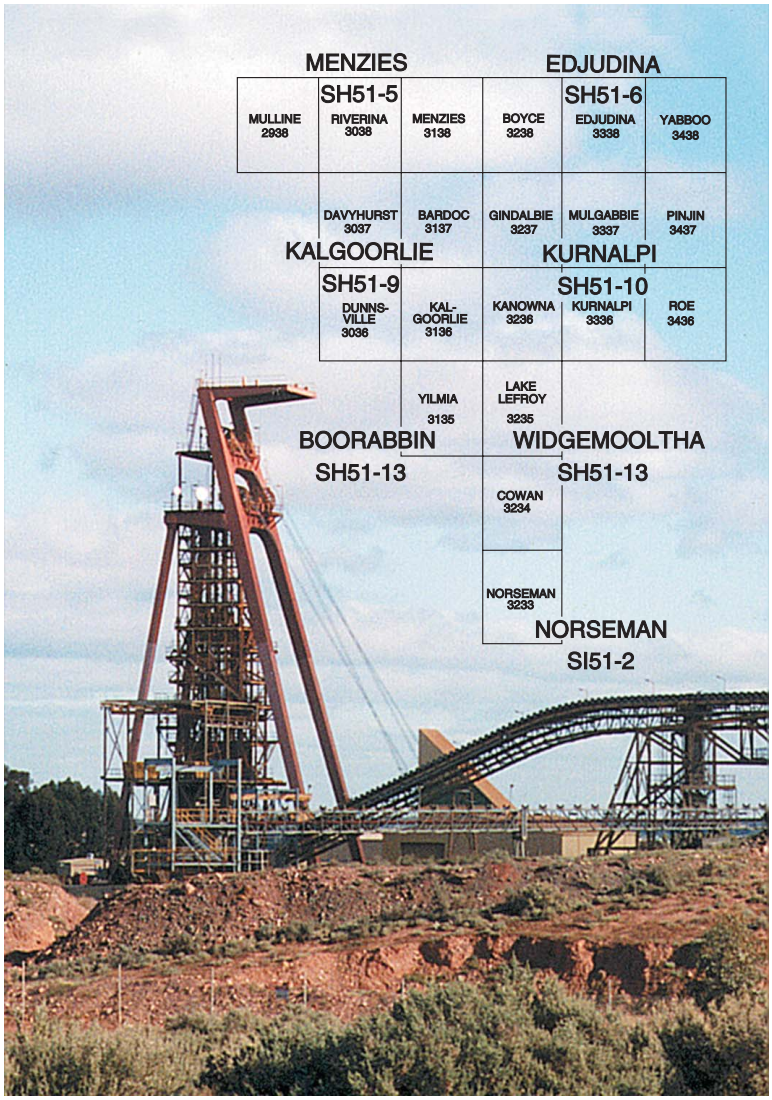

GEOLOGICAL SURVEY OF WESTERN AUSTRALIA

DEPARTMENT OF MINERALS AND ENERGY

GEOLOGICAL SURVEY OF WESTERN AUSTRALIA

REPORT 78

EAST YILGARN GEOSCIENCE DATABASE, 1:100 000 GEOLOGY MENZIES TO NORSEMAN — AN EXPLANATORY NOTE

by
P. B. Groenewald, M. G. M. Painter, F. I. Roberts,
M. McCabe, and A. Fox

Perth 2000

MINISTER FOR MINES
The Hon. Norman Moore, MLC

DIRECTOR GENERAL
L. C. Ranford

DIRECTOR, GEOLOGICAL SURVEY OF WESTERN AUSTRALIA
David Blight

Copy editor: C. D'Ercole

REFERENCE
The recommended reference for this publication is:
GROENEWALD, P. B., PAINTER, M. G. M., ROBERTS, F. I., McCABE, M., and FOX, A., 2000, East Yilgarn Geoscience Database, 1:100 000 geology Menzies to Norseman — an explanatory note: Western Australia Geological Survey, Report 78, 53p.

National Library of Australia
Cataloguing-in-publication entry

East Yilgarn geoscience database : 1:100 000 geology
Menzies to Norseman - an explanatory note.

Bibliography.
ISBN 0 7307 5645 9

1. Geology - Western Australia - Eastern Goldfields - Databases.
2. Geological mapping - Western Australia - Eastern Goldfields - Databases.
I. Groenewald, P. B.
II. Geological Survey of Western Australia. (Series : Report (Geological Surevy of Western Australia) ; 78).

559.416

ISSN 0508–4741

Grid references in this publication refer to the Australian Geodetic Datum 1984 (AGD84)

Printed by Lamb Print Pty Ltd, Perth, Western Australia

Copies available from:
Information Centre
Department of Minerals and Energy
100 Plain Street
EAST PERTH, WESTERN AUSTRALIA 6004
Telephone: (08) 9222 3459 Facsimile: (08) 9222 3444
www.dme.wa.gov.au

Contents

Appendices

Figures

Tables

Digital data (in pocket)

East Yilgarn Geoscience Database, 1:100 000 digital geological data package (2 CDs)

East Yilgarn Geoscience Database, 1:100 000 geology Menzies to Norseman — an explanatory note

by

P. B. Groenewald, M. G. M. Painter, F. I. Roberts, M. McCabe, and A. Fox

Abstract

Published 1:100 000-scale geological maps of the Eastern Goldfields Province of the Archaean Yilgarn Craton, Western Australia, have been combined to form the East Yilgarn Geoscience Database, an integrated dataset for use in a Geographic Information System. This database comprises the twenty maps covering the economically important 55 000 km^2 region between Menzies and Norseman. The data have been rendered seamless through elimination of boundary discrepancies and standardization of rock type and unit definitions throughout the area. To allow detailed analytical access, outcrop geology from published maps is separated into polygon, line, and point themes. The interpreted continuous Archaean geology at 1:250 000-scale beneath the cover is presented in a similar format. Historical mineral workings, current resource location, and statistical data (MINEDEX), as well as recent tenement location, extent, and status data (TENGRAPH) are also provided as separate layers. Digital pseudocolour images based on aeromagnetic and Landsat TM data are also provided. These data sets are available on CD-ROM, or may be accessed at the Geological Survey of Western Australia offices using a map-on-demand program that allows plotting of any combination of data for an area selected by the client.

An overview of the geological characteristics and interpretation is provided in this Report. The Archaean lithostratigraphy of the Eastern Goldfields varies with location. In the western two-thirds, a consistent sequence comprises a lower high-Mg to tholeiitic basalt unit, overlain by a substantial komatiite unit, an upper basalt unit, followed by a felsic volcanic and sedimentary unit, in turn overlain unconformably by locally developed coarse, clastic rock sequences. In the eastern part, a sequence is not readily identified because of poor exposure, higher metamorphic grades, structural complexity, and, probably, much lateral variation in the felsic to intermediate volcanic deposits produced in a tectonically active area. Although not a dominant rock type, calc-alkaline volcanic rocks are important in the eastern area. Geochronology has constrained evolution of greenstones in the Eastern Goldfields to 2715–2670 Ma, with the emplacement of most granites at c. 2673 Ma and 2665–2660 Ma. Xenocrystic zircons in igneous rocks range in age from 2730 to 3450 Ma, providing evidence for pre-existing ensialic crust.

The East Yilgarn Geoscience Database includes nearly 1000 mine sites, exemplifying the considerable value and extent of mineralization in the area. Gold accounts for about 80% of the sites and nickel for many of the remainder. An outline of the characteristics of mineralization is provided in this Report.

KEYWORDS: Archaean geology, greenstones, GIS data base, Yilgarn Craton, Eastern Goldfields, remote sensing, mineral resources, gold, nickel

Introduction

The great mineral wealth of the eastern Yilgarn Craton has led to it being the most extensive block of 1:100 000-scale geological mapping completed to date in Western Australia. The maps have been published by the Geological Survey of Western Australia (GSWA) and the Australian Geological Survey Organisation (AGSO) over the last fifteen years, a period during which advances made in understanding Archaean crustal evolution allowed progressively better interpretation of the regional geology, and successful mineral exploration yielded several large, economic ore deposits. This resulted in the need to revise some earlier mapping and unify the conceptual framework in terms of rock types and structural relationships for the mapped area. Recent advances in information technology allow rapid manipulation and analysis of a great amount of information generated through detailed mapping, remote sensing, and laboratory studies, and hence, the data presented here are being collated in a spatial database encompassing all aspects of the mapping. Furthermore, regular upgrading and further development of this database will be possible, leading to an unrivalled currency of spatial data from which selected types of information may be extracted for viewing and plotting, or for spatial, statistical, and structural analyses in mineral exploration.

The initial digital data package provided in this Report covers the southernmost 55 000 km^2 of the Eastern

Goldfields, between Menzies and Norseman, and is the first phase of a detailed geoscientific database that will encompass the entire eastern Yilgarn Craton. After correction of map-edge and internal unit definition discrepancies, the digital assembly of 20 published 1:100 000-scale geological maps (Table 1; Fig. 1) has been placed in numerous data themes to allow selective access to various types of information. Additional data coverages are as follows: a solid interpretation of Precambrian geology (Swager and Griffin, 1990a; Swager, 1995a); false-colour images derived from Landsat Thematic Mapper (TM) and airborne magnetic survey data; mining and exploration localities; an extract from MINEDEX (the Department of Minerals and Energy (DME) mines and mineral deposits information database); and current tenement holdings from TENGRAPH (DME's electronic tenement-graphics system). The metadata for each theme are provided on CD-ROM. All locality data in the initial dataset are in Transverse Mercator Projection, Australian Map Grid zone 51 coordinates based on the AGD66 datum, but will be transformed to GDA94 and MGA94 in a future edition — users are advised to check the metadata provided on the CDs.

Extent, access, and physiography

The area covered by this dataset encompasses the 1:100 000-scale map sheets from 120° to 123°E with their northern boundary at 29°30'S (6 map sheets), progressively southward through rows of five, five, two, one, and one 1:100 000-scale map sheets to the southern edge of the NORSEMAN* sheet at 32°30'S (Fig. 1).

From the city of Kalgoorlie–Boulder, which is located near the centre of the project area, sealed highways run to the north, west, and south. A good quality gravel road provides access to the east, along the Trans Australian Railway line. Unsealed roads to mining centres and pastoral holdings provide reasonable access throughout the area.

The landscape is relatively subdued in general, with a total elevation range from 270 m to 500 m above the Australian Height Datum (AHD). The extent to which physiography is related to the underlying geology is illustrated by northwesterly trending broad ridges formed by northwesterly striking mafic metavolcanic and banded iron-formation (BIF) units. The latter are responsible for the most prominent ranges of hills on EDJUDINA, MULLINE, and NORSEMAN. Areas underlain by felsic metavolcanic, metasedimentary, and granitic rocks are gently undulating, with low plateaus of duricrust and deeply weathered bedrock. The granitoid expanses on RIVERINA–DAVYHURST, MENZIES–BOYCE–MULGABBIE, and eastern YABBOO–PINJIN–ROE are characterized by undulating plains with sandy soils, commonly resting on lateritic duricrust. Large areas are covered by commonly dry saline lakes and claypans, the relicts of a southeasterly to easterly trending, early

* Capitalized names refer to standard 1:100 000 map sheets, unless otherwise indicated.

Table 1. The twenty 1:100 000-scale geological maps and Explanatory Notes, which accompany them, collated in the first phase of the East Yilgarn Geoscience Database

Year	*Sheet*	*Reference*	*Explanatory Notes*
1988	COWAN, 3234	Griffin (1988a)	Griffin (1990b)
	KALGOORLIE, 3136	Hunter (1988b)	Hunter (1993)
	LAKE LEFROY, 3235	Griffin and Hickman (1988a)	Griffin (1990b)
	YILMIA, 3135	Hunter (1988a)	Hunter (1993)
1989	BARDOC, 3137	Witt and Swager (1989a)	Witt (1994)
	DUNNSVILLE, 3036	Swager (1989a)	Swager (1994a)
1990	MENZIES, 3138	Swager and Witt (1990)	Swager (1994c)
1992	DAVYHURST, 3037	Wyche et al. (1992)	Wyche and Witt (1994)
1993	KURNALPI, 3336	Swager (1993)	Swager (1994b)
	NORSEMAN, 3233	McGoldrick (1993)	not published
1994	EDJUDINA, 3338	Swager and Rattenbury (1994)	Swager (1995b)
	MULGABBIE, 3337	Morris (1994a)	Morris (1994b)
	PINJIN, 3437	Swager (1994d)	Swager (1994e)
	ROE, 3436	Smithies (1994a)	Smithies (1994b)
	YABBOO, 3438	Swager (1994f)	Swager (1995b)
1995	GINDALBIE, 3237	Ahmat (1995c)	not published
	KANOWNA, 3236	Ahmat (1995a)	Ahmat (1995b)
	MULLINE, 2938	Wyche (1995)	Wyche (1999)
	RIVERINA, 3038	Wyche and Swager (1995)	Wyche (1999)
1997	BOYCE, 3238	Chen (1997)	Chen (1999)

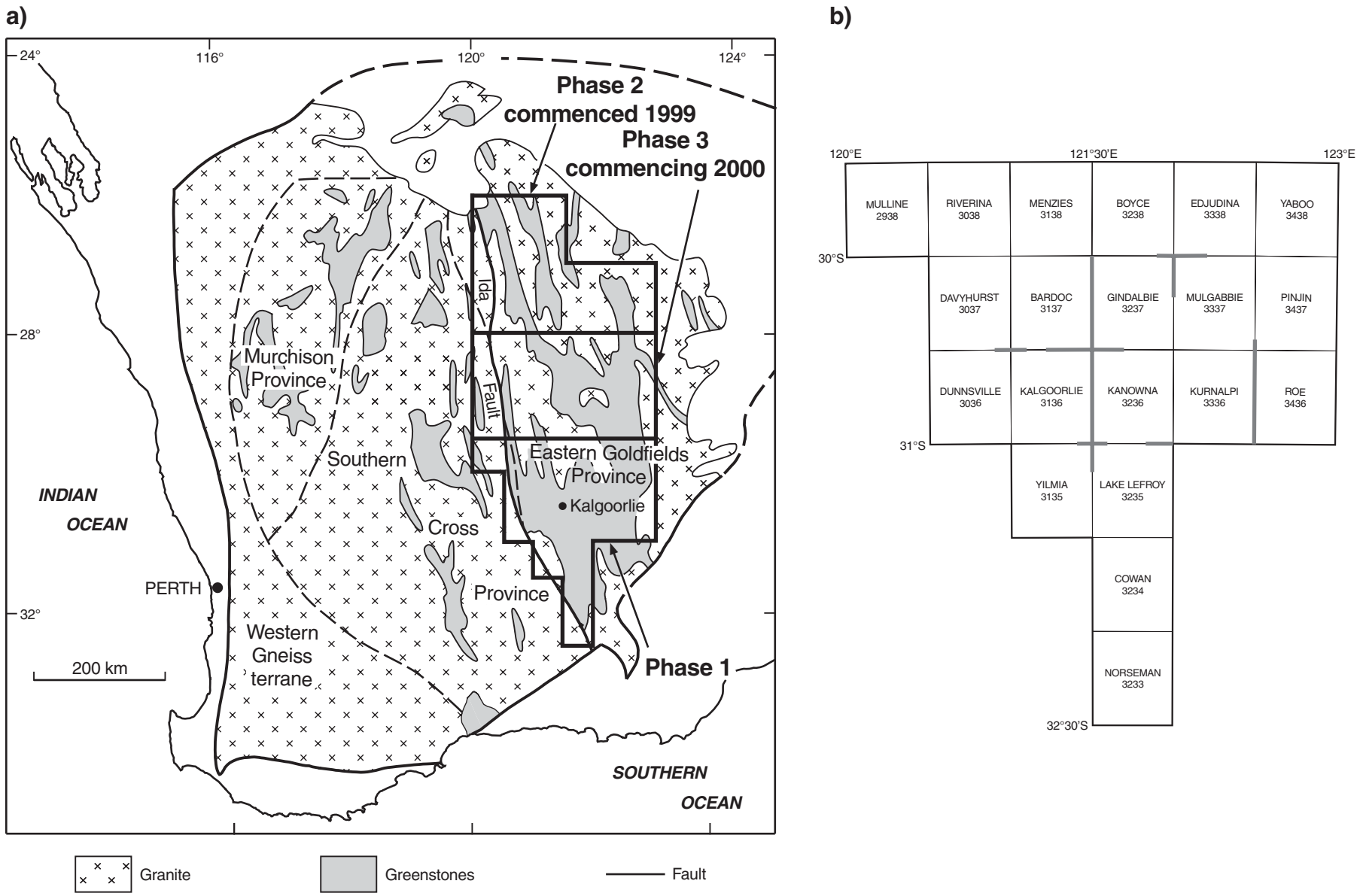

Figure 1. a) Location of the area covered in the first phase of the East Yilgarn Geoscience Database (Gee et al., 1981); b) the distribution of the maps incorporated. The thick grey lines represent map boundaries where fieldwork was required to eliminate discrepancies

Cainozoic palaeodrainage system (van de Graaff et al., 1977; Clarke, 1994). The lakes are flanked by dunes that consist predominantly of quartz sand, but are locally gypsum, which are typically stabilized by vegetation. These dunes separate many small lakes and saltpans. Considerable areas, especially over granitoid rocks, are covered by duricrust, suggesting a considerable period in which no appreciable erosion has taken place. Outcrop is commonly poor and deeply weathered.

The database

The 1:100 000-scale, digital geological map data were generated from digitized, originally hand-drafted, published maps, or through reconversion of the original digital cartographic print files of the published maps. The integrity of data transfer from original compilation sources was maintained through repeated checks of equivalence in the outline and identity of all polygons, the positioning and style of line features, and the orientation, definition, and numerical truth of structural data points.

The elimination of any discrepancies between adjacent primary 1:100 000-scale map sheets to provide seamless continuity of the digital map is essential to the functionality of the database. Commonly, the required minor adjustments to polygon and line positioning along the boundaries are equivalent to, at most, 30 m on the ground. Where greater adjustments were required for precise matching, examination of aerial photographs and Landsat TM images commonly allowed confident repositioning. However, in some areas, remapping along the boundaries between adjacent maps was needed to confirm the identity and distribution of rock types, or the continuity of structural features (Fig. 1). The rectified Landsat TM data have been normalized to provide continuous views without interference from primary scene boundaries.

Careful attention has been paid to the definition of geological rock units or subdivisions on the maps. The original maps show considerable variation in the way individual geologists identified lithological units, rendering application of lithostratigraphic terms outside the area of their primary definition difficult, especially where detailed Explanatory Notes were not produced in conjunction with the map. Although most unit definitions were adequate for the purposes of the standardized legend, some were modified to accommodate variations between the maps.

Application of the standardized codes throughout the area covered by the database required numerous replacements. Reference to Explanatory Notes and adjacent map sheets allowed code substitutions to be made confidently; where Explanatory Notes were not available, some field confirmation was necessary to ensure uniformity and accuracy in application of standardized codes. Definitions of standardized units and the codes applied in the database are in Appendix 1.

Editing and correcting were done using Environmental Systems Research Institute (ESRI) computer software ArcView 3.1, with final assembly and correction of projection parameters made using ArcInfo 7.2.1 to yield seamless layers within a library database. This library was then converted into formats suitable for the application of the popular Geographic Information System (GIS) software packages ArcView, ArcExplorer, and MapInfo. Details of the directory structure, data dictionary, and other metadata are tabulated on the CDs. Access to the database by members of the general public who lack computer facilities has also been provided by an interactive map-on-demand facility (see below).

Themes

Geology

The outcrop geology is recorded in several layers according to data type. The outcrop position and extent are given as either polygons or lines, depending on the form of the rock units (three- or two-dimensional shapes). Attributes of each rock unit include an identification label code, as well as standardized definitions suitable for a map legend in hard copy form (see Appendix 1 for a complete listing). Subsurface records of lithologies (drillholes, costeans) are provided as points in the mine and exploration coverage (see below). Recognized faults or shears are included in the line data layer. The interpreted geological layer shows the position of concealed geological boundary features, inferred faults, and dykes interpreted beneath the surficial cover from aeromagnetic surveys, as shown on the published maps. Structural orientation records are in a point data layer, with measurements provided in the clockwise format, that is, dip direction taken as ninety degrees greater than strike. Outcrop fold annotation is also provided in the point data layer. Figure 2a illustrates the content of these layers and is an example of the type of map that can be generated from the database.

Regional solid geology

A solid geology theme provided in the database is a map of the interpreted distribution of Precambrian rocks beneath younger cover. This has been generated by combining the interpretative maps produced in GSWA Reports 47 (Swager, 1995a) and 48 (Swager et al., 1995). The original hard copy maps have been digitized, with minor extension into areas not covered originally on the MULLINE, MENZIES, BOYCE, and YILMIA maps. Minor adjustments were made to the earlier map (Swager and Griffin, 1990a) in order to bring it into conformity with the more recent one. Once again, polygon, line, and point data are stored in separate layers. Note that the primary maps were interpretations compiled for presentation at a scale of 1:250 000 and thus may not conform precisely to the 1:100 000-scale outcrop maps. This theme is useful for providing the regional contextual setting for areas within the database (Fig. 2b).

Airborne magnetic survey

The airborne magnetic survey theme has been derived from historic Bureau of Mineral Resources (BMR) and

AGSO datasets. The false-colour image has been rendered in red, green, and blue intensity layers to allow replication of the standard geophysical pseudocolour spectrum. Original flight-line spacing of 1.6 km has resulted in a pixel size of 400 m in this coverage, which does not allow detailed interpretation at the 1:100 000 scale of the outcrop geology. Nonetheless, this layer does contribute to the interpretation of geology on a regional scale, particularly in areas of very poor outcrop.

Landsat TM layers

Two images were prepared from Landsat TM data collected in January and February 1998, providing coverage where many of the recent exploration grids are visible. A mosaic of the data provides seamless coverage through correlation of invariant targets in areas of overlap and normalization through robust regression techniques by the Western Australian Department of Land Administration (DOLA). A spatial accuracy better than 50 m and pixel size of 25 m have been preserved. The data have undergone decorrelation stretch processing; raw data may be obtained from the Satellite Remote Sensing Services branch of DOLA.

A monochromatic (grey-scale) layer shows principal component values derived from Landsat TM bands 1, 4, and 7 using standard eigenvector formulae. In addition, a pseudocolour image was prepared using ratios between bands 2, 3, 4, 5, and 7 to distinguish between iron- and silica-rich, vegetation-dominated, and rock outcrop dominated areas. Thus, light-tan colouration is equivalent to recent alluvium, the lakes are light blue, mafic rock outcrops commonly range from purple through Prussian blue to lighter blue-green, lateritic areas are dark brown, whereas kaolinite-enriched areas (granitic) are bluish off-white (Fig. 2c).

Mine workings, exploration sites, and MINEDEX

The East Yilgarn Geoscience Database includes the mining and exploration data points from the published maps, and an extract from MINEDEX (Townsend et al., 1996). The first of these themes provides localities of historic mining centres, mine sites, batteries, prospects, alluvial workings, and mineral occurrences. Points where significant rock types were identified beneath cover during mineral exploration are also included (Fig. 2a). The MINEDEX theme locates index points (Fig. 2d) for access to details of resource identity, commodity, extent, stage of development, and ownership. Details of the abbreviations and classifications are provided in Appendix 2.

Mining tenements

The mining tenement information for the database area, extracted from TENGRAPH, provides geographical positioning and extent of each tenement (Fig. 2d), together with information on its status and type, and the dates and times of application, granting, and expiry of holdings. This theme also provides general topographic data for location of roads, tracks, stations, and town sites. In view of the continuous and on-going changes in the tenement situation, current tenement plans should be consulted at DME offices before any land-use decisions or tenement applications are made.

Map extraction from the database

A computer program has been developed to allow plotting of geological, MINEDEX, and TENGRAPH data, selected in terms of content, scale, and extent, for any area covered by the East Yilgarn Geoscience Database, with automatic creation of appropriate legends and marginalia. This 'map-on-demand' facility may be used by the public at GSWA's Kalgoorlie or Perth offices.

Although data manipulation and processing were completed using ESRI's ArcInfo software, ArcView was chosen to manage the interactive map creation facility. The map layout was modelled on GSWA's standard 1:100 000-scale map sheets, with adjustments to meet the diverse demands of variable scale and size products. In addition to a standard locality diagram showing the extent and position of the map created relative to a quarter-degree index grid, the context of the area plotted is illustrated on a regional interpretation of the Precambrian geology. The currency and source of themes plotted are listed, together with the date and time of extraction.

Clients select primary parameters from three ranges of possibilities when creating a map, as follows:

- page size — A0, A1, A2, A3, or A4;
- scale — 1:25 000, 1:50 000, 1:100 000, or 1:250 000;
- one or more of the themes — outcrop geology, structural line features, structural point features, interpreted geology, MINEDEX, mining–subsurface data, tenements, and topography (localities and roads only). The user may choose whether or not the features selected are labelled individually; and
- each map generated is given a region name based on the 1:50 000 map grid.

Some limitations on the map product are necessary to conform to available space on the various size pages; for example, the 1:250 000-scale maps can only be plotted on an A0 or A1 page, whereas the A4 and A3 plots are limited to a scale of 1:25 000 or 1:50 000. The reason for this is that legends are generated for the area covered by each map, and certain combinations of scale and extent yield legends too large to fit in the space available on the smaller pages. In the case of the A4 page-size, the legend plots as a second page.

The area to be shown on the map is chosen interactively after selection of the three primary parameters. A simplified, solid geology map of the area covered by the database is shown together with a mobile rectangle illustrating the extent of the area allowed by the selected parameters. This mobile rectangle is positioned by the viewer over a selected area and the chosen map is then generated.

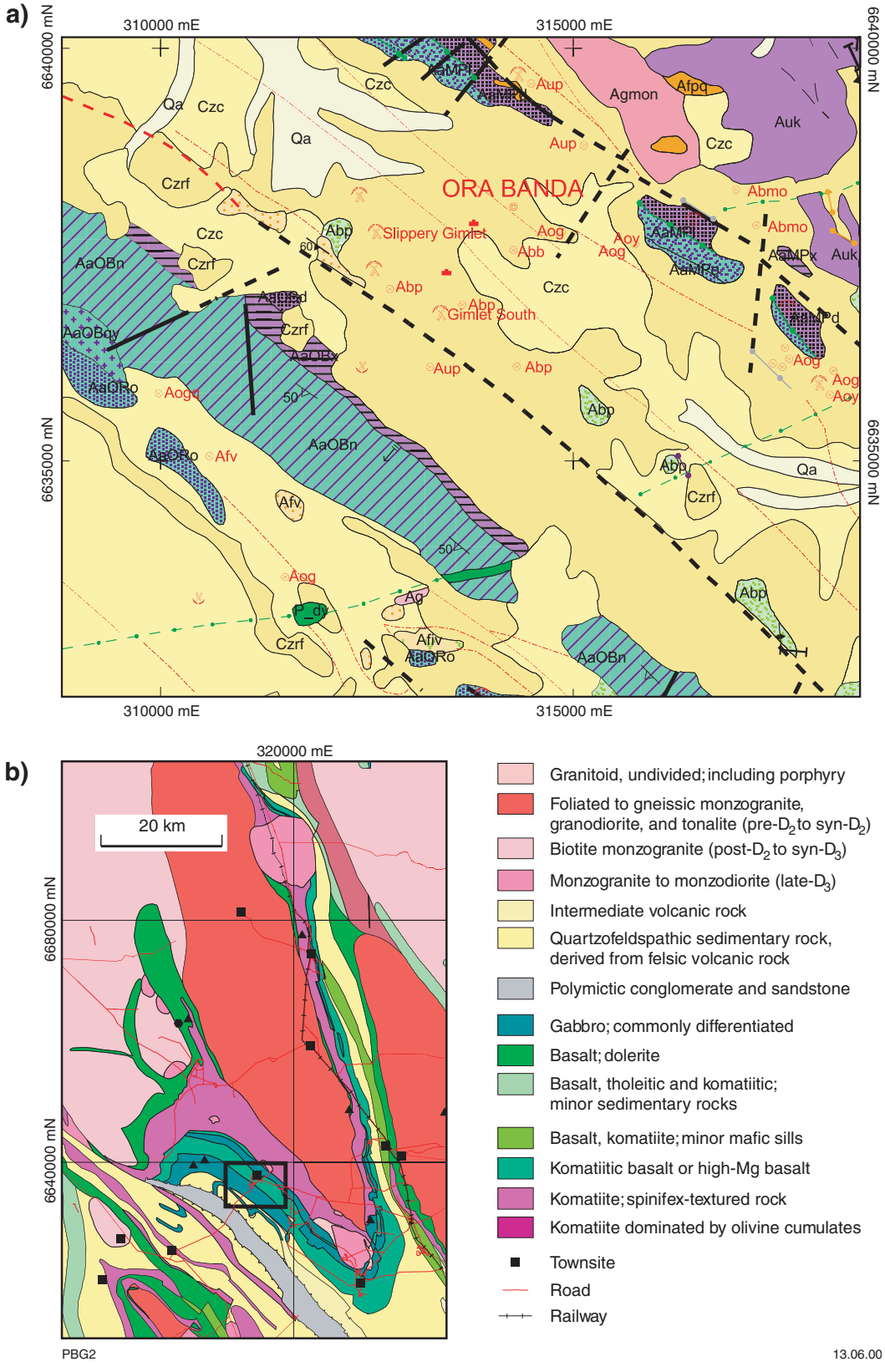

Figure 2. **Illustrative plots generated from the database for a small part of the coverage: a) outcrop geology comprising polygons (from GEOOBS, coded as in Appendix 2), faults (from GEOLIN and GEOCON) shown as observed (solid line), concealed (black dashed), and interpreted (red dashed), and standard structural symbols (from GEOPNT) with mine site, subsurface data points, and battery locations (from MINOCC); b) the geological context of the scene in Figure 2a is shown as a solid black rectangle on an extract from the regional solid geology theme of the database (SIMOBS)**

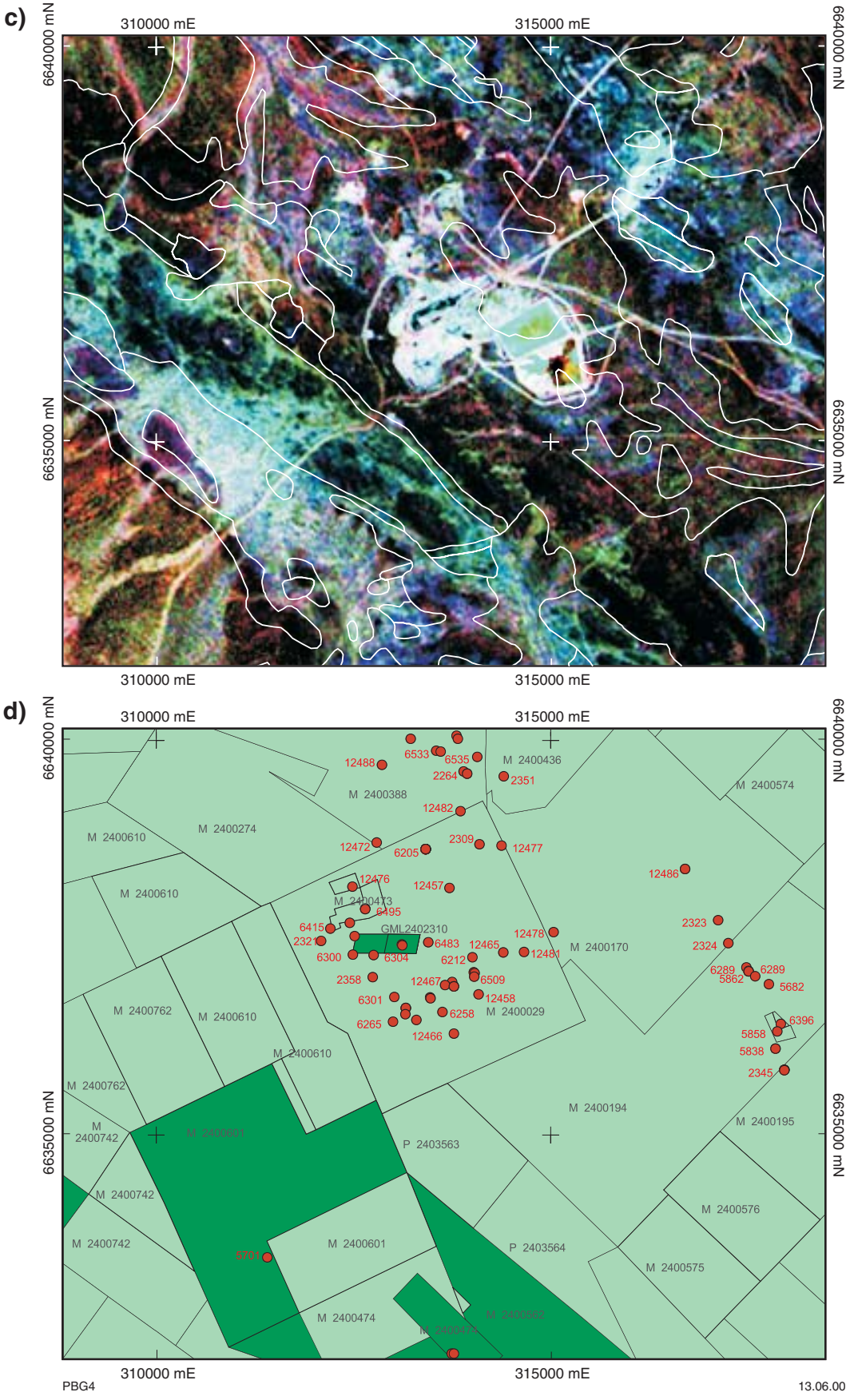

Figure 2. **c) Landsat TM coverage, with outlines of the observed geology superimposed on the pseudocolour image — note that geological mapping preceded development of the mining visible in the image; d) TENGRAPH and MINEDEX coverage, illustrating how tenement extent and status may be shown together with mineral resource indexing — relevant data are provided in look-up tables in the database for each point or polygon**

Archaean geological setting

The Archaean Yilgarn Craton, one of the world's largest granite–greenstone assemblages, is dominated by great expanses of granitoid and granitic gneiss. Supracrustal material, comprising metamorphosed sedimentary and volcanic rocks in greenstone belts, is sparse in the western two-thirds of the craton, but abundant in the east. Outcropping Archaean rocks are limited, with more than 90% of the area covered by regolith and, locally, Palaeozoic rocks. Large arrays of drillhole and aeromagnetic data, produced in the course of mineral exploration, show the real extent of the granites and greenstones beneath this cover. Myers (1995, 1997) subdivided the Yilgarn Craton into 'fault-bounded composite rafts of sialic crust', making up the Eastern Goldfields and Southern Cross Superterranes, the Murchison and Narryer Terranes, and the Southwest Composite Terrane. The Eastern Goldfields and Southern Cross Superterranes closely correspond to the regions more commonly known as the Eastern Goldfields and Southern Cross Provinces (Fig. 1; Gee et al., 1981), terms retained in this document to allow easy reference to the work from which the database has been assembled.

The southern part of the Eastern Goldfields, the area covered by this Report, comprises late Archaean greenstones and granitoids that have a regional tectonostratigraphic architecture dominated by north-northwesterly trending regional folds, with anticlines commonly cored by granitoids and synclines by greenstones, and parallel fault zones that commonly mark apparent truncations of the lithostratigraphy. The greenstones comprise igneous rocks ranging in composition from ultramafic to felsic, largely as komatiitic and basaltic volcanic rocks, but with a widespread andesite to rhyolite population and layered mafic to ultramafic intrusions of likely subvolcanic origin. A sedimentary rock component, making up a substantial proportion of the greenstones locally, ranges from rudaceous to very fine in grain size, marine and terriginous in origin, and epiclastic to mature in character. The granitoids are predominantly monzogranitic to granodioritic in composition, and range in age from synchronous with emplacement of the felsic volcanics to post-tectonic.

There is little evidence in the eastern Yilgarn Craton for any major intracratonic activity subsequent to about 2600 Ma. Numerous mafic dykes with predominantly east-northeasterly and north-northwesterly trends were probably all emplaced in the early Palaeoproterozoic (Sofoulis, 1966; Hallberg, 1987). The Woodline Beds and Mount Barren Formation are deformed, Mesoproterozoic sedimentary successions, possibly 200 m thick, representing a extensive depositional system on the southeastern marginal parts of the Yilgarn Craton (Griffin, 1989; Myers, 1990a). The Albany–Fraser Orogen deformed the southern and southeastern margins, but there is little evidence of this deformation in the interior of the craton (Myers, 1990a). A few localized elevated areas have preserved glacigenic sedimentary rocks of interpreted Permian age (Williams et al., 1976). A subsequent (?Jurassic) major incised drainage system was followed by localized deposition of estuarine–deltaic deposits and shallow-marine limestone in the Eocene (Clarke, 1994). The palaeodrainage channel systems are preserved as the present-day playa-lake systems (Hocking and Cockbain, 1990).

The initial use of tectonostratigraphic terranes for modelling Western Australian crustal evolution by Myers (1990b) coincided with the production of an interpretive geological map of the southwest Eastern Goldfields, which postulated the presence of several terranes (Swager and Griffin, 1990a; Swager et al., 1990, 1992), an interpretation expanded upon with the identification of more terranes further east by Swager (1995a), and modified by Swager (1997). Although a useful method of providing an identity to subareas that differ in observed geological characteristics, the application of terrane subdivisions in the Eastern Goldfields is equivocal because of the poor exposure and lack of critical data. Isotopic age data have proved general contemporaneity of the komatiitic rocks and that the supracrustal sequence accumulated in a short time period (?2670–2710 Ma; Nelson, 1997a). Swager (1997, p. 12) considered the terranes in the Eastern Goldfields to have been '… deposited in adjacent, contemporaneous ensialic basins'. The Ida Fault, an inferred major structural boundary between the Southern Cross and Eastern Goldfields Provinces (Fig. 3), has been interpreted from reflection seismic analysis as a crustal-scale extensional fault that steepens towards the surface, on which normal downthrow to the east postdated metamorphism and most other tectonic history (Goleby et al., 1993; Swager et al., 1997). These characteristics are atypical of a terrane boundary or suture, although it is possible that the normal displacement represents relaxation on a major compressional structure (Griffin, T. J., 1999, pers. comm.). After a detailed study of the structure of another proposed terrane boundary, the Keith–Kilkenny Fault Zone, Passchier (1994, p. 61) concluded that 'a plate tectonic model for events in the Yilgarn is unsatisfactory since no relicts of oceanic crust, accretionary complexes or molasse basins have been recognized'. He also argued that the craton-wide contemporaneity of igneous, metamorphic, and deformational activity, and rapid accumulation of mafic and then felsic volcanic rocks, are unlike anything recognized in any modern plate tectonic setting.

For ease of reference in the following Report, the term 'domain' is used for lithostratigraphic packages that are bounded by the inferred fault lines shown on the interpretive geology layer in the database (Figs 3 and 4). Although some domains are equivalent to the hypothetical terrane units (Swager et al., 1990, 1992; Swager, 1995a, 1997), the subdivision is descriptional and no tectonic implications are intended. The northwestern and central domains, from Gindalbie in the east to Bullabulling and Ora Banda in the west, are grouped together as the Kalgoorlie greenstones. The southernmost and westernmost supracrustal rocks in the study area are demonstrably older, and hence, are separated into the Norseman greenstones (separated by the Mission and Zuleika Faults), and Barlee domain (west of the Ida Fault). Those in the northeast of the area differ in some lithostratigraphic characteristics and are termed the Edjudina–Laverton greenstones (east of the Emu and Avoca Faults; Fig. 4).

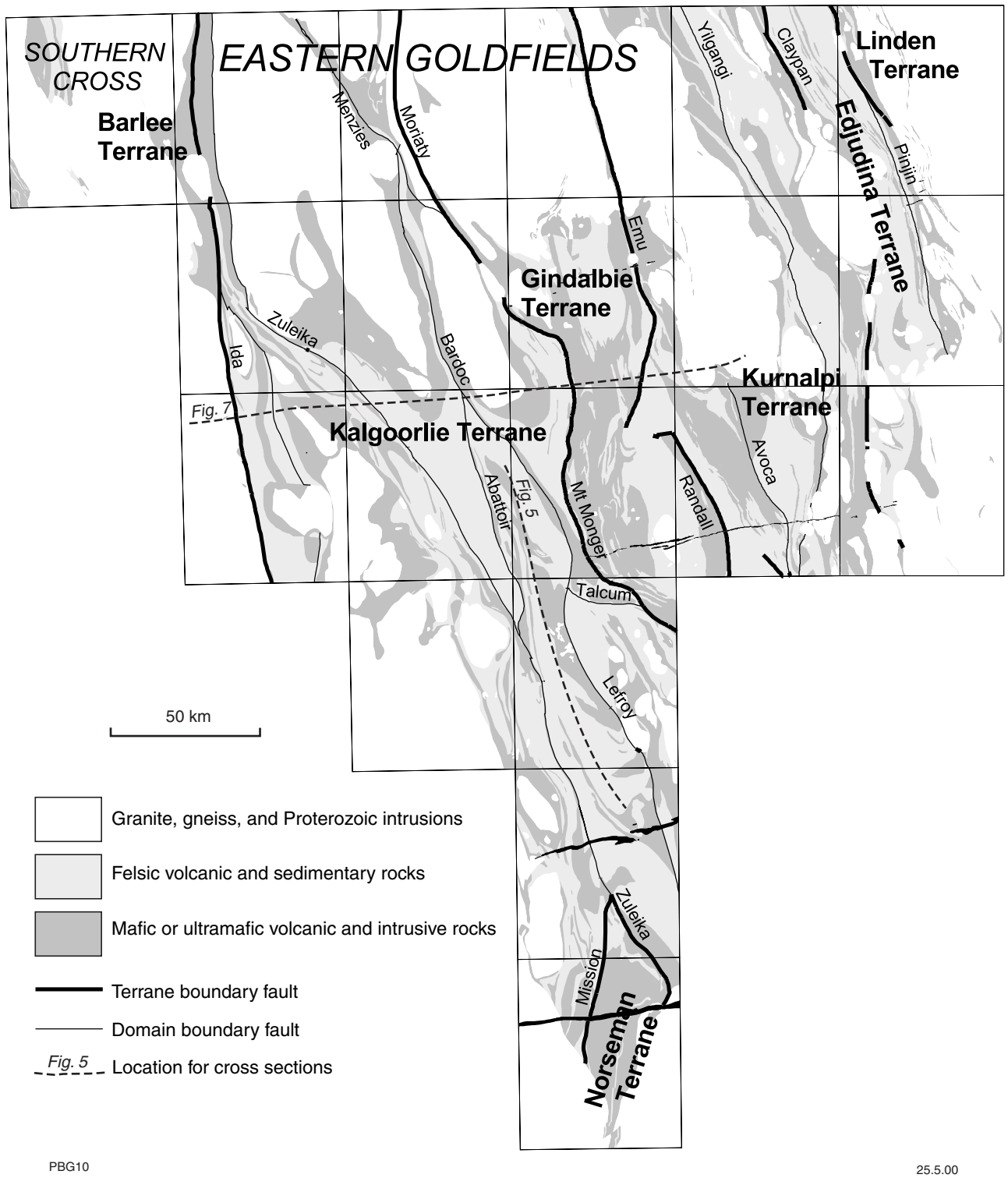

Figure 3. The interpreted distribution of granitoid and greenstone components of the southern Eastern Goldfields Province and the terrane subdivision of Swager et al. (1992) and Swager (1995a, 1997)

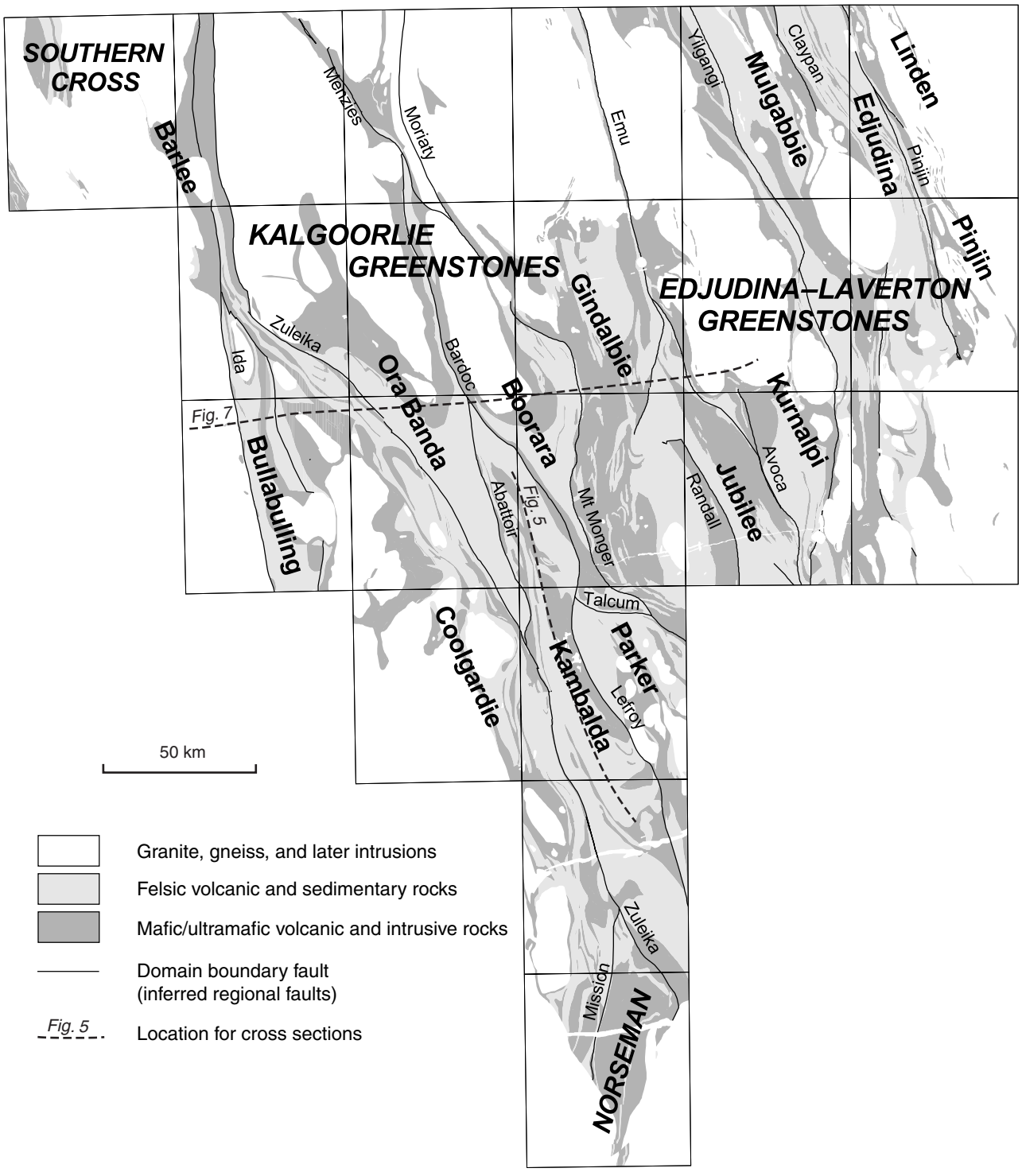

Figure 4. Subdivision of the Eastern Goldfields Province into domains based on mapped lithostratigraphic differences and inferred regional faults

The following sections provide descriptions of the lithostratigraphic successions and a brief review of crustal evolution models for this part of the Yilgarn Craton, followed by the rock unit definitions and general distribution of rock types, metamorphism, structure, and mineralization.

Lithostratigraphy and tectonic domains

The lithostratigraphy and regional variations of the greenstone successions are important for the interpretation of the lateral continuity of the original sequences, the extent of palaeo-(sub) environments, the regional structures, and tectonic setting in which the Eastern Goldfields originated. A paucity of continuous outcrop prevents accurate correlation between separate areas of exposure, exaggerated by a lack of stratigraphic markers, and has hindered identification of detailed successions and accurate structural interpretation. This lack of clear sequences and lateral continuity has led to subdivision into tectonic domains bounded by the largely inferred northerly trending series of anastomosing regional faults. The distribution of primary volcanic activity and sedimentary depositional environments remains only partly understood. Detailed geology and geochronology has revealed that komatiite may be a marker unit that extends the length of the Eastern Goldfields (Hill et al., 1989a, 1995; Nelson, 1997a). Although the domains may differ in detail of apparent lithostratigraphy, they all share clearly recognizable stages of tectonism and granitic magmatism, and progress in isotope chronology reveals closer parallels in the timing of volcanism.

No basal contact to the greenstones has been established. In the southwestern domains of the Kalgoorlie greenstones, banded migmatitic gneisses with evidence of a complex history of deformation were regarded as possible basement remnants (Archibald and Bettenay, 1977). Precise sensitive high-resolution ion microprobe (SHRIMP) zircon ages and detailed mapping have revealed that these gneisses were derived from felsic intrusions into the greenstone sequence. Nonetheless, there are several lines of evidence that felsic rocks did pre-date the greenstones, including the following:

- the geochemistry of komatiitic and basaltic magmas indicates that they were contaminated by evolved sialic crust, to the point that the upper basalts may represent assimilation of up to 25 vol.% felsic crustal rocks by the komatiitic magma (Arndt and Jenner, 1986; Barley, 1986; Morris, 1993; Lesher and Arndt, 1995);
- xenocrystic zircons as old as c. 3.4 Ga have been found in both granites and greenstones (Compston et al., 1986; Campbell and Hill, 1988; Claoué-Long et al., 1988; Hill et al., 1989b); and
- regional granite geochemistry indicates that these rocks were derived from an evolved, sialic lower crustal source (Hill et al., 1992; Champion and Sheraton, 1993; Wyborn, 1993).

Regional mapping has identified significant lithostratigraphic sequences only in the Kalgoorlie (Table 2) and Norseman regions, areas that differ in age (2720–2660 Ma and 2930 Ma respectively) as well as lithological characteristics.

Kalgoorlie greenstones

The Kalgoorlie greenstone sequence consists broadly of a lower basalt unit overlain by a komatiite unit, in turn overlain by an upper basalt unit, followed by felsic volcanic and sedimentary rocks, including late, locally important, conglomeratic deposits (Table 2). It includes layered and differentiated mafic sills at various stratigraphic levels. This sequence is best preserved in the Kambalda (Figs 4 and 5) and Ora Banda domains; similar successions in the Coolgardie and Boorara domains lack the complete upper basalt unit, and komatiite may be overlain directly by felsic volcanic and sedimentary rocks. The Coolgardie domain is characterized by a repetition of the basalt–komatiite interval of the regional succession around Widgiemooltha (Griffin, 1988b; Griffin and Hickman, 1988a,b; Hunter, 1988a,b; Swager, 1989a), a 'double' succession attributed to structural repetition on the basis of a comparison with the stratigraphic successions at Kambalda and Ora Banda (Martyn, 1987; Swager, 1989a). The Kalgoorlie greenstones also include the lithologies of the Bullabulling, Menzies, Boorara, and Parker domains, even though detailed correlation is hampered by the combined effects of poor outcrop and a complex deformational history.

The lower basalt unit consists of commonly fine-grained actinolite–chlorite–albite greenschist facies rocks, with penetrative foliation ranging from weak to intense. Primary structures include pillow lavas, flow-top breccias, and amygdales. This unit has been termed the Kambalda Footwall Basalt (Gresham and Loftus-Hills, 1981; Redman and Keays, 1985), and subdivided into the Lunnon and Scotia Basalts (Nesbitt and Sun, 1976) or Wongi and Missouri Basalts (Witt and Harrison, 1989); a distinct dacitic agglomerate attributed to the same stratigraphic unit north of Bulong provided a SHRIMP crystallization age of 2709 ± 4 Ma (Nelson, 1996).

The lower basalt unit is overlain by a prominent and regionally extensive sequence of ultramafic rocks (Table 2). These include numerous komatiites, which, despite being metamorphosed and highly altered, preserve evidence of original mineral fabrics as well as differentiated flow structures. Considerable thicknesses of olivine cumulate rocks are present at several localities. In addition to the comprehensive observations recorded in the Explanatory Notes for Lake Lefroy and Cowan (Griffin, 1990b), Kalgoorlie (Hunter, 1993), and Bardoc (Witt, 1994), petrographic and field characteristics are given by Hill et al. (1990), and synthesized with geochemical studies by Morris (1993) and Hill et al. (1995).

In the Ora Banda, Kambalda, and Boorara domains, the komatiite unit is overlain by the upper tholeiitic and komatiitic basalt unit. Two subunits are recognized, separated by an intervening sedimentary unit. The lower pillowed to massive komatiitic basalt flows include thick, differentiated flows or subvolcanic sills, whereas the upper basalts consist mainly of massive basalts in which

Table 2. Lithostratigraphy of the Kalgoorlie region

Unit	*Rock types and other characteristics*	*Ora Banda domain*	*Coolgardie domain*	*Kambalda domain*	*Boorara domain*	*Gindalbie domain*	*Edjudina–Laverton greenstones*
Conglomerate (commonly polymictic) and coarse, clastic sandstone	Clast or matrix supported polymictic conglomerate and sandstones; locally stratified, cross-bedded; scour and fill structures, graded beds	Kurrawang Formation 750 m thick, polymictic conglomerate; ~30 m unit with high content of BIF clasts 1300 m sandstone and siltstone		Merougil conglomerate 2300 m thick, mostly pebbly sandstone, sandstone, and siltstone		Penny Dam conglomerate 200 m, pebble to boulder clast-size; quartzofeldspathic sandstone interlayers	Yilgangi conglomerate >200 m thick, local boulders, lithic wacke interlayers
unconformity recognized	~ *?sheared basal contact* ~						
Felsic volcanic, volcaniclastic, sedimentary rocks	Rhyolite to andesite lava, tuff, volcanic breccia. Felsic volcaniclastic sedimentary rocks ranging from sandstone to debris flow deposits, silt and mudstone also present	Black Flag Group 400–3000 m upper part, predominantly felsic volcaniclastic and sedimentary rocks ranging from mudstone to debris flow or diamictite; minor lava flows range from porphyritic dacite to rhyolite; ?0–3000 m lower part, felsic (dacites and andesites) lava flows predominant, more common in southeast				Volcaniclastic units, greywacke, slate, chert. Calc-alkaline dacite–rhyolite suite	No clear stratigraphic sequence. Felsic volcanic, volcaniclastic, sedimentary, and chemical rocks; Intermediate schists; metadacite–andesite
Upper basalt	Komatiitic and tholeiitic basalts, with a tholeiitic plagioclase-phyric upper part and high-Mg variolitic and spinifex-textured lower portion	Victorious Basalt ≤3000 m porphyritic; Bent Tree Basalt ≤3000 m massive to pillowed, includes layered mafic sills (?600 m)	≤200 m porphyritic vesicular basalt; 200–1500 m high-Mg basalt, mafic concordant sills	Upper Hanging Wall Basalt 500–1500 m vesicular tholeiitic basalt, locally schistose; Paringa Basalt 400–800 m mostly high-Mg basalt; Kapai Slate	Absent or thin and discontinuous	Bimodal mafic–felsic volcanic sequence	Basaltic rock types include very fine grained massive units, porphyritic, komatiitic, carbonated varieties; commonly schistose in large areas
Komatiite	Thin, komatiitic basalt cap; thin komatiite flows with minor interflow sedimentary beds overlying thicker komatiitic flows and massive olivine adcumulates	Big Dick Basalt ≤500 m high-Mg basalt; Siberia Komatiite ≤2600 m komatiitic flows; Walter Williams Formation ≤400 m olivine cumulates	≤?2000 m komatiitic, high-Mg, and variolitic basalts; cumulate-textured ultramafics	Devon Consols Basalt 60–300 m variolitic high-Mg basalt; Kambalda Komatiite 300–1500 m ultramafic flows and cumulates	Apparent lower basalt–komatiite sequence around Scotia anticline, limited outcrop	Bulong Complex ~5000 m layered cumulates, komatiite; ponded flows up to 400 m thick	Serpentinite with olivine spinifex or cumulate textures locally
Lower basalt	Komatiitic and tholeiitic basalts, felsic volcanic units locally	Missouri Basalt ≤1500 m massive to pillowed, porphyritic; Wongi Basalt ≥2000 m variolitic high-Mg basalt	500–1500 m spinifex and ocelli textured high-Mg basalt; concordant mafic sills	Kambalda Footwall Basalt ≥2000 m; tholeiitic in upper part, high-Mg basalt in lower		Early basaltic and felsic rocks	
References		Witt (1994); Swager et al. (1995); Swager (1994a)	Hunter (1993); Wyche (1998)	Griffin (1990b); Swager and Griffin (1990b)	Witt (1994)	Ahmat (1995b); Swager (1995a); Nelson (1997b)	Swager (1995a,b)

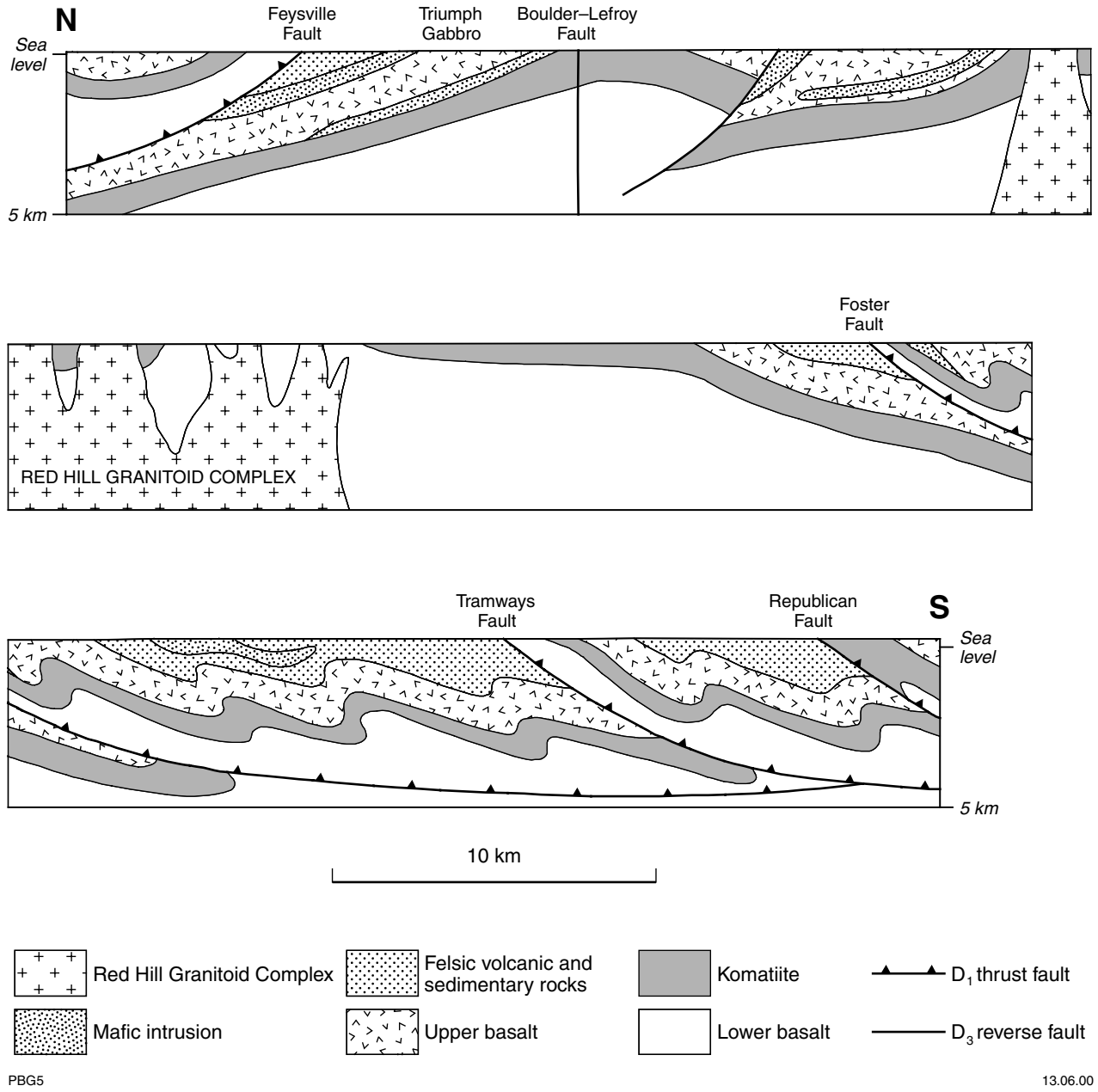

Figure 5. Cross section along the length of the Kambalda domain illustrating the structural interpretation, allowing continuity of the inferred stratigraphic succession (after Swager et al., 1990). The location of this cross section is shown in Figure 3

interleaved pyroxene spinifex-textured, coarser grained gabbroic and cumulate layers are evidence of variably thick, fractionated flows or sills.

The mafic–ultramafic volcanic succession is overlain by the Black Flag Group, a laterally persistent but lithologically highly variable package of rhyolitic to andesitic volcanic rocks and proximal to distal sedimentary rocks. The Black Flag Group is a poorly understood unit — it hosts little-known mineralization and is poorly exposed — with a possible thickness of 3000 m suggested by Groves and Gee (1980), whereas Griffin (1990b) estimated that metamorphosed felsic volcanic rocks in the lower part are 3000 m thick and overlain by an unknown, but substantial thickness of sedimentary rocks.

The uppermost greenstones recognized are the Karrawang Formation and Merougil Conglomerate (Table 2), which comprise rudaceous to arenaceous sedimentary rocks limited to unconformity and fault-bounded synclinal basins, elongate parallel to the regional tectonic trend. The nature, origin, and significance of these sedimentary rocks has been addressed by Glikson (1971),

Witt and Swager (1989a), and Swager (1997), in addition to the descriptions provided in the Explanatory Notes.

Bullabulling, Boorara, Menzies, and Parker domains

Correlation of the Bullabulling, Boorara, Menzies, and Parker domains with the Kalgoorlie greenstones are provisional because outcrop in these areas is of limited lithostratigraphic extent and there are no explicit markers. Fault boundaries have been inferred from aeromagnetic data and locally recognized shear or faulting in outcrop, but the nature and extent of displacements are obscure.

The poorly exposed Bullabulling domain, located between the Bullabulling Shear and Ida Fault (Fig. 4), comprises highly deformed, upper amphibolite facies metamorphic rocks in which no younging directions or regional structures have been established. The most easterly outcrops are sedimentary or felsic volcanic rocks, interlayered with basalts and microgabbro. These are followed westwards by a minor andesite unit, then a more extensive feldspar-phyric, vesicular basalt unit, followed by felsic schists interlayered with lenses of amphibolite. Along the contact between this sequence and the granite to the west are several isolated units of ultramafic schist and silicified serpentinite.

The Boorara domain, extending from the northwestern corner of KANOWNA onto BARDOC, is bounded by the Mount Monger Fault to the east and the Bardoc–Boorara shear zone to the west (Fig. 4). A considerable stratigraphic thickness of basalts and komatiites is present and probably represents tectonic duplication of the same basalt–komatiite–basalt package present in the other Kalgoorlie domains. A felsic unit consisting of sedimentary and volcanic rocks is probably equivalent to the Black Flag Group.

The Menzies domain occupies a highly deformed wedge between the Moriaty and Menzies Shears, north of the Boorara domain (Fig. 4). A highly deformed sequence of ultramafic schist with minor amphibolite and an overlying felsic volcaniclastic unit are in tectonic contact with various basalt units. A geochronological constraint provided by a felsic volcanic rock near the western base of the sequence, a SHRIMP U–Pb zircon date of 2692 ± 6 Ma (Nelson, 1995), indicates emplacement synchronous with the domains further south. The eastern part of this domain is complex and Swager (1994b) inferred a northward lateral facies change from sediment- to basalt-dominant rocks.

The Parker domain lies between the Lefroy, Talcum, and Mount Monger Faults on eastern LAKE LEFROY. It includes felsic volcaniclastic rocks and tholeiitic and komatiitic basalts that are intruded by several granitoid plutons. These greenstones appear to correlate with the upper basalt and felsic volcanic–sedimentary units of the Kambalda domain (Hickman, 1986). In the eastern part of this domain, however, sedimentary rocks contain magnetite-rich BIF horizons, a close similarity to the adjacent BIF-bearing sedimentary rocks of the Mount Belches Formation (Painter and Groenewald, in press).

Gindalbie domain

The Gindalbie domain lies east of the inferred Mount Monger Fault and extends east to a boundary comprising the Emu Fault and Penny Dam conglomerate to the east and Randall Fault to the southeast (Fig. 4). This extensive domain covers a large part of KANOWNA, GINDALBIE, and KURNALPI. It comprises four greenstone successions thought to be separated by regional, early (D_1), low-angle thrust faults. These structures, which must have been folded and displaced by subsequent deformation, are poorly understood because of complex lithostratigraphy in an area of limited outcrop. A description of the inferred structural and stratigraphic relations is provided by Swager (1994c, 1995a) and Ahmat (1995b).

Edjudina–Laverton greenstones

East of the Gindalbie domain are a series of narrow, elongate lithotectonic domains (Fig. 4). These consist of compositionally and chronologically equivalent rock types to the Kalgoorlie greenstones, albeit at higher metamorphic grade with evidence of diverse and locally complex sequences affected by lateral variations, probably caused by syndepositional structural activity and felsic to intermediate volcanic centres. These domains are effectively equivalent to what Swager (1997) termed the Kurnalpi and Edjudina Terranes, and the southern part of what Williams (1974) classified as the Laverton Subprovince. In addition to details provided in the Explanatory Notes, constraints on the stratigraphic relations are given by Swager (1995a, 1997) and Chen (1999).

Norseman greenstones*

The Norseman greenstones are exposed in a restricted area south of the Kambalda and Coolgardie domains (Fig. 4) and differ from the adjacent greenstones in age and lithostratigraphy. Nelson (1995) obtained an age of 2930 ± 4 Ma for rhyolite at a structurally deep level (in the Penneshaw Formation; see below), confirming an age of 2938 ± 10 Ma reported earlier (Campbell and Hill, 1988; Hill et al., 1989b). The rhyolite contains clustered xenocryst populations of 2977 ± 9 Ma and 3106 ± 13 Ma (Nelson, 1995), with single grains having ages as great as c. 3450 Ma (Hill et al., 1989b). The eruption of basalts at a higher tectonic level (Mount Kirk Formation; see below) has been constrained to about 2714 ± 5 Ma, the age of zircons that partially replace baddeleyite within a differentiated subvolcanic sill (Hill et al., 1989b).

The Norseman greenstones have an apparently well-defined, westerly younging stratigraphy, although bedding-parallel, high-strain zones suggest stratigraphic discontinuities, possibly involving structural repetition. The Penneshaw Formation, at the structurally deepest level (Fig. 6), consists mainly of amphibolites and massive to pillowed basalts, with minor felsic volcanic and sedimentary rocks. Along its eastern contact with the intrusive Buldania Granitoid Complex, the Formation includes the Boojerbeenyer Shear Zone, consisting of

* No Explanatory Notes were produced for the NORSEMAN sheet.

interleaved amphibolite, schistose to mylonitic granitoid, banded granitoid gneiss, and, locally, BIF and sedimentary rocks. The interleaving may be tectonic, intrusive, or both. Spray (1985) identified pre-D_1 fabrics in the southern exposures of the granitoid gneiss and suggested that the zone of intense deformation between greenstones and gneiss represents an originally subhorizontal, ductile D_1 shear, a contact subsequently rotated into a steep attitude and which underwent greenschist-facies retrogression. The Penneshaw Formation also contains porphyritic felsic schists with amphibolite intervals (?dykes) near its western contact with the Noganyer Formation.

The Noganyer Formation, which overlies the Penneshaw Formation, is characterized by persistent BIF layers within clastic, partly felsic sedimentary rocks, and is intruded by gabbro sills. Meso- and small-scale structural repetition of BIF layers by folding and faulting has been recognized. The Penneshaw and Noganyer Formations are strongly deformed throughout, and amphibolite facies metamorphism is recorded by garnet-, andalusite-, and cordierite-bearing assemblages in the metasedimentary rocks.

The Woolyeenyer Formation, overlying the Noganyer Formation, is a monotonous sequence of massive basalt flows with a minor ultramafic component. Although apparently 10 km thick, shear zones within the sequence may represent thrust faults and hence, stratigraphic duplication.

The Mount Kirk Formation overlies the Woolyeenyer Formation structurally on a major structural discontinuity called the Mission Fault (Fig. 6). This formation is a tightly folded sequence of sedimentary rocks containing major gabbro sills (Doepel, 1973) and was interpreted as part of the Kalgoorlie Subprovince by Swager et al. (1990). Campbell and Hill (1988) published a preliminary date of 2689 ± 7 Ma for felsic volcanic rocks in the Mount Kirk Formation immediately west of the Mission Fault.

Complete separation of the Norseman and Kalgoorlie greenstones may be equivocal in that the age and geochemistry of the Woolyeenyer Formation are not incompatible with the lower basalt unit immediately further north.

Southern Cross Province

The small expanse of greenstones west of the Ida Fault within the project area is assigned to the Barlee domain of the Southern Cross Province because of the presence of BIF in association with mafic rocks (dominant) and fine-grained sedimentary rocks, a lithological package not present east of the fault. The Barlee domain rocks are similar to those further west in the Southern Cross Province, where SHRIMP zircon ages of 2732 ± 3 Ma and 2734 ± 3 Ma (Nelson, 2000) for the volcanic Marda Complex, which unconformably overlies the remainder of the greenstones, are at least 10 million years older than the oldest part of the Eastern Goldfields Province. The Southern Cross greenstones have quartzite or quartz-pebble conglomerate at, or near, the base of the sequence; basalts with interleaved komatiite and regionally persistent BIF units; and, towards the top, metasedimentary rocks and felsic volcanic complexes. In this province, the supracrustal rocks are exposed in a series of elongate, narrow greenstone domains surrounded by granitoid and granitoid gneiss, and are commonly metamorphosed to relatively high grades (Ahmat, 1986), in contrast to the broad zones of low metamorphic grade in the Kalgoorlie greenstones. The outcrop patterns, the contrast in metamorphic grade, and the normal movement along the crustal-scale Ida Fault, as revealed by seismic profiling (Goleby et al., 1993), suggest that the Barlee domain is exposed at typically deeper crustal levels than the adjoining Bullabulling and Coolgardie domains of the Kalgoorlie greenstones. In central parts of the Southern Cross Province, such as Marda, very low grade metamorphic rocks formed as evidence that these greenstones have always remained at shallow crustal levels.

Models of tectonic settings and crustal evolution in the Eastern Goldfields Province

Considerable research towards interpretation of the crustal evolution of all the major Archaean cratons has led to a large number of models invoking plume, plate, and both plume and plate tectonic settings; comprehensive arguments that Phanerozoic style plate tectonics operated (de Wit, 1998) and were impossible (Hamilton, 1998) illustrate the disparity of opinion. A summary of the established constraints and models that have addressed the origin of the Yilgarn Craton in general and the Eastern Goldfields in particular is pertinent.

A model attributing much of the development in the Eastern Goldfields Province to a mantle plume was formulated (Campbell and Hill, 1988; Campbell et al., 1989; Griffiths and Campbell, 1990; Hill et al., 1992) to account for the evidence of earlier sialic crust in combination with the following petrogenetic constraints:

- komatiitic magmas, such as those of the Eastern Goldfields that have as much as 32 wt% MgO, and represent high fractions of mantle melting that would require thermal anomalies at a depth greater than 250 km (laboratory evidence summary in Arndt et al., 1997);
- the considerable volume and extent of komatiitic lava fields attributed to a single event (Hill et al., 1990, 1995);
- synchronicity of felsic and mafic volcanism from a very early stage (pre-komatiite); and
- generation of felsic melts at sequentially shallower depths.

The East Yilgarn model of Campbell et al. (1989) and Hill et al. (1992) invoked a major plume initiated at the core–mantle boundary that ascended through thermal buoyancy. As the plume head and thermal anomaly approached the lower lithosphere boundary, melting ensued to produce basaltic lavas while the plume mushroomed to a diameter in excess of 1000 km. The first

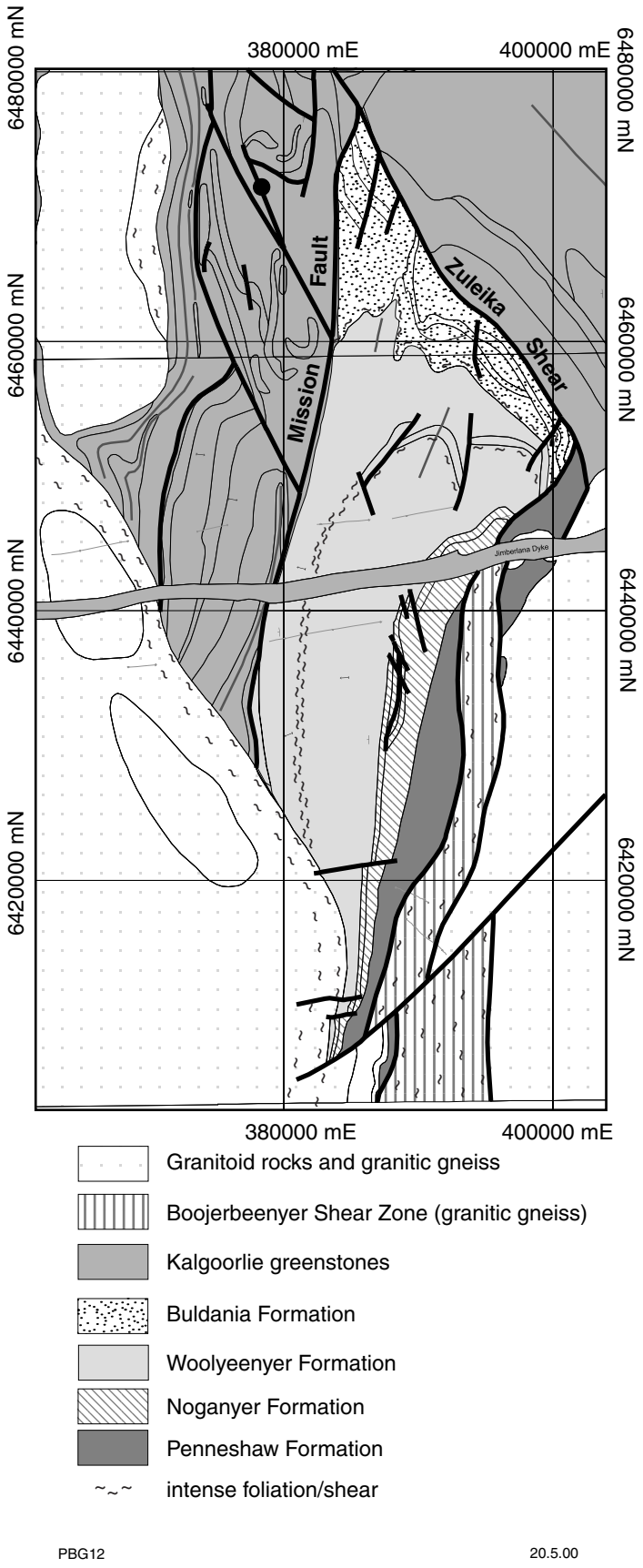

Figure 6. Interpreted Eastern Goldfields solid geology highlighting detail in the Norseman region. After McGoldrick (1993) and Swager et al. (1990, 1995)

melts produced a tholeiitic basalt unit, followed by eruption of the voluminous komatiite magmas comprising the plume axis. The thermal effect on the crust allowed assimilation of up to 25 vol.% of mature quartzofeldspathic crust by the late komatiites to produce compositionally anomalous basalts. The locality of the plume axis was probably central to the Eastern Goldfields, but may have affected the continent in a progressive fashion as the plate moved over the plume (Passchier, 1994).

Typical plume-sourced magmatism, although commonly involving great continental flood basalt outpourings, occurs over a period of only 10–20 million years, but the disturbance of crustal thermal equilibrium lasts considerably longer (White and McKenzie, 1989). Mathematical modelling and time-distance analysis of conduction allowed Campbell and Hill (1988) and Hill et al. (1992) to argue that there would be widespread felsic magmatism in the period 15–30 million years after plume arrival at the lithosphere, with on-going granite magmatism through remelting of precursor granitoids at different levels in the crust for as long as 50 million years. Although this model may explain much of the magmatic history and vertical tectonics of the Eastern Goldfields, it does not directly address the relative abundance of calc-alkaline volcanic rocks in the Edjudina–Laverton greenstones, nor the considerable crustal shortening evident in the regional geological structures.

A convergent plate-margin model for the Eastern Goldfields was proposed by Barley et al. (1989), who recognized two lithostratigraphic associations in the Norseman–Wiluna area: a tholeiite–calc-alkaline volcanic association with felsic sedimentary rocks to the east, and a tholeiite–komatiite assemblage with fine-grained siliceous sedimentary rocks to the west. They suggested that the eastern association corresponds to a volcanic arc succession and that the west represents a back-arc marginal basin sequence. Swager et al. (1992) expanded upon this and preferred an accretionary model with continued transpressional deformation — the accreted terranes not necessarily being exotic and representing '..originally adjacent or closely related geological environments such as island arcs and back arcs.'

Stratigraphic sequence interpretation of the Eastern Goldfields (Krapez et al., 1997) identified five possible tectonic settings: (i) intra-arc rift-basin; (ii) back-arc spreading basin; (iii) arc-related basin; (iv) deep-marine stage (flysch facies) of remnant-ocean basin; and (v) non-marine stage (molasse facies) of remnant-ocean basin. On the basis of these settings, a western Pacific style of multiple marginal basin formation was proposed for the East Yilgarn, with the Eastern Goldfields in an intra-arc frame. This was extended to a model of continental collision with obduction of a mafic and ultramafic lava assemblage generated in a back-arc spreading basin setting over hot continental crust by Archibald (1998). On-going komatiitic magmatism during the closure of the basin produced the suite of contaminated compositions found in the upper basalt unit in the Kalgoorlie greenstones. Arc-related volcanism followed, producing a considerable sequence of volcaniclastic deposits in an intra-arc setting. This evolved into major granitoid emplacement and then shifting of the decoupling plane from the base of the greenstones to the lower crust – middle crust boundary. Archibald (1998) attributed the onset of post-orogenic gold mineralization to fluid-flow focusing in deep crustal shears in the post-collisional stage.

Using analogous settings from eastern South America and the sea of Japan, Morris (1993) concluded that, unlike the plume model, a convergent margin can explain both mafic–ultramafic and calc-alkaline volcanic rocks, and proposed that a northwesterly aligned, continental rift developed in ?continental crust and paralleled to the east by a volcanic arc developed above a westerly dipping subduction zone. A progressive fan-like opening of the rift would account for differences between the different domains in the Kalgoorlie greenstones, with lavas showing advanced crustal contamination in the northern areas (Ora Banda domain) preceding tholeiitic basalts variably fractionated in crustal magma chambers prior to eruption further south (Kambalda and Coolgardie domains). Komatiite behaved as a heat source for melting of the continental crust to produce dacitic and rhyolitic volcanic rocks and associated sedimentary rocks characteristic of the Black Flag Group. Typical arc magmatism would account for the calc-alkaline volcanism in the Edjudina–Laverton greenstones.

The two principal hypotheses of crustal evolution in the Eastern Goldfields are not mutually exclusive because both plume and plate tectonics undoubtedly operated in the Late Archaean, albeit in ways not yet completely understood. As shown by Davies (1992, 1998), subduction in the environment of steeper geothermal gradients could not have operated at the same rate as established in younger settings, and plume activity must have accounted for a significant proportion of the thermal budget. Both models account for many aspects of the granite–greenstone assemblage, but neither is entirely satisfactory. A plume could certainly generate most of the magmatic features, but requires a complex, unknown attribute to account for the calc-alkaline rocks of the eastern domains. The convergent margin model accounts for many of the palaeoenvironments recognized in the felsic sedimentary and intermediate calc-alkaline rocks, but does not explain the komatiites satisfactorily. Recent work has shown that calc-alkaline magmatism may be generated in settings other than those involving subduction (Morris et al., 2000). Similarly, allochthonous crustal fragments generated in an oceanic magmatic environment are not present in any other greenstone belts (Bickle et al., 1994). Although there is little direct negative evidence in either case, the convergent accretionary model has perhaps the most difficulty in accounting for the great majority of the volcanism being tholeiitic to komatiitic, whereas calc-alkaline rocks are located in a series of relatively minor volcanic centres along the eastern shoulder of the Eastern Goldfields basin. Felsic volcanism occurred episodically throughout the emplacement history of the Eastern Goldfields greenstones, commonly with characteristics compatible with crustal derivation. In view of this, the plume model cannot be dismissed and requires continued attention — as suggested by Abbott (1996), where the only greenstones that are preserved may be those produced by interaction between plume, hotspot, and subduction environments.

Archaean rocks and their distribution

In the following outline, most descriptions are based on the Explanatory Notes listed in Table 1. Other sources used for detail or expansion are cited specifically. All rock codes applied in standardizing the maps for the database are listed in Appendix 1. Although all important rock codes are referred to specifically below, a detailed description of all rock units is beyond the scope of these notes. More details of definition and petrography are commonly provided in the original Explanatory Notes. Although all rocks described below have undergone recrystallization under metamorphic conditions ranging between lower greenschist and upper amphibolite facies, igneous or sedimentary names and terminology are used for all those rocks for which protolith characteristics are recognized. Lithostratigraphic sequences are described above (see **Lithostratigraphy and tectonic domains**).

Ultramafic rocks

Ultramafic rocks are present in all the domains, but are most extensive in the Coolgardie, Ora Banda, Boorara, Gindalbie, and Kambalda domains (Fig. 4). Although pervasive metamorphism and further degradation by metasomatism and weathering commonly obscures these rocks in outcrop, a useful identification parameter may be provided by magnetite, a byproduct of serpentinization, which induces high magnetic susceptibility and, hence, identifiable magnetic highs on aeromagnetic maps for many of the ultramafic units. The silica caprock (*Czru*) described above is also useful in many localities. Several publications provide comprehensive descriptions of these lithologies, such as Hill et al. (1990) and Morris (1993).

Undivided ultramafic rocks (*Au*) are those too highly altered or schistose to allow specific classification. Varieties include massive serpentinite (*Aus*), talc–carbonate–serpentine, talc–carbonate(–chlorite–tremolite) (*Aut*), and tremolite–chlorite (*Aur*) rocks. Protoliths for these rocks were probably either olivine cumulates or komatiites, but cannot be identified due to the absence of primary igneous microstructures. Tremolite schists containing small amounts of plagioclase may represent the komatiitic basalt that commonly, but not necessarily, forms with komatiites in ultramafic sequences. Undivided ultramafic rocks outcrop most extensively south and north of the Bulong Complex in the Gindalbie domain and east of Hayes Hill (COWAN AMG 790740*) in the southern Coolgardie domain. Numerous minor occurrences exist in most domains.

Komatiite (*Auk*), the ultramafic volcanic rock identified by relict olivine spinifex-textures, forms flow units that are best developed in the Coolgardie, Ora Banda, Kambalda, Boorara, and Gindalbie domains. Although almost universally serpentinized, olivine is commonly pseudomorphed and the spinifex structure is commonly recognizable, even in highly altered rocks. The spinifex texture is a valuable identifying characteristic comprising relict, large (commonly 5–15 cm, but up to 70 cm across), platy olivine crystals, most commonly stacked in book-like structures, but also occurring randomly in what is interpreted as the uppermost part of lava flows. In areas of low strain, relict textures in lower parts of the komatiite flows allow recognition of original olivine-dominated cumulate rocks.

The dominant mineral assemblages are now serpentine–chlorite or tremolite–chlorite in lower and higher metamorphic grade areas respectively. Talc and magnetite are common minor or accessory minerals. Primary olivine is very rare, whereas chromite is relatively widespread. Locally pervasive carbonation has resulted in areas of talc–carbonate rocks (*Auc*). Despite the ubiquitous metamorphism and alteration, original flow-top breccias have been identified in drillcore, and locally in outcrop, and constrain primary flow thicknesses to a range of 10 to 100 m in general; an apparent unit thickness of 400 m in the Bulong district probably reflects lava ponding. Interflow sedimentary or volcanic ash units also allow recognition of original flow dimensions. The total thickness of komatiites is variable and ranges from about 80 m in outcrops 60 km south of Kambalda, to 1000 m in the Kambalda area, possibly 5000 m in the Bulong area, between 300 and 900 m in the Boorara and Coolgardie domains, and up to 2600 m in the Ora Banda domain. Thin komatiite units have been recorded in all of the eastern domains (Jubilee, Kurnalpi, Mulgabbie, Edjudina, Linden, and Pinjin), and although no estimates have been documented, may be more than 100 m thick. A lateral extent of about 100 km for the flows has been recognized, with major lateral variations being attributed to different subenvironments within the voluminous and regionally extensive eruptions (Hill et al., 1990).

Peridotite (*Aup*) represents massive ultramafic units in which medium- to coarse-grained orthocumulate, mesocumulate, and adcumulate textures can be identified despite pervasive serpentinization. The original matrix has been altered to a fine-grained mass of tremolite, chlorite, serpentine, and magnetite. Primary igneous olivine has survived very low metamorphic grades at a few localities (e.g. Bulong Complex), and metamorphic olivine has reformed in cumulates metamorphosed to amphibolite facies (Hill et al., 1990). Cumulate textures are also seen in the ferruginous silica caprock that commonly forms above the peridotite during the weathering process. Preserved cumulate textures are abundant in the lower part of the regionally extensive komatiite unit in the Ora Banda domain (the Walter Williams Formation of Hill et al., 1990 and Witt, 1994). It is notable that, when seen in isolation, the cumulate lower portion of a komatiite flow is indistinguishable from the peridotites attributed to the layered intrusions. In this northwestern area, minor lenses of peridotite with cumulate textures are associated with the basalt and BIF sequence in the northernmost portion of the Coolgardie domain. The Bulong Complex in the Gindalbie domain (KANOWNA) represents another substantial accumulation of ultramafic lava, of which a

* Localities are specified by the Australian Map Grid (AMG) standard six-figure reference system whereby the first group of three figures (eastings) and the second group (northings) together uniquely define position, on this sheet, to within 100 m.

significant proportion consists of serpentinized cumulate rocks (Ahmat, 1993).

Pyroxenite (*Aux*) forms in large differentiated komatiitic flows (e.g. Bulong) and mafic–ultramafic sills in which pyroxenite may amount to 50% by volume. These rocks are readily recognized in areas where penetrative foliations are not well developed and pseudomorphism of primary pyroxenes by metamorphic amphibole is preserved. Pyroxenite also makes up a large portion of the Carr Boyd Rocks Complex near the northernmost greenstones of the Gindalbie domain. The complex includes layered ultramafic to mafic sequences, recognized in drill core (Purvis et al., 1972), crosscut by bronzitites, which now outcrop over several square kilometres as tremolite and tremolite–chlorite rocks in which cumulate and pegmatoidal textures are recognizably pseudomorphed.

Mafic volcanic rocks

The greenstone sequences consist largely of mafic extrusive rocks. Both tholeiitic and komatiitic (high-Mg) types are present, but may be indistinguishable in the field because characteristic textures are not always preserved. Hence, massive, fine- to medium-grained metabasites (*Ab*) that have not been subdivided are mainly tholeiitic basalts, but may include intercalations of komatiitic basalt. Pillow structures are present at several localities, but are not widely recognized, probably because the rocks are too poorly exposed. The strong deformation in some areas also masks such structures.

Komatiitic or high-Mg basalt (*Abm*) is most common at two lithostratigraphic levels — near the base of the lowermost mafic volcanic unit in the Kalgoorlie sequence, and at low levels in the basaltic unit above the komatiite unit (see below). These basalts are distinguished either by the presence of relict pyroxene-spinifex or variolitic textures, and by chemical analysis providing MgO values in the range 10–18 wt%. Grey to pale-green tremolite–actinolite is the main constituent mineral, and there may be up to about 30% plagioclase, with accessory opaque oxides, typically magnetite. Chlorite is commonly present. The common relict pyroxene-spinifex texture consists of tremolite–actinolite pseudomorphs of acicular clinopyroxene. Individual pseudomorphed blades range in length from a few millimetres up to several centimetres, and clusters of pseudomorphs can assume dendritic or fan-like forms. Komatiitic basalt flows vary laterally in physical characteristics, with spinifex textures completely absent from substantial portions in some cases. Although pillow structures are present, these are rarely well exposed in surface outcrop and probably obscured by deformation in many areas.

The variolitic basalts (*Abmo*) typically consist of a fine, felted groundmass of acicular amphibole(–chlorite) and subordinate (up to 30%), very finely recrystallized plagioclase, with abundant pale, spherical to ovoid cryptocrystalline varioles (termed ocelli on some published maps) that range in diameter from 1 mm to greater than 1 cm. The varioles are mineralogically similar to the groundmass in which they formed, but contain a greater proportion of plagioclase. Variolitic textures are commonly, but not universally, indicative of high MgO content.

Tholeiitic basalts (*Abv*) are typically very fine grained, massive rocks, but may be amygdaloidal (*Aby*) or porphyritic (*Abp*), with plagioclase phenocrysts ranging from 2 to 30 mm in length. Pillow structures and flow-top breccias are seen in outcrop locally, although the poor quality of exposure commonly renders recognition equivocal. Coarser grained parts of basaltic rock packages range from recognizably subophitic basalt to microgabbroic, and may represent either the presence of subvolcanic intrusions or fractionation in thicker, possibly ponded flows. Rocks in which this range of grain size is pronounced have been mapped as basalt–dolerite (*Abd*).

Coarsely plagioclase-phyric basalt (*Abp*) is a distinctive rock, in which large (up to 3 cm), tabular phenocrysts of plagioclase, locally glomeroporphyritic, are set in a fine- to medium-grained hornblende and plagioclase matrix. This rock forms a unit up to 2 km thick at the top of the upper basalt in the Ora Banda domain, whereas a similar basalt south of Coolgardie is interpreted to lie within the lowermost unit of the Kalgoorlie greenstones.

Amphibolite (*Aba*) is used where mafic rocks are completely recrystallized and no vestiges of primary textures or structures remain. Prismatic amphibole and fine, polygonal granoblastic plagioclase, which shows little or no twinning, are the main constituents. Clinopyroxene is present locally. Compositional variations are reflected by different proportions of plagioclase relative to amphibole. In cases where metamorphic foliation is very well developed and the nature of the protolith is obscured by advanced recrystallization and alteration, the metabasites may be classified as 'mafic schists' (*Ala*).

Intermediate rocks

Intermediate volcanic (*Afiv*) and volcaniclastic rocks (*Afix*) make up a significant proportion of the felsic volcanic and sedimentary parts of the greenstone sequence locally.

In the Ora Banda domain, the uppermost part of the primary pre-tectonic sequence, the Black Flag Group (Table 2), includes extensive exposures of intermediate rocks. These volcanic and volcaniclastic rocks include a coarse volcaniclastic conglomerate with angular to subrounded, pebble- to boulder-sized clasts, mainly of a porphyritic felsic lithology. The outcrops of lava include porphyritic plagioclase–hornblende andesite and hornblende dacite. Hunter (1993) described thin beds of lapilli tuff, crystal tuff, and very fine grained ash deposits in this area. Small outcrops of feldspar-phyric andesite outcrop locally within felsic volcanic and volcaniclastic sequences in the Coolgardie and Bullabulling domains.

Intermediate rocks (*Afiv, Afix*) are also present in the Gindalbie domain, where they form the eastern part of the Bulong anticline, extending south along the boundary between Kanowna and Kurnalpi onto the northeastern corner of Lake Lefroy. Most of the massive andesites and

andesitic basalts at this locality are altered. There are also fragmental rocks of andesitic composition in this area. Intermediate rocks that outcrop in several areas in the northern part of the Gindalbie domain are dominantly andesitic to dacitic in composition, but both rhyodacite and basaltic andesite are also present.

Intermediate volcanic rocks make up a substantial proportion of the greenstones in the Yabboo domain. These rocks occupy an elongate area 20 km in length between Red Gate Well (EDJUDINA AMG 280165) and Bore Well (EDJUDINA AMG 360960), and include dacite, andesite, and basaltic andesite that are commonly porphyritic (plagioclase, less commonly hornblende), amygdaloidal, or both. Angular clasts are locally recognizable, indicating volcaniclastic protoliths for these parts. At some localities these rocks grade into greywacke. In the Edjudina domain, intermediate rocks outcrop (~2 km^2) near Edjudina Well (EDJUDINA AMG 497055). Although schistose and strongly carbonated, these rocks were found to be equivalent to andesite and basaltic andesite in composition (Swager, 1995b).

Felsic rocks

Felsic volcanic and volcaniclastic rocks (*Afv*) are widespread, but commonly poorly exposed. They form much of the upper part of the volcanic and sedimentary unit of the Kalgoorlie greenstones, but occur intermittently and locally at levels throughout the sequence, thus yielding radiometric mineral dates ranging from 2720 to 2670 Ma. They are also dominant rock types in the Edjudina–Laverton greenstones. Morris (1998) presented detailed geological and geochemical data for some felsic-dominated volcanic rock successions in the Eastern Goldfields.

The felsic rocks from upper parts of the sequence in the western domains, the Black Flag Group, locally make up a dacite–rhyolite association comprising dacite and rhyolite lavas with associated breccia, volcaniclastic sandstone, and carbonaceous shale. Some dacite and rhyolite units were extruded as subaqueous lava lobes, commonly less than 10 m thick. A variety of clastic sedimentary rocks are associated with the dacite to rhyodacite porphyry, crystal and lapilli tuffs, and volcaniclastic conglomerates in upper parts of the sequence. Whether these rocks represent primary pyroclastic deposits or epiclastic sediments is unclear in the poor exposures available. Oligomictic conglomerate, containing subangular clasts of the porphyritic felsite up to 50 cm in diameter, set in a matrix of similar composition, may be partly volcanic and partly sedimentary in origin. Other interbedded rocks, ranging from shale to pebbly sandstone to conglomerate, have sedimentary structures, such as graded bedding, flame structures, and load casts more commonly than cross-beds and ripples, suggesting deposition in a gravity- rather than stream-flow environment. Some shale and chert units may represent fine ashfall deposits.

The felsic rocks are represented by quartz–feldspar–mica schists in areas of higher metamorphic grade and more intense strain. Although those with volcaniclastic protoliths may remain recognizable because of their oligomictic nature and blastoporphyritic fragments, many quartzofeldspathic schists are of uncertain origin, with possibly extrusive or intrusive igneous protoliths indistinguishable from immature sedimentary protoliths. This applies particularly in the east, where in the Yabboo and Pinjin domains, felsic rocks are commonly so strongly foliated, recrystallized, and weathered that most occurrences can only be recorded as felsic schists (*Afs*). Swager (1995b) recognized finely layered rocks of possibly tuffaceous origin, as well as foliated 'fragmental' rocks inferred to represent volcanogenic conglomerates at some localities.

In a comprehensive study of these rocks, Morris (1998) identified two primary associations. In the western domains, where the felsic rocks were extruded subaqueously, brecciation and resedimentation led to a diverse suite of volcaniclastic rocks. The eastern domains contain a major belt of mainly subaerial lavas and tuffs.

Sedimentary rocks

Sedimentary rocks are most abundant in the upper parts of the greenstone sequences. In the Kalgoorlie greenstones, sedimentary rocks comprise units such as the Black Flag Group and the unconformably overlying Kurrawang Formation and Merougil beds, whereas in the eastern domains, no stratigraphic succession has been established.

Undivided sedimentary rocks (*As*) include shale, siltstone, chert, sandstone, pebbly sandstone, and conglomerate. These typically form in association with the felsic volcanic and sedimentary upper parts of the sequences, and may include a significant felsic volcaniclastic component — poor exposure and deep weathering commonly prevent protolith identification. Similarly, although sedimentary structures are typically obscured by deformation and weathering, graded bedding and cross-bedding are preserved at many localities.

Extensive areas on PINJIN and KURNALPI are underlain by grey slate or siltstone (*Ash*) grading into micaceous quartzofeldspathic schists (*Asf*) that range from fine to coarse in grain size. Although the foliation is commonly the only visible structure, in local areas good surface exposure allows recognition of graded bedding, scours, slumps, and parallel bedding. Interlayering with recognizable lithic wacke or volcaniclastic derived rocks indicates that these rocks probably originated as distal epiclastic deposits.

A metamorphosed association of lithic wackes (*Asw*) is present at several localities. In the Parker domain, graded units of this rock are interleaved with basaltic rocks. In the extensive outcrops to the east of this domain, this rock type and an associated BIF unit have been attributed to the Mount Belches Formation (Painter and Groenewald, in prep.). The best exposures of this formation, on the north shores of Lake Randall, have sedimentary characteristics so well preserved that deposition in relatively deep water as submarine fan, flysch facies, and turbidites was recognized by Dunbar and McCall (1971).

Graphitic black shale (*Ashg*), a widespread rock type on ROE, is very fine grained, moderately foliated to

massive, with some angular grains of quartz and feldspar set in the graphitic matrix.

Chert and siliceous slate (*Ac*) may extend over considerable distances as distinct marker beds, such as the Kapai Slate in the Kambalda domain. Ranging from less than a metre to several tens of metre in thickness, these rocks are locally associated with BIF, whereas in other areas appear to form a lateral facies equivalent (Williams, 1974). In the Norseman greenstones, where these rocks are most common, they form in association with metagreywackes, BIF, and felsic pyroclastic rocks (Doepel, 1973). Some chert within the sedimentary rock sequences may represent silicified shale or mudstone units. Fine-grained sedimentary units (*Ash*) found as interflow layers in mafic volcanic sequences are also silicified to cherty compositions at some localities.

Chert (*Ac*) and BIF (*Aci*) are common in some areas, and absent from others. West of the Ida fault on MULLINE, and in western parts of RIVERINA and DAVYHURST, the greenstones contain abundant chert and BIF, which led Swager et al. (1990) to attribute them to the Southern Cross Province. Banded iron-formation has not been recorded in outcrops of the Kalgoorlie greenstones east of the Ida Fault, but is present as the dominant clast-type in a conglomeratic unit of the Kurrawang Formation (see below). Banded iron-formation becomes progressively more abundant east of Bulong, where units extend several kilometres along strike in the Kurnalpi and Mulgabbie domains, and to the south in the Mount Belches Formation. In the Edjudina domain, BIF forms narrow topographic ridges that coincide with linear magnetic anomalies about 200 km in strike. In the Norseman greenstones, BIF is present as substantial units, up to 70 m thick, with a strike length up to 40 km.

Banded iron-formation is present as both oxide (*Aci*) and silicate (*Acis*) facies. The former is far more common and outcrops as finely layered, fine-grained, quartz–magnetite rock interleaved with chert or siliceous slate. The iron content of these rocks is highly variable, and they range in character from very thinly bedded to laminated, pale to dark-grey banded chert; to grey, pink, and red ferruginous banded chert; to highly magnetic, red and black, magnetite-bearing BIF. Bedding is commonly disrupted by kinks and minor folds. Pronounced folding is characteristic, including sheath and intrafolial folds with variable orientations, possibly reflecting components of early slumping, differential compaction, and regional deformation. The strong magnetic signature of these units provides very strong traces on aeromagnetic images. Silicate facies BIF is of limited extent, typically as a grunerite–quartz lithology, which suggests a metamorphic rather than primary origin for these rocks.

Oligomictic conglomerates (*Ascf*), which are in several of the greenstone sequences, are dominated by clasts of felsic volcanic rocks. For example, they are abundant on KANOWNA, although commonly as units too thin to be shown at map scale. The felsic volcanic clasts are commonly less than 20 cm in diameter, although a few boulders may exceed a metre in diameter. On PINJIN and ROE, conglomerates of this type may be traced along strike from clastic through volcaniclastic to volcanic rocks.

Coarse clastic sedimentary rocks outcrop sporadically for over 80 km along the western boundary of the Ora Banda domain, resting unconformably on older greenstones and occupying the core of the Kurrawang Syncline (the Kurrawang Formation, see below). The lower part of this formation (*Asckw*) consists largely of conglomerates and pebbly sandstone. It is about 750 m thick near White Lake in the south, but thins to the north. The poorly sorted, typically matrix-supported conglomerate contains well-rounded, commonly stretched clasts, typically 5–10 cm, but up to 25 cm in length. Clasts are most commonly felsic and intermediate rocks from the underlying sequence, but there are also clasts of BIF, chert, and quartzite and, less commonly, basalt, amphibolite, and ultramafic rock. The clasts were deformed prior to erosion and deposition. The medium- to coarse-grained matrix consists of poorly sorted, lithic sandstone. Banded iron-formation clasts are common only in a single extensive unit. This layer, about 30 m thick, has a problematic provenance as BIF is not known in the proximal lithostratigraphy, and the nearest outcrops of this rock type are those in the greenstone belts of the Southern Cross Province, about 40 km to the west. The upper part of the Kurrawang Formation (*Astkw*) consists of medium- to coarse-grained, locally pebbly, lithic sandstone. Cross-bedding and graded bedding are common, and there is a common upward-fining trend.

The polymictic Penny Dam and Yilgangi conglomerates (*Asc*) outcrop on the boundaries between the Gindalbie and Jubilee, and Mulgabbie and Kurnalpi domains respectively. These rocks are equivalent in nature to those of the lower Kurrawang Formation, although clasts range more widely in size and may attain a diameter of 40 cm. The compositional range of clasts includes granitoid, quartz–feldspar porphyry, gabbro, chert, and minor schistose metabasites. An immature fluvial origin is suggested by the poorly sorted, poorly bedded, clast- to matrix-supported nature of these conglomerates, although wedge-shaped, faceted clasts in the Penny Dam conglomerate suggest a possible glacigenic origin (Swager, 1993).

Immature sedimentary rocks (*Asm*), the Merougil beds, also outcrop in southwest LAKE LEFROY. These are mainly trough cross-bedded, pebbly sandstones, but include high proportions of conglomerate and siltstone. The beds are up to 2300 m thick, have a polymictic clast assemblage, rest on a sheared disconformity, and are probably of fluvial origin.

Quartz–feldspar porphyry

Porphyritic felsic units, considered to be mainly intrusive, are present at many localities in the greenstone belts. Commonly in the range of 1 to 5 m, rarely exceeding 10 m, in width or thickness, the dykes or sills are variably deformed and commonly strongly foliated along contacts. Evidence of an intrusive origin is provided locally where dykes appear to post-date at least some of the earliest deformation, or are discordant relative to known stratigraphy. Some porphyry units that clearly pre-date the regional deformation are typically concordant with structural trends and may represent original felsic volcanic

layers, or high-level intrusions associated with nearby granitoid rocks. Those that are discordant to early structural features, but have undergone all subsequent deformation, may be useful chronological markers.

Several varieties of felsic porphyry are recognized; quartz–feldspar(–biotite) porphyry (*Afp*) is the most abundant and typically contains 5–10% phenocrysts (commonly less than 2 mm but up to 5 mm across) of quartz and feldspar (dominantly plagioclase), with up to about 5% biotite in a microcrystalline groundmass. Leucocratic plagioclase porphyry is locally abundant, particularly in some areas in the Ora Banda, Gindalbie, and Kurnalpi domains where numerous dykes, typically 1–2 m in width, are spaced 20–50 m apart. The dykes may appear conformable, but are locally transgressive. Similarly, along the western limit of DAVYHURST and RIVERINA, there are numerous thin units (typically less than 2 m thick) of feldspar and quartz–feldspar porphyry with phenocrysts (up to 5 mm but typically less than 2 mm in length) of quartz and sodic plagioclase set in a fine-grained quartzofeldspathic matrix, with subordinate sericite and fine biotite. The units lie within a moderately to strongly deformed tholeiitic basalt sequence that has been metamorphosed at upper greenschist to lower amphibolite facies.

Other varieties of porphyritic dykes are less abundant. A felsic to intermediate hornblende–plagioclase porphyry (*Afih*) contains abundant phenocrysts up to about 2.5 mm in length of both phases in approximately equal amounts, in a microcrystalline groundmass. Dykes of albite-rich, quartz-poor porphyry (*Afpa*) may be a product of sodium metasomatism of the closely associated hornblende–plagioclase porphyry (Witt, 1992). An unusual biotite–quartz–feldspar porphyry (*Afpx*) with abundant greenstone xenoliths lies within the ultramafic sequence in the Ora Banda domain. Two hornblende lamprophyre dykes (*lp*), consisting of abundant amphibole prisms set in a fine-grained quartzofeldspathic matrix, of limited extent are present at Jubilee (AMG 236078) on KURNALPI and near Blow Fly (AMG 711178) on MENZIES.

Mafic to ultramafic intrusions

Medium- to coarse-grained intrusive mafic rocks, with relict cumulate, xenomorphic, subophitic, or ophitic textures, are found throughout the greenstone sequences, most commonly within the mafic rocks. Typical intrusions recognizably pre-date most or all of the deformation history. Where lithostratigraphic relations are recognizable, the units are commonly conformable, but may also be locally transgressive. In many cases, a close compositional similarity to associated basalts suggests a syngenetic origin, either as subvolcanic intrusions or coarser grained portions of thick, ponded flows. These rocks are mainly shown as gabbro (*Aog*) on the maps because the detail of fractionated compositions is either too fine for the map scale or largely obscured by poor outcrop, even though many of the intrusions show clear igneous differentiation trends, which provide younging directions. Of the numerous gabbroic intrusions too small or too poorly exposed to provide 1:100 000-scale map detail for the database, the best known is the Golden Mile Dolerite, a differentiated (micro-) gabbroic sill (Keats, 1987; Clout et al., 1990), which is the main host to gold mineralization at Kalgoorlie–Boulder. A number of large, layered intrusions have been identified within the study area. These typically conformable or semiconformable intrusions have been mapped in detail where possible and subdivided appropriately. In this dataset, the major layered intrusions are identified by a primary code (*Aa*), followed by the initial letters of the intrusion name with suffix letters for subunit compositions.

Dolerite and gabbro (*Aod*, *Aog*) are present throughout the basalt successions and also formed in other parts of the lithostratigraphy, albeit less commonly. They are commonly relatively massive and penetrative foliation is uncommon. The dolerite sills and dykes are narrow, fine grained, and lack clearly differentiated units. Petrographically, these rocks typically consist of fine-grained plagioclase and amphibole (actinolite or hornblende), with chlorite and epidote as common subordinate minerals. Primary subophitic textures are replicated by the metamorphic minerals. Feldspar-phyric dolerite (*Aodp*) has plagioclase phenocrysts set in the typical groundmass. Gabbro is coarser grained, commonly forms sills 50–100 m thick with more or less developed differentiation layering, and varies from pyroxenitic gabbro at the base, to granophyric gabbro at the top. Noritic and gabbronoritic (*Aon*) and pyroxenitic (*Aox*) rocks are also present. Deformation is commonly most intense along contact zones.

The layered mafic intrusions are best exposed and documented in the Ora Banda domain (BARDOC, DAVYHURST) where at least four are distributed around the major Goongarrie – Mount Pleasant granitoid-cored anticlinal arch. The Mount Ellis Intrusion (*AaME*), the lowermost of these, outcrops in the hinge zone of the anticline. Witt (1994, 1995) and Witt et al. (1991) recognized that the four units in this intrusion comprise a basal olivine gabbro–gabbronorite, followed by porphyritic leucogabbro, in which clinopyroxene phenocrysts are variably abundant, a granophyric quartz gabbro, and an uppermost porphyritic dolerite.

Adjacent to, and stratigraphically above, the Mount Ellis Intrusion is the Mount Pleasant Intrusion (*AaMP*), a layered, approximately 550 m-thick mafic–ultramafic sill that forms prominent outcrops over a strike length of more than 70 km around the Goongarrie – Mount Pleasant anticline. Witt (1994) and Witt et al. (1991) found that this sill comprises a melanocratic microgabbro at the base, overlain by an ultramafic layer that includes zones of olivine orthocumulate and pyroxenite, a gabbronorite layer with three zones differing in mineral ratios, a gabbro layer, an ilmenite-rich quartz ferrogabbro with granophyric quartz–albite intergrowths, and another gabbro layer at the top.

Further up in the succession is the Ora Banda Intrusion (*AaOB*), a large, layered mafic and ultramafic sill that intrudes the Black Flag Group (see **Lithostratigraphy and tectonic domains**) and extends southeast in outcrop from southwest of Mount Carnage (DAVYHURST AMG 028395) to Grants Patch (BARDOC AMG 185300). Witt

(1994) identified six zones in this sill, which, from the base up, include: peridotite, orthopyroxene (bronzite) adcumulate, norite, gabbronorite with small, irregular patches of anorthosite, gabbro, and granophyre.

The Orinda Intrusion (*AaOR*), the structurally uppermost sill in this area, is adjacent to the Ora Banda Intrusion. Once more, differentiation has led to compositional layering with a lower unit of gabbronorite and quartz gabbro in the upper portion.

The Powder Sill (*AaPW)* intrudes the predominantly felsic volcanic and sedimentary sequence near the eastern margin of the Coolgardie domain. The sill occupies a southeasterly plunging synform, with the best differentiated and thickest part (possibly 1000 m) of the intrusion in the closure. A lower gabbro and gabbronorite unit underlies an upper portion of leucocratic quartz gabbro with irregular patches of granophyre (Hunter, 1993).

The Three Mile Sill (*AaTM*) intrudes the basalt sequence north and northeast of Coolgardie. Wyche (1998) reported that a section shows distinct igneous layering from pyroxenite at the base, up through gabbro, to porphyritic leucogabbro (locally glomeroporphyritic) with coarse clinopyroxene phenocrysts, in turn overlain by gabbro, then quartz gabbro, capped by a thin unit of more mafic gabbro.

The Mount Thirsty (*AaMT*) and Mission (*AaMI*) Sills, located west to northwest of Norseman, intrude the mafic–ultramafic sequence along a strike length of some 20 km, and amount to about 1500 m of the total greenstone sequence (making up a considerable proportion of the outcrop). These sills comprise lower cumulate-textured pyroxenite, locally underlain by serpentinized peridotite, and overlain by upper units of norite and gabbro.

Several other intrusions have been named and described in the Explanatory Notes, but have not been examined in detail and subdivisions are not shown on the published maps.

Granitoid rocks

Granitoid rocks comprise 50% of the Eastern Goldfields part of the Yilgarn Craton. Although mainly biotite (–hornblende) granodiorite and monzogranite, minor two-mica(–garnet) syenogranite, tonalite, trondhjemite, and syenite intrusions are also recognized. A total of 42 granitoid plutons and 4 complexes have been named (Appendix 1).

Three different styles of intrusion are recognized:

- several plutons of limited extent are entirely surrounded by greenstones, the so-called internal granites of Sofoulis (1966), Bettenay (1988), Hill et al. (1989b), and numerous others;
- extensive composite batholiths that build the domes separating the greenstone belts; and
- small post-tectonic plutons.

This classification does not necessarily match the subdivision of the granites into pre-, syn-, and post-kinematic suggested in several publications, as recognition of the age of emplacement relative to deformation stages has proved difficult to apply. Witt and Swager (1989b) attempted to separate granitoids into pre- to syn-D_2, post- to syn-D_3, and post-tectonic classes. However, the poor quality of outcrop precludes detailed examination of structures in many granitoids. For the purposes of their geochemical study, Witt and Davy (1997) recognized two main groups: pre-regional folding granitoid (pre-RFG) complexes that commonly form composite cores to F_2 anticlines; and circular to ovoid post-RFG plutons. Noting the considerable overlap in geochemical characteristics of granites with very different structural characteristics, Champion and Sheraton (1993, 1997) argued that the complexity of deformation over a protracted period of granite generation renders subdivision using field characteristics equivocal. On-going SHRIMP isotope studies of the granites will help to resolve the classification difficulties. Available geochronological data indicate pre-regional folding magmatism occurred at 2690–2675 Ma, whereas the bulk of the syn- to post-D_2 plutons were emplaced at 2665–2660 Ma. Late plugs and dykes of alkaline granitoids yield emplacement ages ranging from 2630 to 2650 Ma, post-dating the regional deformation (Hill et al., 1992; Nelson, 1997b).

A description of some regional petrographic variations in the granitoids is given in Libby (1978). Details of the petrography and field relations of individual granites, commonly distinctive in terms of mineralogy and texture, are provided in the Explanatory Notes for the map sheets. Although the most extensive granitoids are predominantly monzogranitic, there are variations in the mafic mineral content — biotite is present in many, hornblende in several, clinopyroxene in a few. There are large phenocrysts of K-feldspar in several monzogranites (Bali, Bulyairdie, Cowarna, Galvalley, Menangina, and Widgiemooltha Monzogranites) and not in others. Foliation is most commonly pronounced near the margins, but may not be readily seen in central parts of the plutons.

Geochemical characteristics are typical of I-type granites for all but the youngest intrusions, which are A-type. There is evidence that the chemistry reflects variations in the basement, both in space and age. Wyborn (1993) showed that many granites have trace element patterns that require garnet in their source rocks, whereas others have characteristics indicating stable plagioclase. Champion and Sheraton (1997) found that progressive changes in Nd isotope ratios of the granites reflect variations in the age of their source.

Witt and Davy (1997) recognized a predominance of calc-alkaline granites on geochemical grounds. They suggested hydrous melting of tonalite, granodiorite, and monzogranite in a layered, lower crust to generate the earliest granitoids. The volumetrically predominant later granites were probably derived by hydrous melting of a more-uniform granodioritic to monzogranitic mid-crustal source. Witt and Davy (1997) also invoked fractional crystallization of biotite, feldspars and, in the more mafic magmas, hornblende as the cause of some compositional

variations. There are some rare metal-enriched pegmatites that probably represent incompatible element enrichment of the final magmatic phase in the granitoids, but the general characteristics do not favour the formation of genetically related metalliferous deposits. The most likely orthomagmatic deposits (apart from pegmatites) are small Mo, W, and base metal (Cu, Pb, Zn) concentrations associated with fractionated post-RFG plutons. The predominantly I-type compositions of the Eastern Goldfields granitoids probably reflect an absence of large sedimentary accumulations in the middle to lower crust.

Although a distinction between granitoids of different inferred structural age is shown in the solid geology layer of the database, this subdivision has not been applied in defining the granitoids on the outcrop maps.

Metamorphic rocks

As noted above, although all Archaean rocks in the area have undergone at least low-grade metamorphism, protoliths are commonly recognized, and so the terminology used is based on primary composition. However, there are several areas in which the protolith is not readily inferred, although compositional characteristics and associations may suggest a general primary rock type.

Schists containing aluminous silicates are pelitic in character, but whether derived from truly argillaceous or immature sedimentary precursors is unclear. This is particularly evident where rocks containing andalusite (*Ald*), locally with chloritoid and biotite (*Alld*), are found in close association with fragmental volcanic rocks; for example, on EDJUDINA. It is possible that very early weathering or hydrothermal alteration led to kaolinitic profiles in the vicinity of some of the vents, thus producing aluminous protoliths with no sedimentary history.

Among the mafic rocks, most are readily recognized as being of igneous origin, but immature mafic clastic sediments may be unrecognizable when metamorphosed and foliated. So, although very limited in extent, some mafic schists or amphibolites (*Ala*) have been shown as metamorphic rocks of unknown protolith. Schists of intermediate composition are even more uncertain in this respect, given the more common occurrence of fragmental rocks of volcanic and volcaniclastic origin, and the way in which metamorphosed wackes and greywackes commonly preserve primary compositional characteristics.

A zone in which lithologies of diverse composition are strongly interleaved falls on the boundary between the Boorara, Ora Banda, and Kambalda domains. This melange of mafic, ultramafic, and felsic schists (*Albuf*) was named the 'Bardoc Tectonic Zone' (Witt, 1994).

Gneissic lithologies are restricted to areas where metamorphic grades attained upper amphibolite facies. Mafic to intermediate rocks, ranging from schist to gneiss in character (*Anbai*), have been mapped on GINDALBIE where they occupy an area of at most 50 km^2 in the northeastern corner of the map, completely surrounded by granitoids.

Granitoid gneisses (*Ang*) are present at the northwestern, northeastern, and southwestern edges of the study area. In the northeast, the Kirgella and Barret Well banded gneisses are quartzofeldspathic rocks ranging from monzogranite to tonalite in composition (*Ang*). Banding is mainly the result of varying biotite concentration, although there are also thin aplitic and pegmatitic veins. Deformation of the banding into upright, tight folds indicates a pre-D_2 origin. A U–Pb SHRIMP zircon age of 2675 ± 2 Ma obtained for the gneiss at Barret Well suggests that these are a higher grade equivalent of the monzogranites (Swager and Nelson, 1997). Deeply weathered gneissic granites are present in the northwestern part of the Ora Banda domain.

In the southwest, the Fifty Mile Tank Gneiss (*Anfi*) is a major feature of the Pioneer Dome, making up an area 18 km long and up to 2.5 km wide east of the Pioneer Granitoid Complex. The gneiss is banded at hand specimen and outcrop scales — gneissic banding comprises millimetre-scale variations in biotite content, whereas the macroscopic banding is defined by variation in the abundance of pegmatite in broad (100–300 m wide) bands. Strong foliation is present, parallel to the gneissic banding. There are porphyroclastic fabrics or augen structures locally, particularly where pegmatites have been sheared. The structural discordance of the gneissic banding relative to the greenstones led Griffin (1990a) to discount the possibility that these gneisses may be basement to the greenstones, on the grounds that their emplacement post-dated at least some deformation in the greenstones. This was partly supported by Nelson (1995), who provided a zircon U–Pb SHRIMP age of 2664 ± 5 Ma, but was unable to determine whether this age represented primary crystallization or metamorphic resetting of the high-U zircons.

Structure

General deformational history

The Explanatory Notes for the published maps provide considerable local detail of structures recognized in the field or interpreted from lithostratigraphic and geophysical constraints. In general, the area has a pronounced north-northwesterly structural trend. This is defined by the elongate granitoid bodies that form structural ridges between the greenstones, the general strike of the greenstones, and the regional north-northwesterly trending strike-slip faults. The regional-scale strike-slip faults appear to form an anastomosing network, leading to the apparent lensoid domainal subdivision (Fig. 4). Within the domains, a variety of folds and faults are present, but are only defined accurately locally and precise correlation is impossible because of the poor quality and discontinuous nature of outcrop.

The regional deformation history has been the subject of several interpretations, a summary and integration of

which was written by Swager (1997). Broadly, the recognized deformation involved early D_1 recumbent folding and thrusting, followed by east–west shortening through large-scale, upright D_2 folding, then a period of north-northwesterly trending, mainly sinistral, strike-slip D_3 faulting with associated folding, followed by regional D_4 transpressive north-northeasterly oblique and reverse faulting (Table 3). Early, intermediate, and late periods of extension have been proposed by some authors. The deformation sequences established in different areas are not entirely consistent, probably a consequence of the difficulty of unravelling late structures to elucidate early history in a region of typically poor exposure. An examination of the database will reveal that there are many more measured orientations of foliation than bedding on the maps, a reflection of the general obscurity of bedding in poor outcrop of greenschists on a landscape of low relief, where penetrative foliation has developed during the course of tectonothermal evolution. Furthermore, field examination of areas in which all foliation is shown as vertical in orientation has found that these areas are typically two-dimensional subcrop, where strike is readily measured, but not the dip. Similarly, the lack of topography prevents ascertaining mesoscale bed orientation through the use of three-dimensional geometric constructions. The common assumption that bedding and foliation are commonly coplanar is equivocal in many areas and, therefore, interpretative cross sections created for such areas are largely speculative.

The earliest deformation may have been extensional, but has been very difficult to elucidate. Hammond and Nisbet (1992) proposed that early extension pre-dated D_1 and may represent the last stages of development of the basin in which the greenstones accumulated. They invoked low-angle extensional tectonic slides along the greenstone–granite contacts, in response to an extensional (?rifting) setting, and argued that compressional thrust faulting commonly emplaces basement over cover, a relationship not encountered in the Eastern Goldfields Province. Underplating on the base of sialic crust attenuated through extension may also have generated a significant proportion of the late-stage felsic volcanism, as well as the subsequent widespread granitoids. Similarly, detailed work in the area immediately north of the database coverage led Passchier (1994) to suggest that the D_1 recumbent folds may have formed in an extensional setting. The gneissic characteristics of some early granites, those synchronous in age to volcanic rocks in the greenstones, provide a record of deformation suggesting emplacement at the base of the greenstones in an active tectonic setting. In contrast, a careful study of the age relationships led Swager and Nelson (1997) to argue that high-grade granitic gneisses were emplaced through extensional processes at the base of the low-grade greenstones after the early thrusting and before the second shortening event (Williams and Whitaker, 1993).

The D_1 deformation event, noted in all major domains except Ora Banda, resulted in large-scale stratigraphic repetition. Swager and Griffin (1990b) described a regional-scale thrust duplex structure that extends from Kambalda to Kalgoorlie, duplicating the stratigraphy within the Kambalda domain. The thrusting was regarded as evidence that the earliest deformation was caused by horizontal compression rather than gravity-driven vertical tectonics. In the Boorara domain, at least two stacked, recumbent anticlines were recognized in low-strain areas, although this sequence becomes strongly attenuated northward and D_1 structures are difficult to recognize. Other recognizable D_1 structures include sheared-through recumbent F_1 folds, rotated during D_2 into vertical attitudes (e.g. Kalgoorlie–Boulder mining area), and small-scale thrusts in sedimentary rocks between lava flows.

Stratigraphic repetition on a regional scale was inferred for the Coolgardie domain from a double mafic to ultramafic succession, which can be traced from south of Widgiemooltha to Dunnsville in the north (Martyn, 1987; Swager, 1989a). Although this sequence could be interpreted as an original stratigraphic feature, intense shearing in the lower, thinner komatiite unit probably represents a thrust fault on which the basalt–komatiite unit was repeated. The overlying felsic volcanic sedimentary succession was not affected by this large-scale repetition because the proposed major thrust fault does not ramp to a suitable stratigraphic level.

Regional-scale D_1 thrust slices were inferred in the area between Coolgardie and Widgiemooltha (?Higginsville) where narrow, highly deformed and attenuated mafic–ultramafic rock packages wedge out along strike and appear to be stacked and subsequently folded into steep attitudes. On a more local scale, rootless intrafolial folds and repetitions of gabbro sills are also interpreted as D_1 structures. Early recumbent folds have been observed within the sedimentary pile and are clearly refolded by upright F_2 folds (Archibald et al., 1978, 1981; Archibald, 1987; Griffin, 1988a; Griffin and Hickman, 1988a,b). Two stages of subhorizontal deformation, distinguished by Archibald and co-workers on the basis of large-scale stratigraphic repetition and recumbent folds, may represent different scales (or geometries) of D_1 structures.

Subsequent D_2 folding and D_3 transform faulting have affected all domains. Regional north-northwesterly trending, upright F_2 folds can be traced over long distances and have gently plunging to horizontal fold axes, as shown, for example, by well-preserved, granitoid-cored anticlines such as the Goongarrie – Mount Pleasant and Scotia–Kanowna anticlines (Witt, 1987, 1994). The subvertical regional foliation is interpreted in most cases as a composite $S_1 + S_2$ fabric, particularly outside the main shear zones. Initial foliation development occurred during D_2 folding and intensified during continued regional shortening D_3.

The Boulder–Lefroy Fault and Kunanalling Shear in the Kambalda and Coolgardie domains respectively are well-defined D_3 transform fault zones. These structures vary in width from 100 m to 1 km and comprise anastomosing zones of intensely foliated rock that surround pods of less-deformed rock. They are associated with F_3 en echelon folds, which indicate sinistral displacement. Stratigraphic correlations across these faults suggest displacements of approximately 12 km (Langsford, 1989; Swager, 1989b). The F_3 en echelon folds may show very steep plunges because they formed in already steeply tilted sequences.

Table 3. Summary of proposed regional deformation events in the Eastern Goldfields Province, with constraints provided by magmatic crystallization dates based on mineral geochronology

Event		*Structures*	*Locality or example*	*Timing constraint*
?D_e		Low angle shear on granite–greenstone contacts; N–S movement; synvolcanic granites[a]; polydirectional extension, local recumbent folding[b]	Lawlers; Mount Malcolm (central Eastern Goldfields)	Felsic ash interbedded in komatiites c. 2705 Ma[n]; early granites c. 2680 Ma
D_1	D_{1c}	Low-angle thrust faults and recumbent folds;[c,d,j] ?shear on early granitoid–greenstones contacts; late synvolcanic slides caused by uplift? [a,b]	Between Kalgoorlie and Democrat (south of Kambalda)	Felsic volcanic rocks 2681 ± 5 Ma, 2675 ± 3 Ma [n] maximum age constraint; 2674 ± 6 Ma post-D_1 felsic porphyry dyke[q]
	D_{1e}	Deformed contacts between early granitoid complexes and greenstones; N–S lineations in contact zone; recumbent folds in overlying greenstones[e]	Jeedamya–Kookynie area	
D_e		Roll-over anticlines and E–W extension leading to clastic infill of synclinal basins[f,g]	Kurrawang, Penny Dam, Merougil conglomerates	Post-D_1 and pre-D_2 felsic porphyry; 2674 ± 6 Ma[q]
D_2		Upright folds with shallowly plunging, NNW fold axes[c,e,h]	Kambalda Anticline, Goongarrie – Mount Pleasant anticline, Kurrawang syncline	Minimum: 2660 ± 3 Ma[n] (post-D_2 monzogranite)
D_e		Local extension in final uplift of granite domes[i]	Barret Well (Yabboo)	Maximum: 2675 ± 2 Ma[i] (post-D_1 monzogranite)
D_3		Tightening of F_2 folds[k,l]; NW to NNW sinistral strike-slip faults and shear zones; N to NNE dextral strike-slip faults and shear zones	Boorara–Menzies Fault;[e,k] Boulder–Lefroy Fault;[l,c] Butchers Flat Fault[e]	Minimum: 2658 ± 13 Ma (Brady Well Monzogranite); 2640 ± 8 Ma (Clark Well Monzogranite)
		Transpression on NNW faults, with compressional jogs and fold axes trending N to NNE[m]	Laverton, Yandal (central and northeast Eastern Goldfields)	
Late D_3		Steeply plunging lineations on strike-slip faults Steeply dipping reverse faults	Goongarrie, Bardoc Tectonic Zone;[e] Melita, Niagara[e]	
D_e		Post-metamorphic orogenic collapse[r]	Ida Fault	Late-tectonic granite c. 2640 Ma
D_4		NW to WNW oblique sinistral[e] faults; NE to ENE oblique dextral/reverse faults [e,j]	Paddington area; Mount Charlotte (Kalgoorlie); Black Flag Fault (Mount Pleasant)	2638 ± 26 Ma[o]; 2651 ± 5 Ma[p] alkaline granites, post-tectonic

SOURCE:
(a) Hammond and Nisbet (1992)
(b) Passchier (1994)
(c) Swager and Griffin (1990b)
(d) Gresham and Loftus-Hills (1981)
(e) Witt (1994)
(f) Williams (1993)
(g) Swager (1997)
(h) Hunter (1993)
(i) Swager and Nelson (1997)
(j) Archibald et al. (1981)
(k) Swager et al. (1995)
(l) Swager (1989b)
(m) Chen et al. (in press)
(n) Nelson (1997a)
(o) Hill et al. (1992)
(p) Nelson (1995)
(q) Kent and McDougall (1995)
(r) Goleby et al. (1993)

Syntectonic granitoid intrusions are associated with 'accommodation' folds and faults, which are of local extent only, have various orientations, and commonly post-date the regional F_2 folds (e.g. around Coolgardie).

Continued regional shortening (D_3) is particularly evident in the major mining centres. At Kalgoorlie, Swager (1989b) described late-stage foliations (developed in sericite–carbonate–quartz schist of the gold lode system) and sets of reverse strike faults compatible with continued shortening after D_3 sinistral shearing. Prominent, oblique faults, which crosscut and offset these late-stage structures, have been described as a separate D_4 event (Mueller et al., 1988), but could be attributed to a small rotation in the main shortening direction. At gold-mining localities near

Kambalda, there is evidence for late-stage reverse faulting and steep movements on the Boulder–Lefroy Fault (Clark et al., 1986).

Late extensional faulting, recognized only in the crustal-scale Mount Ida fault through seismic reflection and the change in metamorphic grade across the fault, represents about 5 km of vertical displacement. The age constraint provided by crosscutting granitoids (see Table 3) places this event before 2640 ± 8 Ma, but after peak metamorphism at around 2650 Ma (Goleby et al., 1993; Swager et al., 1997). The orientation of this fault parallel to the D_2 compressional structures suggests some relationship with main orogenic activity, possibly as a post-orogenic collapse feature.

Validity of interpreted structural boundaries

Wide zones of intense foliation, with associated widespread carbonate alteration, are recognized in outcrop, but direct evidence of the kinematics is found at few localities and commonly only late stages of displacement can be identified. Aeromagnetic data reveal disruption of the greenstone successions in the form of truncations of numerous, parallel magnetic lineaments that probably reflect lithostratigraphy. Apparent drag structures on the lineaments close to the truncation may indicate the sense of displacement. In some cases, the positions of major faults are further constrained by adjacent, discontinuous en echelon folds evident on the magnetic maps. These features have been interpreted as boundary faults that subdivide the greenstones into domains or terranes, albeit that displacements are unknown and their continuity poorly constrained. Some boundaries are better defined than others; for example, the Ida Fault. This boundary between the Kalgoorlie greenstones and Southern Cross Province is delineated by pronounced aeromagnetic 'highs' corresponding to variably sheared ultramafic rocks, which outcrop locally. Interpretation as a terrane boundary is equivocal in that early displacement on this structure is unknown, and late displacement was extensional.

The Zuleika Shear separates the Coolgardie domain from the Ora Banda domain in the north and the Kambalda domain in the south (Fig. 4), and forms the northeastern boundary of the Norseman domain. The shear can be traced from northwest RIVERINA for at least 250 km to the south-southeast. The shear zone is defined by a complex zone of attenuation and stratigraphic mismatch in places over 1 km wide. No unequivocal marker units have been recognized across it. Evidence for both horizontal and vertical movements can be found at specific localities, but these are late-stage and possibly reflect only minor displacements. Earlier movements (i.e. pre-D_2) are suggested by the different D_2 geometries across the shear. The Zuleika Shear may thus have acted as a major D_2 tear fault that brought greenstones, in which there is evidence of thrust fault repetition of stratigraphy (Coolgardie domain), into juxtaposition with a sequence without any apparent repetition (Ora Banda domain).

Two major elongate areas, delineated by outcrops of coarse clastic sedimentary rocks (the Kurrawang Formation and Merougil Conglomerate) east of the Zuleika Shear, were possibly synclinal basins formed during D_2 folding. Movements along precursors to the Zuleika Shear and Lefroy Fault may have played an important, but as yet little understood, role in the development of these basins. Conglomerates in the Kurrawang Formation contain internally folded BIF pebbles, which were possibly derived from the nearest BIF outcrop in the Barlee Terrane to the northwest.

The eastern boundary of the Ora Banda domain is along the Menzies Shear in the far north of the map area, followed southwards by the Bardoc Tectonic Zone. This branches southwards to become the Abattoir and Boorara Shears, forming the boundaries between the Boorara, Kambalda, and Ora Banda domains. The Boorara Shear continues south, as the Woolibar Fault, north-northeast of Kambalda, and then becomes the Lefroy Fault. The Menzies–Bardoc–Boorara shear zone, locally up to 3 km wide, consists of many interleaved and attenuated slices of various greenstone lithologies, commonly very strongly foliated. Several late-stage (horizontal, oblique, and vertical) displacements have been recognized along this break by Swager and Witt (1990), Swager (1994b), and Witt (1994).

The Abattoir Shear, which separates the Kambalda domain from the Ora Banda domain, lies west of a narrow, sheared sequence of mafic and ultramafic rocks. These greenstones overlie, and are similar to, the sequence in the Kambalda domain, and may represent a further structural repetition thereof. Evidence for this fault in outcrop and geophysical coverage is limited.

In the northeastern part of the area, major fault zones are present partly along granite–greenstone boundaries (Emu and Claypan Faults) and largely within the greenstones (Yilgangi Fault, Pinjin Fault). Limited outcrop information is available for these faults, but on aeromagnetic survey maps, local truncations of anomalies representing stratigraphic units provide evidence of displacement. The lithostratigraphy east of the Emu Fault differs in that felsic volcanic and sedimentary rocks are more abundant than in the Kalgoorlie greenstones, some felsic volcanic rocks differ in petrogenetic characteristics, BIF is a common rock type, and komatiite is less common. However, high precision SHRIMP U–Pb zircon geochronology (Nelson, 1997a) has constrained the emplacement of these eastern greenstones to the same time period as the Kalgoorlie greenstones, as follows:

- dates of 2711 ± 5 Ma and 2699 ± 4 Ma bracket komatiite emplacement to the same interval as further west;
- dates of 2708 ± 6 Ma and 2713 ± 4 Ma on felsic rocks demonstrate that felsic volcanism was widespread, albeit only locally voluminous, at this early stage; and
- the ages obtained for dacitic rocks of 2673 ± 7 Ma at Yindi Woolshed (Mulgabbie domain), 2672 ± 12 Ma in the Bulong antiform (Gindalbie domain), and 2675 ± 3 Ma at Perkolilli (Boorara domain) indicate

that the upper felsic volcanic rocks were synchronous in both the eastern and western greenstone tracts.

Similarly, structural studies (Swager, 1995a,b; Chen, 1999) have shown that the eastern domains have undergone the same deformational history as those further west.

It has been argued that all major shear zones may be long-lived structures, initiated in an extensional regime during deposition and repeatedly reactivated by subsequent complex compressional and transform movements during the regional deformation (Hallberg, 1985; Chen et al., 1998). The total amount of displacement is impossible to determine, but the common similarity of greenstone lithostratigraphy and age on either side of many of the faults support correlation of the various lithologies across faults equivocally interpreted as terrane boundaries.

Seismic reflection profiling

Although many regional structures in the Eastern Goldfields appear to be very steep or vertical at surface, their vertical geometry is poorly understood from outcrop mapping because of the general low-relief landscape and poor exposure. The earliest seismic reflection work, comprising several short, low-resolution profiles, revealed that the regional faults have no effect on underlying mid-crustal reflectors and this implied a listric geometry for these structures (Mathur et al., 1977). Subsequently, in the first part of an ongoing seismic reflection project, a 213 km traverse recorded by AGSO in 1991 yielded important results (Drummond et al., 1993; Drummond and Goleby, 1993; Goleby et al., 1993; Williams, 1993). Although the details of this traverse are beyond the scope of this Report, a summary is provided of the interpretations, as synthesized by Swager et al. (1997). Despite the difficulty of imaging from the low-amplitude reflections provided by the metamorphic and igneous rocks, interpretation of the seismic data in conjunction with field geology, gravity, and aeromagnetic surveys yielded constraints on the geometry of the Eastern Goldfields. The most notable findings, as illustrated in Figure 7, are as follows:

- Crustal thickness, already known to be about 33 km (Drummond et al., 1993), increases eastwards across the boundary between the Southern Cross and Eastern Goldfields Provinces. This change from 33 to 38 km, which occurs along a 50 km gentle downwarp, is almost equivalent to the estimated total thickness of the upper crustal greenstone sequence in the Kalgoorlie greenstones.
- The Ida Fault, interpreted as the boundary between the provinces, is an inclined, late-stage extensional feature. This indicates that the Kalgoorlie greenstones once continued west of the fault and possibly overlaid the Southern Cross successions prior to uplift and erosion.
- The Eastern Goldfields greenstones extend only to a depth of 4–7 km, and internal reflectors are truncated at depth against an abrupt reflection surface, beneath which no greenstones can be imaged. This basal surface is most likely to represent a regional detachment or decollement.
- Several stages of large scale deformation are required to explain the geometry above the basal surface. These may include early subhorizontal movement (D_1 thrusting, ?early extension), east–west extension (post-D_1, pre-D_2), and east–west shortening (D_3 stacking and folding). Movements out of the east–west plane of this seismic line are recognized in both D_1 thrust faults and D_3 strike slip faults, a limitation on the initial seismic interpretation to be resolved through the three-dimensional series of traverses measured in September 1999.
- Concealed imbricate wedges resting upon the detachment have reflection characteristics of strongly foliated rocks, and are likely to be quartzofeldspathic on the basis of regional gravity data. They are likely to be either granitic gneisses or disrupted felsic volcanics not yet recognized in the greenstones.
- Several granites are imaged as seismically opaque bodies of thin, tabular form with steep sides and a flat base. Truncation of stratigraphic markers by these bodies reveals their clearly transgressive intrusive form.

It is notable that the vertical faults inferred from field mapping and aeromagnetic lineaments are difficult to see because there are few marked reflectors, resulting in typically low resolution data and thus poor resolution of stratigraphic truncations by steep structures. Faults that penetrate through the decollement, the Ida, Bullabulling, Bardoc, and Avoca Faults (Fig. 7), appear to be partly listric in form. The faults inferred from aeromagnetic and field observations, such as the Mount Monger and Emu Faults, but unresolved seismically, may also be listric or represent branching upwards from the detachment.

Metamorphism

Despite the common preservation of primary structural and textural characteristics, all Archaean rocks in the area covered were metamorphosed under conditions ranging from very low to medium grade. The greater proportion of the greenstones are greenschist to epidote amphibolite facies metamorphic rocks, with amphibolite facies rocks forming in parts along the western and eastern margins, and small areas of prehnite–pumpelleyite or lower greenschist facies restricted to the uppermost central parts of the greenstone belts. Metasomatic alteration has led to serpentinization, carbonation, and silicification in numerous areas, both as very early diagenetic effects and as part of the regional metamorphic evolution.

Regional metamorphism

A general interpretation of regional metamorphism in the Eastern Goldfields by Binns et al. (1976) documented an overall variation in grade and style throughout the area. Grades range from medium grade in peripheral areas, to low or very low grade in the core areas of the greenstones (Fig. 8), and style encompasses ‘static’ (massive) and ‘dynamic’ (foliated) end members. Large parts of the very

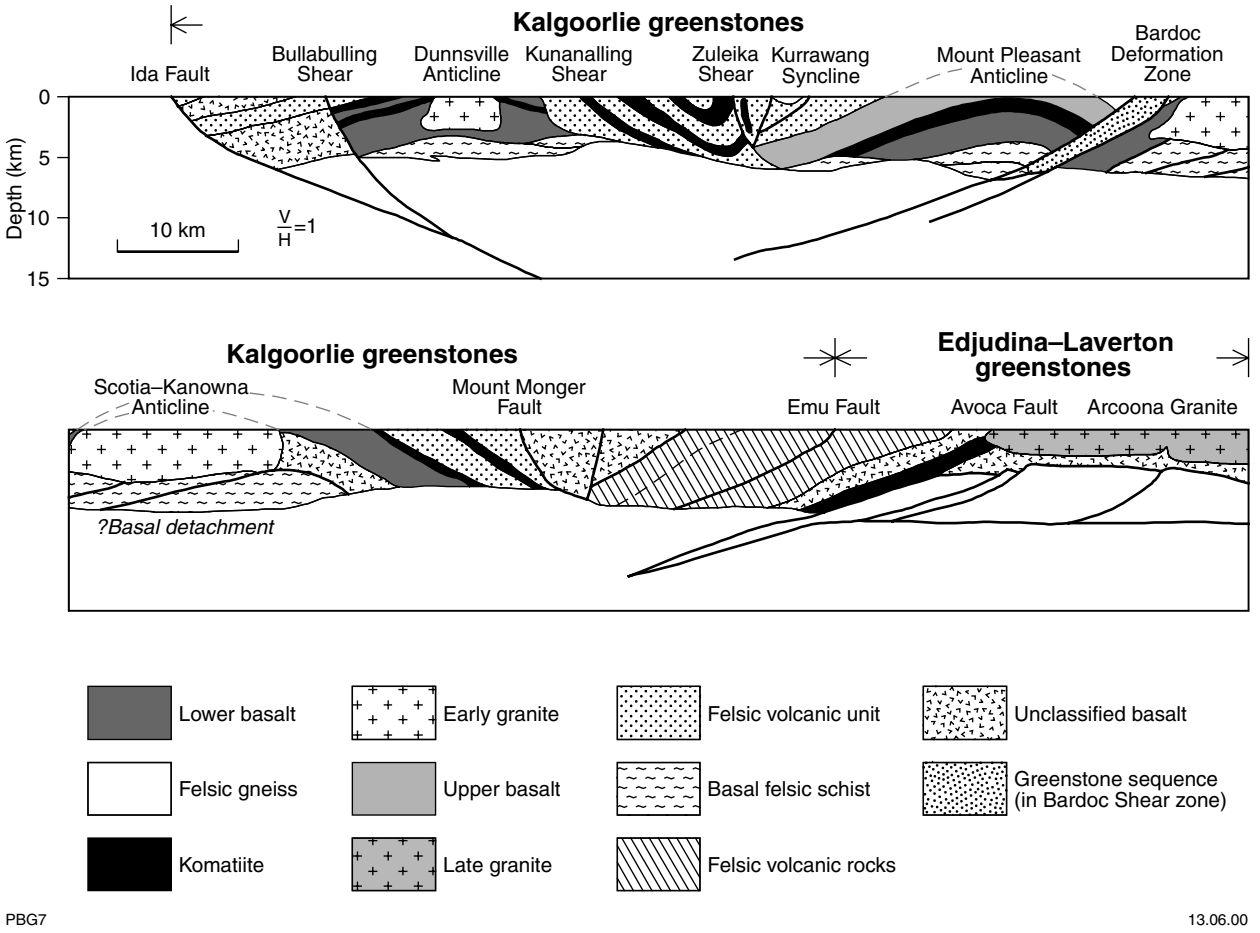

Figure 7. Cross section created through geological interpretation of seismic line EGF1 (from Swager et al., 1995)

low and low grade areas have little penetrative foliation and, although the mineralogy is commonly entirely metamorphic, there is excellent preservation of primary structural and textural features, such as pillows in basalts, spinifex textures in komatiitic rocks, volcaniclastic fragments, and sedimentary structures. Heterogeneous deformation is a feature in these areas, with narrow zones of penetrative foliation and shear separating broad expanses of weakly deformed rocks. In contrast, the higher grade areas are characterized by pervasive penetrative foliation, accompanied by general disruption of primary fabrics and, in some areas, total destruction of protolith features.

The metamorphism had at least three main stages of development: the earliest foliation, although not commonly distinct, is defined by metamorphic mineralogy; S_2 is locally far more pronounced and also comprises metamorphic mineralogy; and decussate sprays of amphibole and porphyroblasts of feldspar cut across both generations of foliation, revealing the likely occurrence of peak metamorphic temperatures subsequent to the deformation.

Binns et al. (1976, p. 307) noted that '. . . amphiboles in complexly folded metasediments . . . cut indiscriminately across axial surfaces . . .'. These authors recorded that, although the areas of higher grade metamorphism are adjacent to the granites that bound the greenstones, it is difficult to attribute the thermal variations entirely to heat conduction from the intrusions.

There is considerable evidence that regional metamorphism occurred at low pressure. In the highest grade rocks recognized, assemblages involving cordierite–staurolite–garnet, quartz–staurolite–andalusite, and quartz–cordierite–andalusite–biotite indicate that pressure did not exceed 5 kbar. Quantitative thermobarometry by various authors has been consistent with this, giving temperatures in the range of 500 to 650°C, with pressures of 2.5 to 5 kbar, as summarized by Swager et al. (1995), who also recorded arguments for a post-tectonic thermal peak. Binns et al. (1976) documented the coincidence of highest Bouguer gravity anomalies with lowest metamorphic grades in the central parts of the greenstone belts. They argued that this suggests a broadly synformal structure for the belts, with a relationship between historic depth and metamorphic grade being preserved. Swager (1997) also noted the interesting coincidence of lowest metamorphic grades with areas where the greatest thickness of underlying greenstones is proved by reflection seismic results. This may reflect maximum separation from the granitic heat sources rather than record the shallowest depth of burial.

As noted above, a large proportion of the granitoids, which altogether make up about 50% of the Eastern Goldfields, were emplaced between 2675 and 2660 Ma. The heat advection that would have accompanied this magmatism must have been considerable. The concentric arrangement of isograds around the granites suggests that the aureoles may coalesce to create the regionally extensive, amphibolite facies metamorphic effect (Bickle and Archibald, 1984; Ridley, 1993). Although Bickle and Archibald (1984) argued that the heat from the granites was inadequate to account for the high-grade metamorphism, in other low pressure metamorphic terrains it is recognized that the granites are themselves the product of an anomalous thermal effect at deeper levels in the crust (?underplating, ?delamination) and act as a particularly efficient transfer mechanism to advect a considerable amount of thermal energy to shallow levels (Lux et al., 1986; De Yoreo et al., 1989; Warren and Ellis, 1996).

The timing of metamorphism was diachronous in that early foliation (S_1) is defined by metamorphic minerals, but is crosscut by later metamorphic assemblages. Further support for this is the way in which porphyroblasts of biotite and andalusite post-dated the regional upright foliation that was generated synchronously with emplacement of the granitoids. Kent and McDougall (1995, 1996) argued that the earlier metamorphism predated an intrusion from which a SHRIMP zircon date of 2674 ± 6 Ma was obtained. In view of the fact that the Ida Fault brings areas of different metamorphic grade into juxtaposition, and hence post-dates metamorphism, a minimum age of 2640 ± 8 Ma for a granite intruded after the fault movement constrains the minimum age of peak metamorphism.

The relatively consistent metamorphic pattern, revealed by the lowest grades being central to the greenstone belts and higher grades occurring in marginal areas, and the broader variation in metamorphic grade with higher grades occurring in eastern and western parts of the Eastern Goldfields, is not the product of differential erosion of an irregular thermal topography (thermal ridges or domes and depressions). The regular distribution of isograds and commonly low pressure conditions suggests the establishment of a high geothermal gradient, not necessarily relative to depth but to distance from the margins of the greenstone belts, given that the peak metamorphic conditions post-dated the most intense deformation, which generated the large anticlinal ridges separating the belts. This implies that the greenstone successions may have cooled to a normal geothermal profile before the D_2 event. The highest grade metamorphism does affect the uppermost supercrustals locally; for example, in the eastern Gindalbie domain, high-grade assemblages in stratigraphically high-level metasedimentary rocks reflect the close proximity to the granite immediately east of this locality.

The regional extent and abundance of granitoid rocks for which ages are restricted to a short period, provides an indication of major mafic underplating and intracrustal reworking. Underplating and hence subcrustal mafic accretion has considerable implications for the genesis of the greenstones in general, as well as for the genesis of the gold deposits. As shown by De Yoreo et al. (1989), crustal anatexis and magma migration in the deep crust need not accompany particularly great temperature rises in the lower crust where the melting buffers temperatures in the range of 700 to 850°C. Migration of the melt to shallow levels and accompanying heat advection leads to a thermal profile in which gradients are very steep to depths of 10–15 km, and relatively flat at deeper levels.

Hydrothermal metamorphism

Metasomatic alteration is also a factor in the region. Very early hydrothermal metamorphism characteristic of a seafloor setting was recognized in the Kambalda domain from a shortened metamorphic profile, wherein a rapid increase in grade from greenschist to amphibolite facies is similar to that seen in Palaeozoic ophiolites (Barley and Groves, 1989). Local silicification, particularly in very fine grained rocks such as slate, is also likely to have occurred at an early stage and may pre-date much of the deformation, and was probably hydrothermal.

Widespread carbonation has been found both in low strain domains (e.g. around Kalgoorlie) and regional shear zones. The timing is apparently retrograde relative to the peak metamorphism in some lower grade areas (Clark et al., 1986), whereas a prograde environment has been recognized in at least some higher grade areas (Groves et al., 1988). These conflicting relative age interpretations are all based upon microstructural fabric and assemblage relations, and suggest either diachronous or prolonged carbonic fluid activity, both acceptable models in a thermally evolving metamorphic system. Witt et al. (1997) noted that textural evidence in a dynamic setting is difficult to constrain reliably, and the association of carbonation with D_3 structures suggests a close relationship with the regional metamorphic culmination.

Within shear zones, more than one stage of hydrothermal alteration is evident at some localities. For example, gold mineralization in the Menzies–Boorara shear zone is associated with subhorizontal quartz veins that clearly post-date the steep chlorite–carbonate shear fabric of the more widespread carbonation. Potassic minerals, such as biotite and sericite, and sulfides, such as pyrite, pyrrhotite, and arsenopyrite, commonly accompanied the dispersed to massive ankeritic carbonation and formation of quartz stockworks associated with gold mineralization. The hydrothermal alteration related to gold mineralization was variable, with assemblages differing with the composition and metamorphic grade of the host rocks. This was documented by Witt et al. (1997) who identified the systematic relationship of these alteration assemblages to regional metamorphic grade as evidence that the thermal gradients related to the orogenic environment were still in place at the time of mineralization. Within this setting, lateral thermal gradients related to granitoid emplacement probably induced lateral, up-temperature fluid flow of a metamorphic fluid phase, and thus provided the transport medium for the mineralization. The number of widespread and contemporaneous gold deposits suggests large-scale fluid circulation. Although

Figure 8. Regional distribution of metamorphic facies in the Menzies to Norseman part of the Eastern Goldfields, based on data from Binns et al. (1976), Swager et al. (1990, 1995), Witt (1993d), Swager (1995a), and Wyche (1998)

potassium metasomatism is a feature of all the deposits, sodium and calcium introduction was also involved in some of the high-grade gold deposits. Isotopic characteristics of the mineralization support a lateral fluid flow model, with a correlation between Pb isotopes in ore minerals and granites, and more radiogenic Pb and Sr in deposits near the margins of the greenstones than in those further from the granites.

Proterozoic geology

Mafic and ultramafic dykes

Undeformed dykes, mainly gabbroic, but ranging in composition from pyroxenite to gabbronorite to granophyre, intrude the Archaean granitoids and greenstones with general east to east-northeasterly and north-northwesterly trends. These were termed the Widgiemooltha dyke suite by Sofoulis (1966), described in some detail by Hallberg (1987), and their early Proterozoic age confirmed by Nemchin and Pidgeon (1998). Although locally exposed as prominent ridges, most dykes are covered by surficial deposits. A distinctive regolith unit comprising red-brown soils demarcates the extent of some of these dykes, but recognition of their widespread distribution, abundance, and extent has depended upon the availability of regional aeromagnetic surveys.

The Binneringie Dyke (*Pdyb**) is the largest of these intrusions and can be traced for 600 km across almost the entire Yilgarn Craton, from the Albany–Fraser Orogen in the east to the Boddington area in the west. It is best exposed along the northern shore of Lake Cowan as a chain of hills, and attains a maximum width of 3 km. Despite its size, only vertical layering has been recognized in this intrusion, unlike the Jimberlana Dyke (see below). A precise baddeleyite U–Pb age of 2418 ± 3 Ma was determined for this dyke using a sample collected near its western extremity (Nemchin and Pidgeon, 1998).

Another major Proterozoic intrusion, the Jimberlana Dyke (*Pdyn*), outcrops on NORSEMAN. Magnetic, gravity, and diamond drillcore data have revealed a structure in which compositional layering defines listric conical intrusions at several points along the 180 km length of this intrusion. These canoe-shaped complexes have a well-developed rhythmic differentiation pattern similar to the Great Dyke in Zimbabwe, as described by Campbell (1968, 1978) and McClay and Campbell (1976).

Several other dykes have been named in the south Eastern Goldfields. These are the Celebration (*Pdyc*), Randalls (*Pdyr*), Pinjin(*Pdyp*), Gidgi (*Pdyg*), Kalpini (*Pdyk*), and Ballona (*Pdyl*) Dykes. All trend approximately 075° and, together with the Binneringie and Jimberlana Dykes, have positive magnetic anomalies. In contrast, three prominent, negative magnetic anomalies that trend ~085° represent unexposed dykes between the Randalls and Binneringie intrusions. Less substantial magnetic anomalies parallel to these trends suggest that there are many more minor dykes in this swarm. The different palaeomagnetic characteristics may reflect different periods of magmatism (Williams, 1970).

Other post-tectonic dykes, which trend north-northwest, are possibly equivalent in age and origin to the more abundant easterly trending dykes. Outcrops of these intrusions are sparse, but the trends are strongly evident in detailed aeromagnetic surveys. One particular intrusion of this type, the Parkeston Dyke (*Pdyp*), has been drilled during exploration and found to be petrographically similar to the Widgiemooltha dykes (Bateman, R., 1999, pers. comm.). Other major linear, negative magnetic anomalies that trend 045° and 020–030° in central and eastern parts of the area may also represent mafic dykes.

Phanerozoic geology

Permian sedimentary rocks

Thin layers of undeformed, unmetamorphosed, matrix-supported conglomerate and coarse, poorly sorted sandstone (*Ps*), locally overlain by silcrete, are preserved as small mesas on EDJUDINA. The presence of striated, angular quartz pebbles supports an interpretation that these are glacigene deposits, equivalent to the Permian Wilkinson Range Beds that overlie the Officer Basin some distance to the east (Williams et al., 1976).

Tertiary — Eundynie Group

Upper Eocene Eundynie Group (*TE*) sedimentary rocks (Cockbain, 1968a,b) are found in the southern part of the study area within the Cowan and Lefroy palaeodrainage channels. These deposits reflect deposition in shallow-water settings and comprise fluviodeltaic channelled and cross-bedded sandstone, siltstone, and conglomerates, increasingly interspersed with spongolite and macrofossiliferous limestone to the south (Clarke, 1994). The only outcrops of this unit that fall within the area of the present database were described by Griffin (1989).

Regolith and surficial deposits

Cainozoic regolith covers the major proportion (~90%) of the area, with 17 types being distinguished. Detailed descriptions of the Cainozoic geology in the area were provided by Kriewaldt (1969, 1970), Williams (1970), Doepel (1973), and Griffin (1989). Available regolith maps are Chan (1991), which covers the entire area at a scale of 1:1 000 000, and Craig and Churchward (1995), a 1:250 000-scale map of the Menzies area. Kojan and Faulkner (1994) provided a regolith geochemistry map of the MENZIES 1:250 000 sheet.

Playa deposits, which fill the salt lakes and claypans (*Czl*), consist of interbedded argillites, arenites, and evaporite minerals (gypsum, halite), locally intermixed with sandplain deposits (*Czls*). These are commonly surrounded by dunes of sand, silt, and gypsum (*Czld*)

* *P* appears as P_ in the digital data.

derived from the lakes and sandplains. Many of these dunes are now stabilized by vegetation. Colluvium (*Czc*), a widely developed type of regolith, includes locally derived, coarse-grained proximal debris and distal, finer grained material as a matrix, which is locally ferruginous. Areas of distinctly proximal colluvium are indicated by composite codes; for example, areas where colluvium rests upon mafic volcanic rock (*Czc/Abv*). Quartzofeldspathic colluvium to eluvium (*Czcg*) derived by weathering and erosion of granitoid is commonly very proximal; scattered fragments of granitoid are commonly present. These deposits, where partially reworked, grade laterally into sheetwash and sandplains. Sheetwash (*Czw*) consists of reddish, ferruginous fine sand to clay in thick packages, the material having been transported and substantially reworked. Plains and dunes of eolian sand (*Czs*) cover extensive areas as sheets of variable thickness adjacent to salt-lake margins and on duricrust plateaus overlying granitoid. This fine-grained, clean quartz sand may contain layers of ferruginous nodules.

Ferricrete or ferruginous duricrust (*Czrf*), previously termed laterite on several of the published 1:100 000 maps, is widespread. Although interpreted as isolated, eroded remnants of an old, extensively lateritized peneplain by Jutson (1934), Davy and Gozzard (1995) found the occurrences to be distributed at a wide range of altitudes, either as residual or transported material, formed at different times in the last 50 million years. Breakaways or erosional scarps commonly bound the ferruginous duricrust outcrops and reveal highly weathered (bleached and mottled) rocks that can be identified by locally preserved textural features. These lateritization profiles are up to 100 m thick. The ferricrete is typically yellowish brown to dark brown, locally black, and commonly massive to nodular or pisolitic. Where duricrust has formed directly from the underlying bedrock, original structures and textures are commonly preserved, as represented by the use of composite codes (e.g. *Czrf/Ab*).

On several of the published maps, units shown as 'laterite' included ferricrete, reworked ferricrete (e.g. scree slopes), 'hardpan', and gravelly or pisolitic soils, together with nodular carbonate ('kankar') or calcrete, which although relatively common, is rarely extensive enough to warrant separation at 1:100 000 scale. On maps where these relict lithologies were grouped, the code (*Czr*) is applied in the database.

Silica caprock (*Czru*) is a subvitreous siliceous rock, typically light brown to off-white in colour, developed mainly over deeply weathered ultramafic rocks. This rock is locally very abundant over serpentinized peridotite, and olivine cumulate textures may be well preserved. Chrysoprase and jasperoidal chalcedony are present locally. Although commonly less than a metre thick, substantial units up to several metres thick occur locally.

Silcrete (*Czrz*) commonly forms a thin (0.5 m), discontinuous layer over granitic or other quartzo-feldspathic rocks. A widely distributed and locally abundant rock type, silcrete is a light-grey to white, subvitreous, siliceous rock, typically with angular, medium-grained quartz grains. Silcrete may directly overlie the original primary rock type or be separated from it by an intensely kaolinitized unit up to 2 m thick.

Quaternary alluvium (*Qa*) occupies present-day drainage channels and floodplains, and consists of unconsolidated clay, silt, sand, and pebbles. No sub-division of these deposits is made in the database.

Exploration and mining

The discovery of gold and subsequent development of a mining industry in the Menzies to Norseman region contributed much to the early economic growth of Western Australia. The gold rush began with the discovery of Bayleys Find at Coolgardie in 1892 and many more finds were made as prospectors concentrated in the region. In 1893, gold was found at Kalgoorlie and led to a field that yielded considerable quantities of gold and became recognized as one of the world's largest gold deposits. Until the mid-1960s, when exploitation of iron ore resources of the Hamersley region began, the contribution from the Golden Mile at Kalgoorlie dominated mining revenue in the state. Levels of gold production in the region have fluctuated, with peak production in 1903, a decline to low levels by the 1920s, followed by resurgence in the 1930s. There was a further decline in the 1960s. The 1980s and 1990s have seen a return to high levels of production and exploration throughout what is certainly one of the world's major metallogenic gold provinces (Barley et al., 1998).

The discovery of high-grade nickel sulfide ore at Kambalda in 1966 stimulated intense mineral exploration and led to the development of one of the world's most productive nickel mining areas. The so called 'nickel boom' of the late 1960s and early 1970s commenced with production of nickel concentrates from the Lunnon Shoot at Kambalda in mid-1967, followed by the discovery of numerous similar deposits in the Kambalda – Widgiemooltha – Spargoville – St Ives area, at Nepean to the west, and Scotia to the north. By the end of 1973, the annual production of nickel exceeded 45 000 tons. In addition to the major search for sulfide nickel deposits, some exploration was carried out for nickeliferous laterites. Several discoveries were made in the region, including those at Bulong and Ora Banda. These significant nickel resources are now economically viable given the development of efficient low-cost processing methods. More recent exploration has substantially increased the known extent of nickeliferous laterites, and also led to the discovery of an extremely high-grade nickel sulfide deposit at Silver Swan in 1995.

Apart from the nickel and gold resources, no other major ore deposits have been found, despite considerable exploration for base metal, platinum group element, and diamond deposits in the south Eastern Goldfields. There has been minor exploitation of copper, rare metal, and gemstone deposits, and some dimension stone has been mined intermittently. Construction and road materials have been quarried, mostly around the City of Kalgoorlie–Boulder and along the main roads and railways.

Database themes

The themes in the database particularly relevant to the exploration and mining industry are discussed below.

MINOCC — localities of mine workings, prospects, and subsurface observations

Information in this theme has been taken directly from the twenty published 1:100 000-scale geological maps for the region, which show localities of historical and currently operating (at map publication date; see Table 1) mines and batteries, as well as prospects, mineral occurrences, and subsurface rock types revealed by mineral exploration. In view of the great predominance of gold workings in the area, mine sites in the database are only labelled with a commodity code when it is something other than gold. The high level of exploration activity throughout the region in the 1980s and 1990s resulted in a marked increase in the resource inventory, particularly in the vicinity of abandoned mines. For this reason, the more recent findings, as shown by MINEDEX (see below), may bear historical names for localities slightly different from those shown in the historical mine workings database. Similarly, present large-scale opencut mining operations have commonly amalgamated several historical mine sites.

MINEDEX layer

The extract from MINEDEX included in the present database provides the following information, either directly as point attribute information, or in look-up tables:

- commodity groups, projects, and sites;
- corporate ownership and percentage holding;
- site type and stage of development;
- site coordinates; and
- current (at date of CDs) mineral resource estimates.

The abbreviations used in the tables are provided in Appendix 2.

TENGRAPH record of the extent, location, and status of tenements

The tenement information within the database (current at the date given on the CDs) demarcates extent and location of tenements, with the following additional data in the attribute table:

- tenement identification (Tenid); for example, M 2600261 refers to mining licence M 26/261;
- survey status (Survstatus) indicating whether or not the tenement has been surveyed;
- status of the tenement (Tenstatus) referring to whether the tenement application has been granted (L) or is under application (P); and
- dates and times of submission of application, granting, and expiry of tenement holding.

The data in these layers, although voluminous in view of the great number of both historical and current mine sites, and the continuous prospecting activity, are but an index to a vast pool of information. Details of exploration activities are recorded in statutory annual and completion reports now stored in Western Australian mineral exploration database (WAMEX) and is accessible at DME's Perth and Kalgoorlie offices. Resource and production statistics are provided in MINEDEX and annual publications such as the DME Statistics Digest. The Explanatory Notes for the map sheets provide overviews of the mine localities and some production statistics for major mines. Among the great number of manuscripts addressing the many aspects of mineralization, some recent works that provide insight are as follows: for nickel, Elias et al. (1981) and Marston (1984); and for gold, Witt (1993a,b,c,d), Groves (1993), Groves et al. (1995, 1998), Witt et al. (1997), Cassidy et al. (1998), Witt and Vanderhor (1998), Yeats and Vanderhor (1998), Phillips and Zhou (1999), and Yeats et al. (1999). Base metals and other commodities have been less well documented, because of their relative insignificance, but overviews are provided in Witt et al. (1998) and Hocking and Preston (1998).

Gold

Major gold-mining centres in the southern Eastern Goldfields are at Kalgoorlie, Norseman, Coolgardie, Ora Banda, Menzies, St Ives, Paddington, and Kanowna (Fig. 9). Most of the gold deposits are present in the vicinity of major zones of faulting and shearing within, and at the margins of, the greenstone belts, predominantly in mafic greenschist facies metavolcanic rocks or gabbro. Gold deposit formation took place at c. 2.63 – 2.65 Ga, with volumetrically less-significant mineralizing events at c. 2.66 Ga and 2.63 Ga (Solomon and Groves, 1994; Witt et al. 1996; Yeats and McNaughton, 1997).

A continuum model for this mineralization has been proposed, according to which gold deposits may have formed at any level in the crust in the course of the same mineralizing event (Groves, 1993; Solomon and Groves, 1994). The model recognizes an association of gold with major structural breaks in the craton, with fault and joint systems produced by regional compression or transpression, including major listric reverse faults and second- and third-order splays. These high-strain regions provide a high density of anastomosing deformation zones, in which fluid flow was focused at various levels in the crust.

Subsequent research, dedicated to the major localities of mineralization that account for a great majority of the production, interpreted the gold deposits as products of ‘a small number of large-scale, mid-crustal, synmetamorphic hydrothermal systems that involved a significant component of lateral, up-temperature fluid flow towards regions of late tectonic uplift and granitoid intrusion’ (Witt et al., 1997, p. 407). Most recent attempts at modelling the mineralization have introduced the terms ‘late-orogenic structurally controlled’ (Witt and Vanderhor, 1998) and ‘orogenic’ (Groves et al., 1998) to describe the Yilgarn gold deposits.

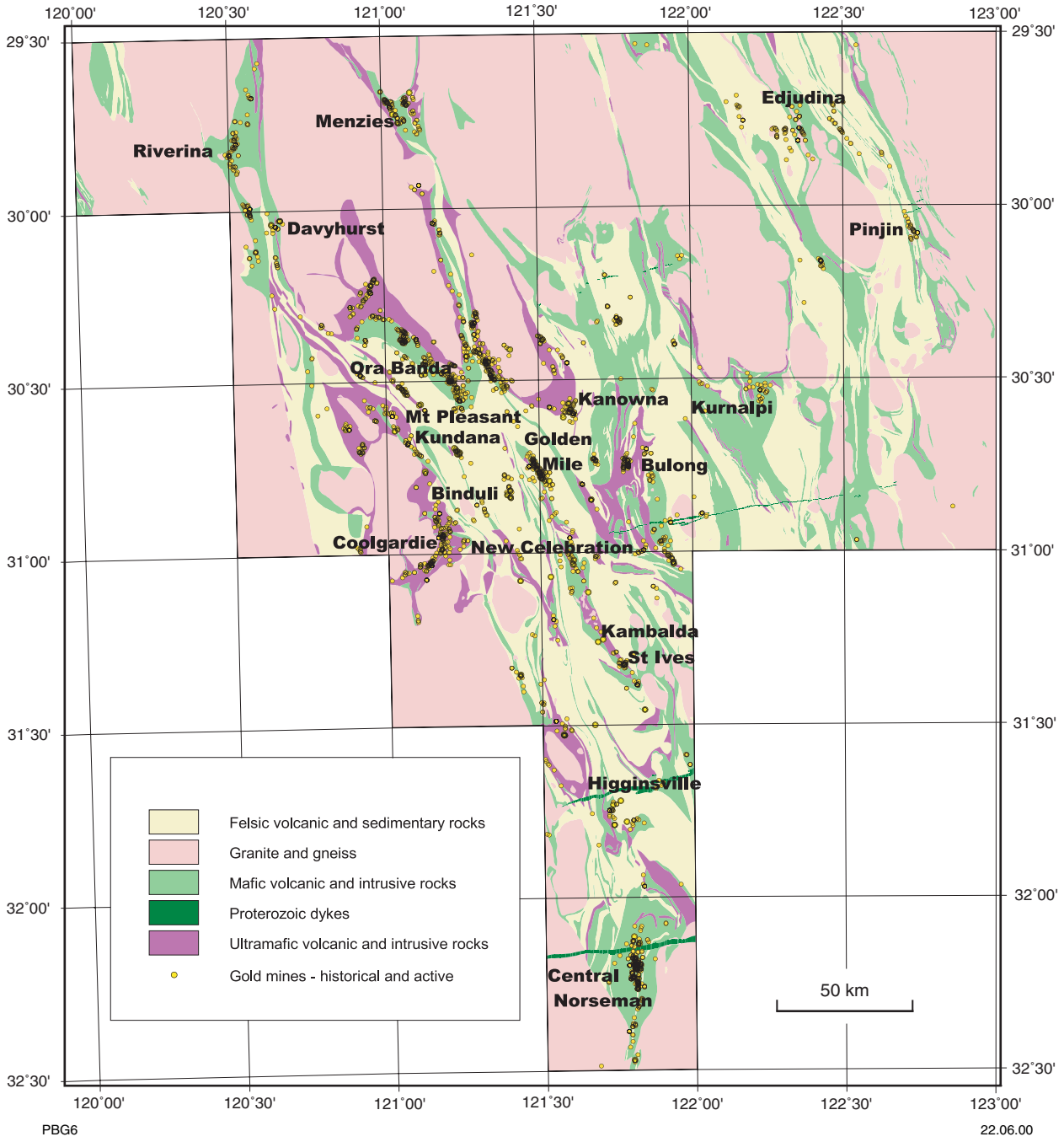

Figure 9. Plot from the database showing general distribution of gold mines on a simplified map of the solid geology of the southern Eastern Goldfields

The most favourable host rocks in the Eastern Goldfields (basalt, gabbro, dolerite, and BIF) have high Fe:(Fe+Mg) values, are of middle to upper greenschist facies, and show evidence that transitional brittle–ductile deformation occurred at depths of between 6 and 12 km. The vein and hydrothermal deposits may also be present in komatiites, intermediate to felsic volcanic or intrusive rocks, and sedimentary rocks. They are metamorphosed with metasomatic addition of SiO_2, K_2O, CO_2, H_2O, S, and Au. Gold is commonly associated with relatively low normal accumulations of As, Ag, W, Sb, Te, B, Cu, Pb, Zn, and Mo. Fluid sources may have been either metamorphic or magmatic, or a combination of both. In general, it is believed that gold deposition was controlled by fluid-wall rock reactions, such as the sulfidation of iron-rich hosts, and hence the favouring of rock types with a high iron–magnesium ratio (Groves et al., 1990).

Gold is present in the ferricretes and supergene zones, which overlie many gold occurrences and deposits in the area, to the extent that development in many of the early workings did not go far beyond the 'laterite ore' (Davy and Gozzard, 1995). Alluvial deposits were also common in early gold workings in the Eastern Goldfields, where

some of the mined gold came from eluvial or alluvial mantles or fringes adjacent to eroded source deposits. The resurgence of the gold mining industry in the 1980s and 1990s was based not only on developments in gold processing technology, but also on the opencut mining of large, low-grade oxide resources formed as a result of supergene enrichment.

Nickel

Since the discovery of nickel mineralization in the Lunnon shoot at Kambalda in 1966, ores of this metal have been mined at numerous localities (Fig. 10) and become a major part of the known and potential mineral resources in the south Eastern Goldfields. The great majority of nickel mined until very recently has been in the form of sulfide associated with large flows of high-temperature, high-Mg komatiitic lava (Hill et al., 1990, 1996). High-grade sulfide deposits form as adcumulates at the basal contacts of lava pathways. Larger, low-grade disseminated adcumulate sulfide deposits are centrally located in olivine-rich bodies within very large lava pathways (Barnes et al., 1987).

The work by Hill et al. (1989, 1990, 1996) showed that the komatiite- and dunite-associated nickel deposits in the Eastern Goldfields are extrusive in origin and can be subdivided into two types. In the first type, the komatiite flows are thin (20–100 m); massive sulfides (2–15% nickel) and olivine-sulfide cumulates (about 2.5% nickel) formed at the base of lava-flow channels in komatiite flow fields. In the second type, disseminated sulfides are present in the central zones of large bodies of olivine cumulate that occupy subvolcanic lava feeder zones. They range from olivine-sulfide orthocumulate to olivine-sulfide adcumulate, with grades averaging 0.6% nickel (reaching a maximum of 1.5% nickel).

The distribution of nickel sulfide deposits in ultramafic igneous rocks in the southern Eastern Goldfields is directly related to the volcanogenic setting of the host rocks and the process of sulfide segregation (Hill et al., 1996). In Type 1 deposits, the basal, massive, and matrix sulfide ores accumulated along preferred lava pathways in komatiitic flow fields. These deposits are found in relatively narrow olivine cumulate and adcumulate lenses. In Type 2 deposits, the disseminated sulfide ore form olivine adcumulate lenses in broader, more continuous sheet flows within erosional pathways. Locating such deposits requires detailed interpretation of the flow-field stratigraphy and morphology from mapping and drilling, in an environment affected by complex structural reworking of the original volcanic deposits and the effects of deep weathering.

The Kambalda deposits have been among the richest komatiite-hosted nickel sulfide deposits in the world. Copper, cobalt, platinum-group metals, and gold have been important byproducts. Although some mines have faced difficulties during times of low nickel price, komatiite-hosted sulfides are still being mined profitably. High-grade deposits, such as Silver Swan, can be particularly profitable.

The only important nickel sulfide deposit not associated with komatiites is at Carr Boyd Rocks, where sulfides were mined from an intrusive breccia pipe within a larger peridotite–gabbro complex. Proterozoic mafic dykes have also been of interest in nickel exploration, with a detailed study of the Jimberlana Dyke east of Norseman revealing some subeconomic occurrences.

Laterite nickel(–cobalt) resources are now being exploited at Cawse and Bulong (Fig. 10) using high temperature and pressure acid leach processes, which allow for economical production from low grade deposits. The nickeliferous laterites in the Menzies to Norseman region developed above, or adjacent to, ultramafic rocks and thus reflect the abundance of komatiites and the preservation of their weathering profiles.

Base metals and other commodities

The discovery in 1974 of the Teutonic Bore base metal deposit in the Leonora area, north of the present project area, led to considerable exploration of the Eastern Goldfields greenstones for volcanic-hosted base-metal sulfides. Although this yielded very little in comparison with other similar Archaean cratons, such as the Superior Province in Canada, minor finds in areas immediately north of the database coverage suggest that the eastern parts of the Eastern Goldfields may be more promising. The potential for volcanogenic base metal mineralization in the southern Eastern Goldfields may depend primarily on the presence and distribution of deep-water felsic volcano-sedimentary suites in the greenstone belts. Although felsic rocks may amount to around 40% of the Eastern Goldfields greenstones, and have some characteristics in common with mineralized felsic rocks of the Superior Province in Canada, exploration to date has failed to locate economic base metal deposits. Witt et al. (1996) examined the geochemistry of the south Eastern Goldfields felsic rocks and argued that those in the western domains have light rare-earth element (LREE) enrichment, unlike the flat REE patterns typical of the Canadian metallogenic province, and suggested rather low potential for volcanic-hosted massive sulfide in this area. However, felsic rocks in the eastern domains have trace element characteristics more like those in the Superior Province and hence may have greater volcanic-hosted massive sulfide potential (Witt et al., 1996; Morris, 1998). The recognition of a calc-alkaline volcanic suite, with andesites in close proximity to a contemporaneous tonalite intrusion (Nelson, 1996), led Witt et al. (1998) to advise closer examination of these eastern greenstones.

Although production of other metals has been low to insignificant, the potential of further findings cannot be dismissed. There are traces of copper mineralization in pyrite–chalcopyrite–quartz veins, commonly in association with gold. A small amount has been produced from shales in the hanging wall of the Mount Pleasant sill and from chalcopyrite-bearing quartz veins at Corsair, some 10 km east of Kalgoorlie. Minor occurrences of tin, in the form of a cassiterite-bearing, lepidolite–albite pegmatite, were worked in the Norseman area between

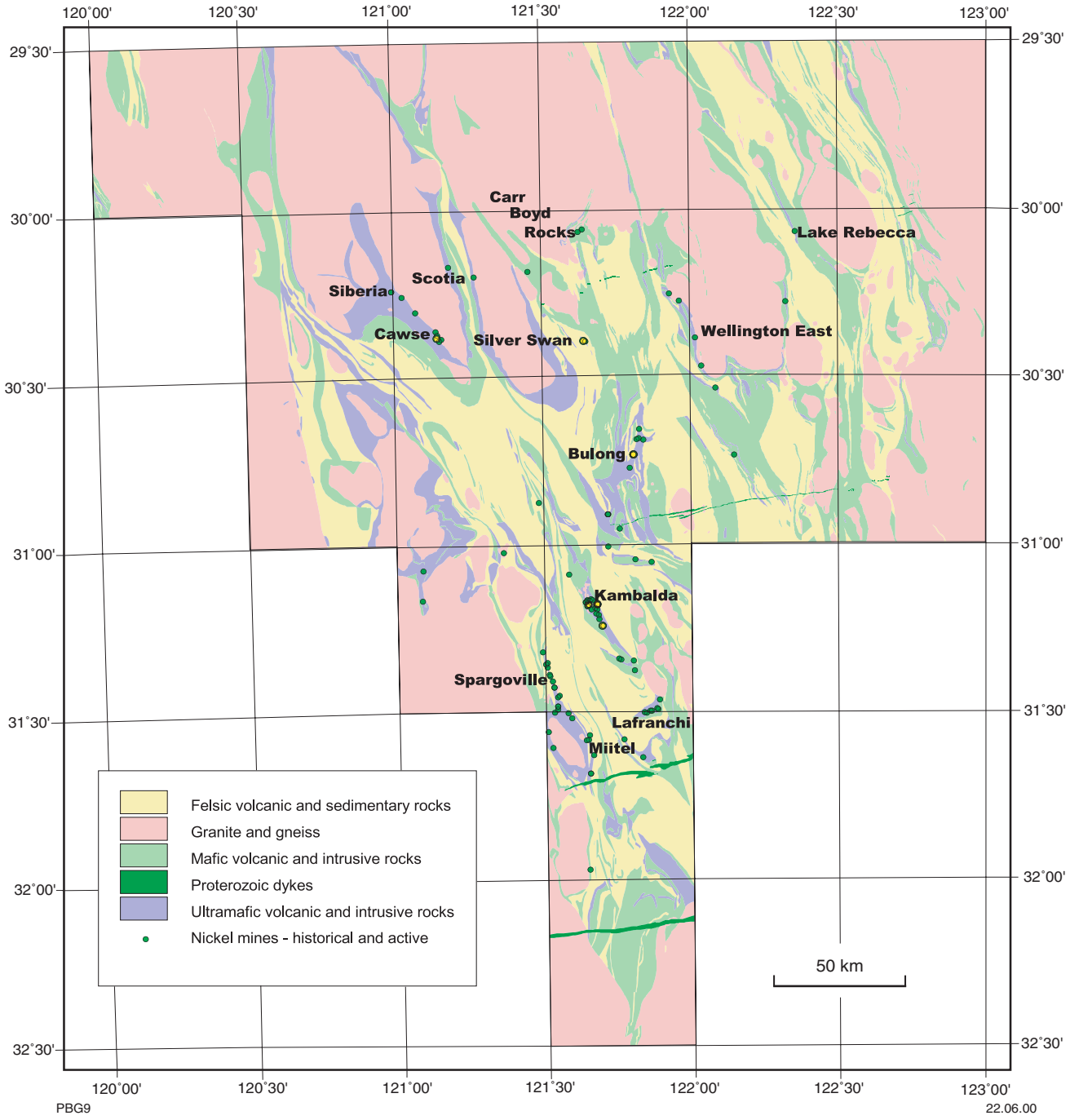

Figure 10. Plot from the database showing the general distribution of nickel mines on a simplified map of the solid geology of the southern Eastern Goldfields

1966 and 1968, yielding about 7 t of concentrate (Doepel, 1973). The Londonderry and Spargoville pegmatites on YILMIA have yielded almost 300 t of beryl, 130 t of lepidolite, 8000 t of petelite, and 9 t of tantalite–columbite. Tungsten has been mined, as wolframite, from the quartz and pegmatite veins around Ora Banda, and from scheelite concentrates recovered as a byproduct of gold processing at Coolgardie, Davyhurst, and Higginsville. Minor production has also been recorded for alunite, asbestos, dimension stone, gemstones, magnesite, opal, spodumene, and vermiculite.

References

ABBOTT, D. H., 1996, Plumes and hotspots as sources of greenstone belts: Lithos, v. 37, p. 113–127.

AHMAT, A. L., 1986, Metamorphic patterns in the greenstone belts of the Southern Cross Province, Western Australia: Western Australia Geological Survey, Report 19, Professional Papers, p. 1–21.

AHMAT, A. L., 1993, Mafic–ultramafic rocks of the Gindalbie Terrane: a review of the Bulong and Carr Boyd Complexes, *in* Kalgoorlie 93 — an international conference on crustal evolution, metallogeny, and exploration in the Eastern Goldfields *compiled by* P. R. WILLIAMS and J. A. HALDANE: Australian Geological Survey Organisation, Record 1993/54, p. 23–27.

AHMAT, A. L., 1995a, Kanowna, W.A. Sheet 3236: Western Australia Geological Survey, 1:100 000 Geological Series.

AHMAT, A. L., 1995b, Geology of the Kanowna 1:100 000 sheet: Western Australia Geological Survey, 1:100 000 Geological Series Explanatory Notes, 28p.

AHMAT, A. L., 1995c, Gindalbie, W.A. Sheet 3237: Western Australia Geological Survey, 1:100 000 Geological Series.

ARCHIBALD, N. J., 1987, Geology of the Norseman–Kambalda area, *in* The Second Eastern Goldfields Geological Field Conference *edited by* W. K. WITT and C. P. SWAGER: Geological Society of Australia (W.A. Division); 2nd Eastern Goldfields Geological Field Conference, 1987, Abstracts and Excursion Guide, p. 13–14.

ARCHIBALD, N. J., 1998, An allochthonous model for the greenstone belt evolution in the Menzies–Norseman area, Eastern Goldfields Province: implications for gold mineralisation, *in* Geodynamics and gold exploration in the Yilgarn: Australian Geodynamics Cooperative Research Centre, Workshop abstracts, p. 10–16.

ARCHIBALD, N. J., and BETTENAY, L. F., 1977, Indirect evidence for tectonic reactivation of a pre-greenstone sialic basement in Western Australia: Earth and Planetary Science Letters, v. 33, p. 370–378.

ARCHIBALD, N. J., BETTENAY, L. F., BICKLE, M. J., and GROVES, D. I., 1981, Evolution of Archaean crust in the Eastern Goldfields Province of the Yilgarn Block: Geological Society of Australia, Special Publication, no. 7, p. 491–504.

ARCHIBALD, N. J., BETTENAY, L. F., BINNS, R. A., GROVES, D. I., and GUNTHORPE, R. J., 1978, The evolution of Archaean greenstone terrains, Eastern Goldfields Province, Western Australia: Precambrian Research, v. 6, p. 103–131.

ARNDT, H. T., and JENNER, G. A., 1986, Crustally contaminated komatiites and basalts from Kambalda, Western Australia: Chemical Geology, v. 56, p. 229–255.

ARNDT, H. T., KERR, A. C., and TARNEY, J., 1997, Dynamic melting in plume heads: the formation of Gorgona komatiites and basalts: Earth and Planetary Science Letters, v. 146, p. 289–301.

BARLEY, M. E., 1986, Incompatible-element enrichment in Archean basalts: a consequence of contamination by older sialic crust rather than mantle heterogeneity: Geology, v. 14, p. 947–950.

BARLEY, M. E., EISENLOHR, B. N., GROVES, D. I, PERRING, C. S., and VEARNCOMBE, J. R., 1989, Late Archean convergent margin tectonics and gold mineralization: a new look at the Norseman–Wiluna belt, Western Australia: Geology, v. 17, p. 826–829.

BARLEY, M. E., and GROVES, D. I., 1989, Exploration significance of regional and local scale hydrothermal alteration patterns in greenstone belts: Minerals and Energy Research Institute of Western Australia, Report 43, 211p.

BARLEY, M. E., KRAPEZ, B., GROVES, D. I., and KERRICH, R., 1998, The Late Archaean bonanza: metallogenic and environmental consequences of the interaction between mantle plumes, lithospheric tectonics and global cyclicity: Precambrian Research, v. 91, p. 96–90.

BARNES, S. J., GOLE, M. J., and HILL, R. E. T., 1987, The Agnew nickel deposit, Yilgarn Block, Western Australia: stratigraphy, structure, geochemistry and origin: Western Australian Mining and Petroleum Research Institute, Report 38, 187p.

BETTENAY, L. F., 1988, The nature and origin of batholithic granitoids in the Yilgarn Block, Western Australia and their significance to gold mineralization, *in* Advances in understanding Precambrian gold deposits, Volume 2 *edited by* S. E. HO and D. I. GROVES: University of Western Australia, Geology Department and University Extension, Publication no. 12, p. 227–237.

BICKLE, M. J., and ARCHIBALD, N. J., 1984, Chloritoid and staurolite stability: implications for metamorphism in the Archaean Yilgarn Block in Western Australia: Journal of Metamorphic Petrology, v. 2, p. 179–203.

BICKLE, M. J., NISBET, E. G., and MARTIN, A., 1994, Archaean greenstone belts are not oceanic crust: Journal of Geology, v. 102, p. 121–138.

BINNS, R. A., GUNTHORPE, R. J., and GROVES, D. I., 1976, Metamorphic patterns and development of greenstone belts in the Eastern Yilgarn Block, Western Australia, *in* The early history of the Earth *edited by* B. F. WINDLEY: New York, John Wiley and Sons, p. 303–313.

CAMPBELL, I. H., 1968, The origin of heteradcumulate and adcumulate textures in the Jimberlana Norite: Geological Magazine, v. 105, p. 378–383.

CAMPBELL, I. H., 1978, Some problems with cumulus theory: Lithos, v. 11, p. 311–328.

CAMPBELL, I. H., GRIFFITHS, R. W., and HILL, R. I., 1989, Melting in an Archaean mantle plum: heads it's basalts, tails it's komatiites: Nature, v. 339, p. 697–699.

CAMPBELL, I. H., and HILL, R. I., 1988, A two-stage model for the formation of the granite–greenstone terrains of the Kalgoorlie–Norseman area, Western Australia: Earth and Planetary Science Letters, v. 90, p. 11–25.

CASSIDY, K. F., GROVES, D. I., and McNAUGHTON, N. J.,1998, Late-Archean granitoid-hosted lode-gold deposits, Yilgarn Craton, Western Australia: Ore Geology Reviews, v. 13, p. 65–102.

CHAMPION, D. C., and SHERATON, J. W., 1993, Geochemistry of granitoids of the Leonora–Laverton region, Eastern Goldfields Province, *in* Kalgoorlie 93 — an international conference on crustal

evolution, metallogeny, and exploration of the Eastern Goldfields *compiled by* P. R. WILLIAMS and J. A. HALDANE: Australian Geological Survey Organisation, Record 1993/54, p. 39–46.

CHAMPION, D. C., and SHERATON, J. W., 1997, Geochemistry and Nd isotope systematics of Archaean granites of the Eastern Goldfields, Yilgarn Craton, Australia: implications for crustal growth processes: Precambrian Research, v. 83, p. 109–132.

CHAN, R. A., 1991, Regolith terrains of the Kalgoorlie area 1:1 000 000 (first edition): Australia Bureau of Mineral Resources.

CHEN, S. F., 1997, Boyce, W.A. Sheet 3238 (1st edition plot): Western Australia Geological Survey, 1:100 000 Geological Series.

CHEN, S. F., 1999, Edjudina, W.A. (2nd edition): Western Australia Geological Survey, 1:250 000 Geological Series Explanatory Notes, 32p.

CHEN, S. F., LIU, S., and WITT, W. K., 1998, Strike-slip-induced local compressional deformation in the Archaean greenstone belts, northeastern Yilgarn Craton, Western Australia: Geological Society of Australia, Abstracts no. 49, p. 79.

CHEN, S. F., WITT, W. K., and LIU, S., in press, Transpression and restraining jogs in the northeastern Yilgarn Craton, Western Australia: Precambrian Research.

CLAOUÉ-LONG, J. C., COMPSTON, W., and COWDEN A., 1988, The age of the Kambalda greenstones resolved by ion-microprobe: implications for Archaean dating methods: Earth and Planetary Science Letters, v. 89, p. 239–259.

CLARK, M. E., ARCHIBALD, N. J., and HODGSON, C. J., 1986, The structural and metamorphic setting of the Victory Gold mine, Kambalda, Western Australia, *in* Gold '86 — an international symposium on the geology of gold deposits *edited by* A. J. MacDONALD: Gold '86 Symposium, Toronto, 1986, Proceedings, p. 243–254.

CLARKE, J. D. A., 1994, Evolution of the Lefroy and Cowan palaeodrainage channels, Western Australia: Australian Journal of Earth Sciences, v. 41, p. 55–68.

CLOUT, J. M. F., CLEGHORN, J. H., and EATON, P. C., 1990, Geology of the Kalgoorlie gold field, *in* Geology of the Mineral Deposits of Australia and Papua New Guinea, Volume 1 *edited by* F. E. HUGHES: Australasian Institute of Mining and Metallurgy, Monograph 14, p. 411–431.

COCKBAIN, A. E., 1968a, Eocene foraminifera from the Norseman Limestone of Lake Cowan, Western Australia: Western Australia Geological Survey, Annual Report 1967, p. 59–60.

COCKBAIN, A. E., 1968b, The stratigraphy of the Plantagenet Group, Western Australia: Western Australia Geological Survey, Annual Report 1967, p. 61–63.

COMPSTON, W., WILLIAMS, I. S., CAMPBELL, I. H., and GRESHAM, J. J., 1986, Zircon xenocrysts from the Kambalda volcanics: age constraints and direct evidence for older continental crust below the Kambalda–Norseman greenstones: Earth and Planetary Science Letters, v. 76, p. 299–301.

CRAIG, M. A., and CHURCHWARD, H. M, 1995, Menzies regolith–landforms (1:250 000): Australian Geological Survey Organisation.

DAVIES, G. F., 1992, On the emergence of plate tectonics: Geology, v. 20, p. 963–966.

DAVIES, G. F., 1998, Plates, plumes, mantle convection, and mantle evolution, *in* The Earth's mantle — composition, structure, and evolution *edited by* I. JACKSON: Cambridge, Cambridge University Press, p. 228–258.

DAVY, R., and GOZZARD, J. R., 1995, Lateritic duricrusts of the Leonora area, Eastern Goldfields, Western Australia: a contribution to the study of transported laterites: Western Australia Geological Survey, Record 1994/8, 122p.

DE WIT, M. J., 1998, On Archaean granites, greenstones, cratons and tectonics: does the evidence demand a verdict?: Precambrian Research, v. 91, p. 181–226.

DE YOREO, J. J., LUX, D. R., and GUIDOTTI, C. V., 1989, The role of crustal anatexis and magma migration in the thermal evolution of regions of thickened continental crust, *in* Evolution of metamorphic belts *edited by* J. S. DALY, R. A. CLIFF, and B. W. D. YARDLEY: Geological Society of London, Special Publication, no. 43, p. 187–202.

DOEPEL, J. J. G., 1973, Norseman, W.A.: Western Australia Geological Survey, 1:250 000 Geological Series Explanatory Notes, 40p.

DRUMMOND, B. J., and GOLEBY, B. R., 1993, Seismic reflection images of the major ore-controlling structures in the Eastern Goldfields Province, Western Australia: Exploration Geophysics, v. 24, p. 473–478.

DRUMMOND, B. J., GOLEBY, B. R., SWAGER, C. P., and WILLIAMS, P. R., 1993, Constraints on Archaean crustal composition and structure provided by deep seismic sounding in the Yilgarn Block: Ore Geology Reviews, v. 8, p. 117–124.

DUNBAR, G. J., and McCALL, G. J. H., 1971, Archaean turbidites and banded ironstones of the Mt Belches area (Western Australia): Sedimentary Geology, v. 5, p. 93–133.

ELIAS, M., DONALDSON, M. J., and GIORGETTA, N., 1981, Geology, mineralogy, and chemistry of lateritic nickel–cobalt deposits near Kalgoorlie, Western Australia: Economic Geology, v. 76, p. 1775–1783.

GEE, R. D., BAXTER, J. L., WILDE, S. A., and WILLIAMS, I. R., 1981, Crustal development in the Yilgarn Block, Western Australia, *in* Archaean Geology *edited by* J. E. GLOVER and D. I. GROVES: Geological Society of Australia; 2nd International Archaean Symposium, Perth, W.A., 1980, Proceedings; Special Publication, no. 7, p. 275–286.

GLIKSON, A. Y., 1971, Archaean geosynclinal sedimentation near Kalgoorlie, Western Australia, *in* Symposium on Archaean rocks *edited by* J. E. GLOVER: Geological Society of Australia, Special Publication, no. 3, p. 443–460.

GOLEBY, B. R., RATTENBURY, M. S., SWAGER, C. P., DRUMMOND, B. J., WILLIAMS, P. R., SHERATON, J. E., and HEINRICH, C. A., 1993, Archaean crustal structure from seismic reflection profiling, Eastern Goldfields, Western Australia: Australian Geological Survey Organisation, Record 1993/15, 54p.

GRESHAM, J. J., and LOFTUS-HILLS, G. D., 1981, The geology of the Kambalda nickel field, Western Australia: Economic Geology, v. 76, p. 1373–1416.

GRIFFIN, T. J., 1988a, Cowan, W.A. Sheet 3234: Western Australia Geological Survey, 1:100 000 Geological Series.

GRIFFIN, T. J., 1988b, Widgiemooltha, W.A. (2nd edition): Western Australia Geological Survey, 1:250 000 Geological Series.

GRIFFIN, T. J., 1989, Widgiemooltha, W.A. (2nd edition): Western Australia Geological Survey, 1:250 000 Geological Series Explanatory Notes, 43p.

GRIFFIN, T. J., 1990a, Eastern Goldfields Province, *in* Geology and mineral resources of Western Australia: Western Australia Geological Survey, Memoir 3, p. 77–119.

GRIFFIN, T. J., 1990b, Geology of the granite–greenstone terrane of the Lake Lefroy and Cowan 1:100 000 sheets, Western Australia: Western Australia Geological Survey, Report 32, 53p.

GRIFFIN, T. J., and HICKMAN, A. H., 1988a, Lake Lefroy, W.A. Sheet 3235: Western Australia Geological Survey, 1:100 000 Geological Series.

GRIFFIN, T. J., and HICKMAN, A. H., 1988b, Widgiemooltha, W.A. Sheet SH 51-14 (2nd edition): Western Australia Geological Survey, 1:250 000 Geological Series.

GRIFFITHS, R. W., and CAMPBELL, I. H., 1990, Stirring and structure in mantle plumes: Earth and Planetary Science Letters, v. 99, p. 66–78.

GROVES, D. I., 1993, The crustal continuum model for late-Archaean lode-gold deposits of the Yilgarn Block, Western Australia: Mineralium Deposita, v. 28, p. 366–374.

GROVES, D. I., and GEE, R. D., 1980, Regional geology and mineral deposits of the Kalgoorlie–Norseman region — an excursion guide: Geological Society of Australia (W.A. Division); 2nd International Archaean Symposium, Perth, W.A., 1980, Abstracts and Excursion Guide, 112p.

GROVES, D. I., GOLDFARB, R. J., GEBRE-MARIAM, M., HAGEMANN, S. G., and ROBERT, F., 1998, Orogenic gold deposits: a proposed classification in the context of their crustal distribution and relationship to other gold deposit types: Ore Geology Reviews, v. 13, p. 1–27.

GROVES, D. I., GOLDING, S. D., ROCK, N. M. S., BARLEY, M. E., and McNAUGHTON, N. J., 1988, Archaean carbon reservoirs and their relevance to the the fluid source for gold deposits: Nature, v. 331, p. 254–257.

GROVES, D. I., KNOX-ROBINSON, C. M., HO, S. E., and ROCK, N. M. S., 1990, An overview of Archaean lode-gold deposits, *in* Gold deposits of the Archaean Yilgarn Block, Western Australia: nature, genesis and exploration guides *edited by* S. E. HO, D. I. GROVES, and J. M. BENNETT: University of Western Australia, Geology Department and University Extension, Publication no. 20, p. 2–18.

GROVES, D. I., RIDLEY, J. R., BLOEM, E. M. J., GEBRE-MARIAM, M., HAGEMANN, S. G., HRONSKY, J. M. A., KNIGHT, J. T., McNAUGHTON, N. J., OJALA, J., VIELREICHER, R. M., MCCUAIG, T. C., and HOLYLAND, P. W., 1995, Lode-gold deposits of the Yilgarn block: products of Late Archaean crustal-scale overpressured hydrothermal systems, *in* Early Precambrian processes *edited by* M. P. COWARD and A. C. RIES: Geological Society of London, Special Publication, no. 95, p. 155–172.

HALLBERG, J. A., 1985, Geology and mineral deposits of the Leonora–Laverton area, northeastern Yilgarn Block, Western Australia: Perth, Western Australia, Hesperian Press, 140p.

HALLBERG, J. A., 1987, Postcratonization mafic and ultramafic dykes of the Yilgarn Block: Australian Journal of Earth Sciences, v. 34, p. 135–149.

HAMILTON, W. B., 1998, Archean magmatism and deformation were not products of plate tectonics: Precambrian Research, v. 91, p. 143–179.

HAMMOND, R. L., and NISBET, B. W., 1992, Towards a structural and tectonic framework for the Norseman–Wiluna greenstone belt, Western Australia, *in* The Archaean: Terrains, processes and metallogeny *edited by* J. E. GLOVER and S. E. HO: University of Western Australia, Geology Department and University Extension, Publication no. 22, p. 39–50.

HICKMAN, A. H., 1986, Stratigraphy, structure and economic geology of the Mount Monger area, Eastern Goldfields Province: Western Australia Geological Survey, Report 16, 21p.

HILL, R. E. T., BARNES, S. J., GOLE, M. J., and DOWLING, S. E., 1990, Physical volcanology of komatiites — a field guide to the Norseman–Wiluna greenstone belt, Eastern Goldfields Province, Yilgarn Block, Western Australia (2nd edition): Geological Society of Australia (W.A. Division); Excursion Guidebook no. 1, 100p.

HILL, R. E. T., BARNES, S. J., GOLE, M. J., and DOWLING, S. J., 1995, The volcanology of komatiites as deduced from field relationships in the Norseman–Wiluna greenstone belt, Western Australia: Lithos, v. 34, p. 159–188.

HILL, R. E. T., BARNES, S. J., and PERRING, C. S., 1996, Komatiite volcanology and the volcanogenic setting of associated nickel deposits, *in* Nickel '96 — mineral to market *edited by* E. J. GRIMSBY and I. NUESS: Australian Institute of Mining and Metallurgy, Publication Series no. 6/96, p. 91–95.

HILL, R. E. T., GOLE, M. J., and BARNES, S. J., 1989a, Olivine adcumulates in the Norseman–Wiluna greenstone belt, Western Australia: implications for the volcanology of komatiites, *in* Magmatic sulphides — the Zimbabwe volume, *edited by* M. D. PRENDERGAST and M. J. JONES: London, Institue of Mining and Metallurgy, p. 189–206.

HILL, R. I., CAMPBELL, I. H., and COMPSTON, W., 1989b, Age and origin of granitic rocks in the Kalgoorlie–Norseman region of Western Australia: implications for the origin of the Archaean crust: Geochimica et Cosmochimica Acta, v. 53, p. 1259–1275.

HILL, R. I., CHAPPELL, B. W., and CAMPBELL, I. H., 1992, Late Archaean granites of the southeastern Yilgarn Block, Western Australia: age, geochemistry, and origin: Royal Society of Edinburgh, Transactions, v. 83, p. 211–226.

HOCKING, R. M., and COCKBAIN, A. E., 1990, Regolith, *in* Geology and mineral resources of Western Australia: Western Australia Geological Survey, Memoir 3, p. 591–602.

HOCKING, R. M., and PRESTON, W. A., 1998, Western Australia: Phanerozoic geology and mineral resources: Australian Geological Survey Organisation, Journal of Australian Geology and Geophysics, v. 17, p. 245–260.

HUNTER, W. M., 1988a, Yilmia, W.A. Sheet 3135: Western Australia Geological Survey, 1:100 000 Geological Series.

HUNTER, W. M., 1988b, Kalgoorlie, W.A. Sheet 3136: Western Australia Geological Survey, 1:100 000 Geological Series.

HUNTER, W. M., 1993, The geology of the granite–greenstone terrane of the Kalgoorlie and Yilmia 1:100 000 sheets, Western Australia: Western Australia Geological Survey, Report 35, 80p.

JUTSON, J. T., 1934, The physiography (geomorphology) of Western Australia: Western Australia Geological Survey, Bulletin 95, 366p.

KEATS, W., 1987, Regional geology of the Kalgoorlie–Boulder gold-mining district: Western Australia Geological Survey, Report 21, 44p.

KENT, A. J. R., and McDOUGALL, I., 1995, ^{40}Ar–^{39}Ar and U–Pb age constraints on the timing of gold mineralization in the Kalgoorlie Gold Field, Western Australia: Economic Geology, v. 90, p. 845–859.

KENT, A. J. R., and McDOUGALL, I., 1996, ^{40}Ar–^{39}Ar and U–Pb age constraints on the timing of gold mineralization in the Kalgoorlie Gold Field, Western Australia — a reply: Economic Geology, v. 91, p. 795–799.

KOJAN, C. J., and FAULKNER, J. A., 1994, Geochemical mapping of the Menzies 1:250 000 sheet: Western Australia Geological Survey, 1:250 000 Regolith Geochemistry Series Explanatory Notes, 55p.

KRAPEZ, B., BROWN, S., and HAND, J., 1997, Stratigraphical signatures of depositional basins in the Archaean volcano-sedimentary successions of the Eastern Goldfields Province, *in* Kalgoorlie 97 — an international conference on crustal evolution, metallogeny, and exploration of the Yilgarn craton — an update *compiled by* K. F. CASSIDY, A. J. WHITAKER, and S. F. LIU: Australian Geological Survey Organisation, Record 1997/41, Extended Abstracts, p. 33–38.

KRIEWALDT, M., 1969, Kalgoorlie, W.A.: Western Australia Geological Survey, 1:250 000 Geological Series Explanatory Notes, 18p.

KRIEWALDT, M., 1970, Menzies, W.A.: Western Australia Geological Survey, 1:250 000 Geological Series Explanatory Notes, 11p.

LANGSFORD, N., 1989, The stratigraphy of locations 48 and 50, *in* The 1989 Kalgoorlie gold workshops *edited by* I. M. GLACKEN: Australasian Institute of Mining and Metallurgy and the Eastern

Goldfields Geological Discussion Group, Kalgoorlie, Western Australia, p. B1–B8.

LESHER, C. M., and ARNDT, N. T., 1995, REE and Nd isotope geochemistry, petrogenesis and volcanic evolution of contaminated komatiites at Kambalda, Western Australia: Lithos, v. 34, p. 127–157.

LIBBY, W. G., 1978, The felsic alkaline rocks, *in* Contributions to the geology of the Eastern Goldfields Province of the Yilgarn Block, Western Australia *edited by* W. G. LIBBY, J. D. LEWIS, and C. F. GOWER: Western Australia Geological Survey, Report 9, p. 111–137.

LUX, D. R., DE YOREO, J. J., GUIDOTTI, C. V., and DECKER, E. R., 1986, The role of plutonism in the formation of low pressure metamorphic belts: Nature, v. 323, p. 794–797.

McCLAY, K. R., and CAMPBELL, I. H., 1976, The structure and shape of the Jimberlana Intrusion, Western Australia, as indicated by an investigation of the Bronzite Complex: Geological Magazine, v. 113, p. 129–139.

McGOLDRICK, P. J., 1993, Norseman, W.A. Sheet 3233: Western Australia Geological Survey, 1:100 000 Geological Series.

MARSTON, R. J., 1984, Nickel mineralization in Western Australia: Western Australia Geological Survey, Bulletin 14, 271p.

MARTYN, J. J., 1987, Evidence for structural repetition in the greeenstones of the Kalgoorlie district, Western Australia: Precambrian Research, v. 37, p. 1–18.

MATHUR, S. P., MOSS, F. J., and BRANSON, J. C., 1977, Seismic and gravity investigations along the Geotraverse: Australia Bureau of Mineral Resources, Bulletin 191, 63p.

MORRIS, G. A., LARSON, P. B., and HOOPER, P. R., 2000, 'Subduction style' magmatism in a non-subduction setting: the Colville Igneous Complex, NE Washington state, USA: Journal of Petrology, v. 41, p. 43–67.

MORRIS, P. A., 1993, Archaean mafic and ultramafic volcanic rocks, Menzies to Norseman, Western Australia: Western Australia Geological Survey, Report 36, 107p.

MORRIS, P. A., 1994a, Mulgabbie, W.A. Sheet 3337: Western Australia Geological Survey, 1:100 000 Geological Series.

MORRIS, P. A., 1994b, Geology of the Mulgabbie 1:100 000 sheet: Western Australia Geological Survey, 1:100 000 Geological Series Explanatory Notes, 18p.

MORRIS, P. A., 1998, Archaean felsic volcanism in the Eastern Goldfields Province, Western Australia: Western Australia Geological Survey, Report 55, 80p.

MUELLER, A. G., HARRIS, L. B., and LUNGAN, A., 1988, Structural control of greenstone-hosted gold mineralization by transcurrent shearing: a new interpretation of the Kalgoorlie mining district, Western Australia: Ore Geology Reviews, v. 3, p. 359–387.

MYERS, J. S., 1990a, Albany–Fraser Orogen, *in* Geology and mineral resources of Western Australia: Western Australia Geological Survey, Memoir 3, p. 255–274.

MYERS, J. S., 1990b, Precambrian tectonic evolution of part of Gondwana, southwestern Australia: Geology, v. 18, p. 537–540.

MYERS, J. S., 1995, The generation and assembly of an Archaean supercontinent: evidence from the Yilgarn Craton, Western Australia, *in* Early Precambrian processes *edited by* M. P. COWARD and A. C. RIES: Geological Society of London, Special Publication, no. 95, p. 143–154.

MYERS, J. S., 1997, Archaean geology of the Eastern Goldfields of Western Australia — a regional overview: Precambrian Research, v. 83, p. 1–10.

NELSON, D. R., 1995, Compilation of SHRIMP U–Pb zircon geochronology data, 1994: Western Australia Geological Survey, Record 1995/3, 244p.

NELSON, D. R., 1996, Compilation of SHRIMP U–Pb zircon geochronology data, 1995: Western Australia Geological Survey, Record 1996/5, 168p.

NELSON, D. R., 1997a, Evolution of the Archaean granite–greenstone terranes of the Eastern Goldfields, Western Australia: SHRIMP U–Pb zircon constraints: Precambrian Research v. 83, p. 57–81.

NELSON, D. R., 1997b, Compilation of SHRIMP U–Pb zircon geochronology data, 1996: Western Australia Geological Survey, Record 1997/2, 189p.

NELSON, D. R., 2000, Compilation of SHRIMP geochronology data, 1999: Western Australia Geological Survey, Record 2000/2, 251p.

NEMCHIN, A. A., and PIDGEON, R. T., 1998, Precise conventional and SHRIMP baddeleyite U–Pb age for the Binneringie Dyke, near Narrogin, Western Australia: Australian Journal of Earth Sciences, v. 45, p. 673–675.

NESBITT, R. W., and SUN, S.-S., 1976, Geochemistry of Archaean spinifex textured peridotites and magnesian and low magnesian tholeiites: Earth and Planetary Science Letters, v. 31, p. 433–453.

PAINTER, M. G. M., and GROENEWALD, P. B., in prep., Mount Belches, W.A. Sheet 3335: Western Australia Geological Survey, 1:100 000 Geological Series.

PASSCHIER, C. W., 1994, Structural geology across a proposed Archaean terrane boundary in the eastern Yilgarn craton, Western Australia: Precambrian Research, v. 68, p. 43–64.

PHILLIPS, N., and ZHOU, T., 1999, Gold-only deposits and Archean granite: Society of Economic Geologists, Newsletter, no. 37, p. 1–13.

PURVIS, A. C., NESBITT, R. W., and HALLBERG, J. A., 1972, The geology of part of the Carr Boyd Rocks Complex and its associated nickel mineralization, Western Australia: Economic Geology, v. 67, p. 1093–1113.

REDMAN, B. A., and KEAYS, R. R., 1985, Archaean basic volcanism in the Eastern Goldfields Province, Yilgarn Block, Western Australia: Precambrian Research, v. 30, p. 113–152.

RIDLEY, J., 1993, Implications of metamorphic patterns to tectonic models of the Eastern Goldfields, *in* Kalgoorlie 93 — an international conference on crustal evolution, metallogeny, and exploration of the Eastern Goldfields *compiled by* P. R. WILLIAMS and J. A. HALDANE: Australian Geological Survey Organisation, Record 1993/54, p. 95–100.

SMITHIES, R. H., 1994a, Roe, W.A. Sheet 3436: Western Australia Geological Survey, 1:100 000 Geological Series.

SMITHIES, R. H., 1994b, Geology of the Roe 1:100 000 sheet: Western Australia Geological Survey, 1:100 000 Geological Series Explanatory Notes, 15p.

SOFOULIS, J., 1966, Widgiemooltha, W.A.: Western Australia Geological Survey, 1:250 000 Geological Series Explanatory Notes, 26p.

SOLOMON, M., and GROVES, D. I., 1994, The geology and origin of Australia's mineral deposits: Oxford Monographs in Geology and Geophysics, v. 24, 951p.

SPRAY, J. G., 1985, Dynamothermal transition zone between Archaean greenstone and granitoid gneiss at Lake Dundas, Western Australia: Journal of Structural Geology, v. 7, p. 187–203.

SWAGER, C. P., 1989a, Dunnsville, W.A. Sheet 3036: Western Australia Geological Survey, 1:100 000 Geological Series.

SWAGER, C. P., 1989b, Structure of the Kalgoorlie greenstones — regional deformation history and implications for the structural

setting of the Golden Mile gold deposits: Western Australia Geological Survey, Report 25, Professional Papers, p. 59–84.

SWAGER, C. P., 1993, Kurnalpi, W.A. Sheet 3336: Western Australia Geological Survey, 1:100 000 Geological Series.

SWAGER, C. P., 1994a, Geology of the Dunnsville 1:100 000 sheet: Western Australia Geological Survey, 1:100 000 Geological Series Explanatory Notes, 22p.

SWAGER, C. P., 1994b, Geology of the Kurnalpi 1:100 000 sheet: Western Australia Geological Survey, 1:100 000 Geological Series Explanatory Notes, 19p.

SWAGER, C. P., 1994c, Geology of the Menzies 1:100 000 sheet (and adjacent Ghost Rocks area): Western Australia Geological Survey, 1:100 000 Geological Series Explanatory Notes, 31p.

SWAGER, C. P., 1994d, Pinjin, W.A. Sheet 3437: Western Australia Geological Survey, 1:100 000 Geological Series.

SWAGER, C. P., 1994e, Geology of the Pinjin 1:100 000 sheet: Western Australia Geological Survey, 1:100 000 Geological Series Explanatory Notes, 22p.

SWAGER, C. P., 1994f, Yabboo, W.A. Sheet 3438: Western Australia Geological Survey, 1:100 000 Geological Series.

SWAGER, C. P., 1995a, Geology of the greenstone terranes in the Kurnalpi–Edjudina region, southeastern Yilgarn Craton: Western Australia Geological Survey, Report 47, 31p.

SWAGER, C. P., 1995b, Geology of the Edjudina and Yabboo 1:100 000 sheets: Western Australia Geological Survey, 1:100 000 Geological Series Explanatory Notes, 35p.

SWAGER, C. P., 1997, Tectono-stratigraphy of late Archaean greenstone terranes in the southern Eastern Goldfields, Western Australia: Precambrian Research, v. 83, p. 11–42.

SWAGER, C. P., GOLEBY, B. R., DRUMMOND, B. J., RATTENBURY, M. S., and WILLIAMS, P. R., 1997, Crustal structure of the granite–greenstone terranes in the Eastern Goldfields, Yilgarn Craton, as revealed by seismic reflection profiling: Precambrian Research, v. 83, p. 43–56.

SWAGER, C. P., and GRIFFIN, T. J., 1990a, Geology of the Archaean Kalgoorlie Terrane (northern and southern sheets): Western Australia Geological Survey, 1:250 000 Geological Map.

SWAGER, C. P., and GRIFFIN, T. J., 1990b, An early thrust duplex in the Kalgoorlie–Kambalda greenstone belt, Eastern Goldfields Province, Western Australia: Precambrian Research, v. 48, p. 63–73.

SWAGER, C. P., GRIFFIN, T. J., WITT, W. K., WYCHE, S., AHMAT, A. L., HUNTER, W. M., and McGOLDRICK, P. J., 1990, Geology of the Archaean Kalgoorlie Terrane — an explanatory note: Western Australia Geological Survey, Record 1990/12, 54p.

SWAGER, C. P., GRIFFIN, T. J., WITT, W. K., WYCHE, S., AHMAT, A. L., HUNTER, W. M., and McGOLDRICK, P. J., 1995, Geology of the Archaean Kalgoorlie Terrane — an explanatory note: Western Australia Geological Survey, Report 48, 26p.

SWAGER, C. P., and NELSON, D. R., 1997, Extensional emplacement of a high-grade granite gneiss complex into low-grade granite greenstones, Eastern Goldfields, Western Australia: Precambrian Research, v. 83, p. 203–219.

SWAGER, C. P., and RATTENBURY, M. S., 1994, Edjudina, W.A. Sheet 3338: Western Australia Geological Survey, 1:100 000 Geological Series.

SWAGER, C. P., and WITT, W. K., 1990, Menzies, W.A. Sheet 3138: Western Australia Geological Survey, 1:100 000 Geological Series.

SWAGER, C. P., WITT, W. K., GRIFFIN, T. J., AHMAT, A. L., HUNTER, W. M., McGOLDRICK, P. J., and WYCHE, S., 1992, Late Archaean granite–greenstone of the Kalgoorlie Terrane, Yilgarn Craton, Western Australia, *in* The Archaean: Terrains, processes and metallogeny *edited by* J. E. GLOVER and S. E. HO: University of Western Australia, Geology Department and University Extension, Publication no. 22, p. 107–122.

TOWNSEND, D. B., PRESTON, W. A., and COOPER, R. W., 1996, Mineral resources and locations Western Australia: digital dataset from MINEDEX: Western Australia Geological Survey, Record 1996/13, 19p.

van de GRAAFF, W. J. E., CROWE, R. W. A., BUNTING, J. A., and JACKSON, M. J., 1977, Relict early Cainozoic drainages in arid Western Australia: Zeitschrift für Geomorphologie N. F., v. 21, p. 379–400.

WARREN, P. H., and ELLIS, D. J., 1996, Mantle underplating, granite tectonics, and metamorphic P-T-t paths: Geology, v. 24, p. 663–666.

WHITE, R., and McKENZIE, D., 1989, Magmatism at rift zones: the generation of volcanic continental margins and flood basalts: Journal of Geophysical Research, v. 94(B6), p. 7685–7729.

WILLIAMS, I. R., 1970, Kurnalpi, W.A.: Western Australia Geological Survey, 1:250 000 Geological Series Explanatory Notes, 37p.

WILLIAMS, I. R., 1974, Structural subdivision of the Eastern Goldfields Province, Yilgarn Block: Western Australia Geological Survey, Annual Report 1973, p. 53–59.

WILLIAMS, I. R., GOWER, C. F., and THOM, R., 1976, Edjudina, W.A.: Western Australia Geological Survey, 1:250 000 Geological Series Explanatory Notes, 29p.

WILLIAMS, P. R., 1993, A new hypothesis for the evolution of the Eastern Goldfields Province, *in* Kalgoorlie 93 — an international conference on crustal evolution, metallogeny, and exploration in the Eastern Goldfields *compiled by* P. R. WILLIAMS and J. A. HALDANE: Australian Geological Survey Organisation, Record 1993/54, p. 77–83.

WILLIAMS, P. R., and WHITAKER, A. J., 1993, Gneiss domes and extensional deformation in the highly mineralized Archaean Eastern Goldfields Province, Western Australia: Ore Geology Reviews, v. 8, p. 141–162.

WITT, W. K., 1987, Stratigraphy and layered mafic/ultramafic intrusions of the Ora Banda sequence, Bardoc 1:100 000 sheet, Eastern Goldfields — an excursion guide, *in* The Second Eastern Goldfields Geological Field Conference *edited by* W. K. WITT and C. P. SWAGER: Geological Society of Australia (W.A. Division); 2nd Eastern Goldfields Geological Field Conference, 1987, Abstracts and Excursion Guide, p. 49–63.

WITT, W. K., 1992, Porphyry intrusions and albitites in the Bardoc–Kalgoorlie area, Western Australia, and their role in Archean epigenetic gold mineralization: Canadian Journal of Earth Sciences, v. 29, p. 1609–1622.

WITT, W. K., 1993a, Gold deposits of the Menzies and Broad Arrow areas, Western Australia — Part 1 of a systematic study of the gold mines of the Menzies–Kambalda region: Western Australia Geological Survey, Record 1992/13, 156p.

WITT, W. K., 1993b, Gold deposits of the Mt Pleasant – Ora Banda areas, Western Australia — Part 2 of a systematic study of the gold mines of the Menzies–Kambalda region: Western Australia Geological Survey, Record 1992/14, 104p.

WITT, W. K., 1993c, Gold deposits of the Kalgoorlie – Kambalda – St Ives, Western Australia areas — Part 3 of a systematic study of the gold mines of the Menzies–Kambalda region: Western Australia Geological Survey, Record 1992/15, 108p.

WITT, W. K., 1993d, Lithological and structural controls on gold mineralization in the Archaean Menzies–Kambalda area, Western Australia: Australian Journal of Earth Sciences, v. 40, p. 65–86.

WITT, W. K., 1994, Geology of the Bardoc 1:100 000 sheet: Western Australia Geological Survey, 1:100 000 Geological Series Explanatory Notes, 50p.

WITT, W. K., 1995, Tholeiitic and high-Mg mafic–ultramafic sills in the Eastern Goldfields Province, Western Australia: implications for tectonic settings: Australian Journal of Earth Sciences, v. 42, p. 407–422.

WITT, W. K., and DAVY, R., 1997, Geology and geochemistry of Archaean granites in the Kalgoorlie region of the Eastern Goldfields, Western Australia: a syn-collisional tectonic setting?: Precambrian Research, v. 83, p. 133–183.

WITT, W. K., DAVY, R., and CHAPMAN, D., 1991, The Mount Pleasant sill, Eastern Goldfields, Western Australia: iron-rich granophyre in a layered high-Mg intrusion: Western Australia Geological Survey, Report 30, Professional Papers, p. 73–92.

WITT, W. K., and HARRISON, N., 1989, Volcanic rocks and bounding shear zones of the Ora Banda greenstone sequence, *in* The 1989 Kalgoorlie gold workshops *edited by* I. M. GLACKEN: Australasian Institute Mining and Metallurgy and Eastern Goldfields Geological Discussion Group, Kalgoorlie, Western Australia, p. A2–A7.

WITT, W. K., HICKMAN, A. H., TOWNSEND, D., and PRESTON, W. A., 1998, Mineral potential of the Archaean Pilbara and Yilgarn Cratons, Western Australia: Australian Geological Survey Organisation, Journal of Australian Geology and Geophysics, v. 17, p. 201–221.

WITT, W. K., KNIGHT, J. T., and MIKUCKI, E. J., 1997, A synmetamorphic lateral fluid flow model for gold mineralization in the Archean southern Kalgoorlie and Norseman Terranes, Western Australia: Economic Geology, v. 92, p. 407–437.

WITT, W. K., and SWAGER, C. P., 1989a, Bardoc, W.A. Sheet 3137: Western Australia Geological Survey, 1:100 000 Geological Series.

WITT, W. K., and SWAGER, C. P., 1989b, Structural setting and geochemistry of Archaean I-type granites in the Bardoc–Coolgardie area of the Norseman–Wiluna belt, Western Australia: Precambrian Research, v. 44, p. 323–351.

WITT, W. K., SWAGER, C. P., and NELSON, D. R., 1996, $^{40}Ar/^{39}Ar$ and U–Pb constraints on the timing of gold mineralization in the Kalgoorlie gold field, Western Australia — a discussion: Economic Geology, v. 91, p. 792–795.

WITT, W. K., and VANDERHOR, F., 1998, Diversity within a unified model for Archaean gold mineralization in the Yilgarn Craton of Western Australia: an overview of the late-orogenic, structurally controlled gold deposits: Ore Geology Reviews, v. 13, p. 29–64.

WYBORN, L. A. I., 1993, Constraints on interpretations of lower crustal structure, tectonic setting and metallogeny of the Eastern Goldfields and Southern Cross Provinces provided by granite geochemistry: Ore Geology Reviews, v. 8, p. 125–140.

WYCHE, S., 1995, Mulline, W.A. Sheet 2938: Western Australia Geological Survey, 1:100 000 Geological Series.

WYCHE, S., 1998, Kalgoorlie, W.A. (2nd edition): Western Australia Geological Survey, 1:250 000 Geological Series Explanatory Notes, 31p.

WYCHE, S., 1999, Geology of the Mulline and Riverina 1:100 000 sheets: Western Australia Geological Survey, 1:100 000 Geological Series Explanatory Notes, 28p.

WYCHE, S., HUNTER, W. M., and WITT, W. K., 1992, Davyhurst, W.A. Sheet 3037: Western Australia Geological Survey, 1:100 000 Geological Series.

WYCHE, S., and SWAGER, C. P., 1995, Riverina, W.A. Sheet 3038: Western Australia Geological Survey, 1:100 000 Geological Series.

WYCHE, S., and WITT, W. K., 1994, Geology of the Davyhurst 1:100 000 sheet: Western Australia Geological Survey, 1:100 000 Geological Series Explanatory Notes, 21p.

YEATS, C. J., and McNAUGHTON, N. J., 1997, Significance of SHRIMP II U–Pb geochronology on lode-gold deposits of the Yilgarn Craton, *in* Kalgoorlie 97 – an international conference on crustal evolution, metallogeny, and exploration of the Yilgarn craton — an update *compiled by* K. F. CASSIDY, A. J. WHITAKER, and S. F. LIU: Australian Geological Survey Organisation, Record 1997/41, Extended Abstracts, p. 125–130.

YEATS, C. J., McNAUGHTON, N. J., RUETTGER, D., BATEMAN, R., GROVES, D. I., HARRIS, J. L., and KOHLER, E., 1999, Evidence for Archean lode gold mineralization in the Yilgarn Craton, Western Australia: a SHRIMP U–Pb study of intrusive rocks: Economic Geology, v. 94, p. 1259–1276.

YEATS, C. J., and VANDERHOR, F., 1998, Archaean lode-gold deposits, *in* Exploration models for major Australian mineral deposit types: Australian Geological Survey Organisation, Journal of Australian Geology and Geophysics, v. 17, p. 253–258.

Appendix 1

Rock codes and definitions

Regolith — Quaternary rocks and features

Qa	Alluvium — clay, silt, sand, and gravel in channels and floodplains
Qrbs	Residual, deep-red, unconsolidated soil overlying Proterozoic mafic and ultramafic dykes

Cainozoic rocks and features

Czc	Colluvium — gravel and sand as proximal sheetwash and talus
Czcf	Ferruginous gravel or reworked laterite
Czcg	Quartzofeldspathic sand and gravel over and adjacent to granitic rocks
Cze	Weathered rock; protolith unrecognizable
Czl	Playa deposits — saline and gypsiferous evaporites, clay, silt, and sand in playa lakes
Czld	Dune deposits — sand, silt, and gypsum in stabilized dunes adjacent to playa lakes
Czls	Mixed playa and sandplain terrain, commonly palaeodrainages
Czr	Residual regolith and reworked products, undivided; mainly ferruginous and carbonaceous duricrust; minor silcrete and calcrete
Czrf	Ferruginous duricrust or ferricrete or both; massive to rubbly; locally reworked
Czrk	Calcrete
Czrm	Magnesite, derived from ultramafic rock
Czru	Siliceous caprock over ultramafic rock; locally includes chalcedony and chrysoprase
Czrz	Silcrete
Czs	Sandplain deposits — yellow sand with minor silt and clay; limonitic pisoliths near base; low, vegetated dunes locally common; lateritic pebbles
Czw	Sheetwash — clay, silt, and sand as extensive fans; locally ferruginous or gravelly or both

Tertiary rocks

TE	EUNDYNIE GROUP: sandstone; siltstone, mudstone, spongolitic or bituminous, calcareous sandstone, bioclastic calcarenite; poorly indurated, laterized cap
Ts	Sandstone and silcrete; coarse, angular, poorly sorted quartz sand in a clay-rich matrix; partly silicified Permian rocks

Permian rocks

Ps	Permian sedimentary rocks; quartz–pebble conglomerate and poorly sorted sandstone; glacigene deposit

Proterozoic mafic dykes

P_dy	Proterozoic mafic and ultramafic dykes; locally known as the Widgiemooltha dyke suite
P_dyb	Binneringie Dyke; as for *P_dy*
P_dyc	Celebration Dyke; as for *P_dy*
P_dyg	Gidgi Dyke; as for *P_dy*
P_dyi	Pinjin Dyke; as for *P_dy*
P_dyjn	Norite in Jimberlana Dyke; as for *P_dy*
P_dyjx	Pyroxenite in Jimberlana Dyke; as for *P_dy*
P_dyk	Kalpini Dyke; as for *P_dy*
P_dyl	Ballona Dyke; as for *P_dy*
P_dyp	Parkeston Dyke; as for *P_dy*
P_dyr	Randalls Dyke; as for *P_dy*

Dykes and veins

a	Aplite dyke
g	Granite dyke
lp	Lamprophyre dyke
p	Pegmatite dyke or pod
q	Quartz vein or pod

Granitoid rocks

Ag	Granitoid rock, undivided
Agba	Foliated granitoid interleaved with subordinate amphibolite
Agd	Quartz diorite to quartz monzodiorite, with clinopyroxene, amphibole or biotite or both; small dykes and stocks
Agdp	Diorite or monzodiorite; plagioclase phenocrysts, K-feldspar megacrysts; locally quartz phyric
Agf	Strongly foliated granitoid; locally gneissic; includes amphibolite lenses
Agg	Granodiorite; microgranitoid enclaves locally
Agm	Monzogranite, undivided; biotite bearing; local hornblende; commonly medium to coarse grained; minor granodiorite

Agmf Strongly foliated biotite monzogranite, medium to coarse grained; minor granodiorite and pegmatite dykes

Agmh Hornblende–biotite monzogranite; alkali feldspar megacrysts present locally

Agmp Porphyritic monzogranite

Agp Porphyritic granitoid, undivided

Agq Quartz syenite to quartz monzonite; horneblende bearing; minor clinopyroxene locally; numerous mafic enclaves

Agr Granitoid, recrystallized (hornfelsed)

Ags Syenite and quartz syenite; numerous mafic schlieren and xenoliths; porphyritic locally

Agsq Quartz syenite

Ag Tonalite

Agy Syenogranite

Granitoid rocks — named

Aggcb CROWBAR GRANODIORITE: medium- to coarse-grained, equigranular granodiorite; domal within regional anticline; pervasive foliation

Aggcr CREDO GRANODIORITE: medium-grained biotite granodiorite; domal within regional anticline; foliation strongest on contacts with greenstones

Aggdd DOYLE DAM GRANODIORITE: post-D_2 to syn-D_3, K-feldspar-phyric; massive to weakly foliated; discordant to greenstones

Aggde DEPOT GRANODIORITE: medium- to coarse-grained hornblende leuco-granodiorite –tonalite; foliation moderate except in numerous shear zones; intrusive western contact

Aggdn DUNNSVILLE GRANODIORITE: medium to coarse grained; penetrative foliation, sub-horizontal mineral lineation; sheared contacts with greenstones

Agglb LIBERTY GRANODIORITE: fine to coarse grained; locally monzogranitic; massive; contacts discordant with greenstones and early foliation

Aggot OLIVER TWIST GRANODIORITE: biotite granodiorite, locally monzogranitic; domal within D_2 antiform; sheared contacts with greenstones

Agmbl BALI MONZOGRANITE: coarse grained, K-feldspar megacrysts; internally massive, intense contact-parallel foliation with down-dip mineral lineation

Agmbo BORA MONZOGRANITE: equigranular, medium-grained biotite monzogranite; scattered mafic enclaves and strong foliation

Agmbr BURRA MONZOGRANITE: coarse grained, biotite bearing, K-feldspar megacrysts; commonly homogeneous, deformed at margins; possibly composite

Agmby BULYAIRDIE MONZOGRANITE: medium grained, hornblende bearing, perthitic K-feldspar megacrysts; unfoliated

Agmca CAWSE MONZOGRANITE: coarse grained, equigranular, biotite bearing; domal in D_2 anticlines; moderate to weak foliation; sheared contacts

Agmcl CALOOLI MONZOGRANITE: equigranular, medium to coarse grained, biotite bearing; commonly massive, foliated near margins

Agmco COWARNA MONZOGRANITE: leucocratic, medium grained, biotite bearing; K-feldspar phenocrysts

Agmcv COMET VALE MONZOGRANITE: fine to medium grained; porphyritic; local foliation; discordant contacts with greenstones

Agmcw CLARK WELL MONZOGRANITE: biotite bearing, seriate grain size

Agmga GALVALLEY MONZOGRANITE: K-feldspar-phyric biotite monzogranite; aligned K-feldspar, biotite, and xenoliths define foliation locally

Agmgd GOAT DAM MONZOGRANITE: equigranular biotite monzogranite; strongly deformed mafic enclaves locally

Agmgi GOODIA MONZOGRANITE: equigranular, fine- to medium-grained biotite monzogranite to granodiorite; strongly foliated margins

Agmgo GOONGARRIE MONZOGRANITE: locally K-feldspar-phyric; biotite bearing; domal within D_2 anticline; weak to moderate foliation; deformed contacts

Agmjo JORGENSON MONZOGRANITE: equigranular monzogranite; strongly sheared marginal areas

Agmju JUNGLE MONZOGRANITE: biotite monzogranite

Agmka KARRAMINDIE MONZOGRANITE: fine- to medium-grained biotite monzogranite; unfoliated

Agmld LAKE DUNDAS MONZOGRANITE: sub-equigranular, medium- to coarse-grained biotite monzogranite

Agmmn MENANGINA MONZOGRANITE: biotite monzogranite with prominent K-feldspar megacrysts; cut by pegmatite and aplite

Agmmu MUNGARI MONZOGRANITE: medium-grained, equigranular, two-mica monzogranite; massive

Agmmy MYSTERY MONZOGRANITE: fine-grained, equigranular biotite monzogranite

Agmnm NINE MILE MONZOGRANITE: coarse grained, porphyritic, biotite bearing; penetrative foliation moderate to weak, strongest at contacts with greenstones; domal core to D_2 anticline

Agmon LONE HAND MONZOGRANITE: leuco-granite; massive; contacts discordant with greenstones and foliation in early granite

Agmro ROWLES LAGOON MONZOGRANITE: medium- to coarse-grained biotite monzo-granite; locally plagioclase-phyric; foliated

Agmst SILT DAM MONZOGRANITE: seriate biotite monzogranite; marginal zones have contact-parallel foliation with steep mineral lineation

Agmtg TWO GUM MONZOGRANITE: medium-grained, porphyritic, biotite–hornblende monzogranite

Agmtr THEATRE ROCKS MONZOGRANITE: sub-equigranular, fine- to medium-grained biotite monzogranite to granodiorite; post-D_2 to syn-D_3

Agmul ULARRING MONZOGRANITE: even-grained monzogranite

Agmwi WIDGIEMOOLTHA MONZOGRANITE: foliated porphyritic monzogranite; microcline porphyroclasts

Agmwo WOOLGANGIE MONZOGRANITE: recrystallized monzogranite and granodiorite

Agmya YARRI MONZOGRANITE: biotite monzogranite; K-feldspar phenocrysts; pervasive foliation and quartz veins are folded locally

Agmyi YINDI MONZOGRANITE: fine- to medium-grained, equigranular monzogranite

Agtkn KINTORE TONALITE: medium-grained biotite tonalite

Agtlb LAKE BRAZIER TONALITE: highly variable biotite- and hornblende-bearing tonalite to granodiorite

Agyad FAIR ADELAIDE SYENOGRANITE: medium grained, equigranular and massive; contacts discordant with greenstones and early granite foliation

Agzpo PORPHYRY QUARTZ MONZONITE: medium to coarse grained; biotite after hornblende; prominent K-feldspar phenocrysts

Granitoid complexes

Ag_B BULDANIA GRANITOID COMPLEX: major composite batholith; predominantly seriate biotite–hornblende granodiorite

Ag_E ERAYINIA GRANITOID COMPLEX: syenite to monzogranite; hornblende or clinopyroxene bearing; variable foliation; strong shear in mafic enclaves

Ag_{PI} PIONEER GRANITOID COMPLEX: foliated biotite monzogranite; gneiss enclaves

Ag_{RH} RED HILL GRANITOID COMPLEX: syenogranite, monzogranite porphyry, and granodiorite porphyry

Gneisses

An Complexly deformed, massive and foliated quartzofeldspathic rocks; gneissic in part; minor calc-silicate and mafic components

Anbai Amphibolitic and intermediate gneiss; commonly foliated or lineated or both; commonly clinopyroxene bearing, locally garnet bearing

Anbi Intermediate to basic schist or gneiss; includes some acid components

Anfi FIFTY MILE TANK GNEISS: quartzofeldspathic gneiss, porphyroclastic; minor monzogranite; schistose mafic to ultramafic enclaves common

Anfip FIFTY MILE TANK GNEISS: as for above (*Anfi*), with numerous deformed pegmatite veins

Ang Quartzofeldspathic or banded granitoid gneiss; locally migmatitic; mafic bands

Anga Granodiorite and tonalite gneiss with streaky augen of quartz and granular feldspar

Ano Orthogneiss; interleaved with amphibolite

Metamorphic rocks — low to moderate grades

Ala Amphibolite; schistose; clinopyroxene, cummingtonite, with or without garnet present locally; protolith unknown

Alai Grunerite–hornblende–magnetite–plagioclase rock type; moderately to weakly foliated

Alan Banded amphibolite

Alb Fine- to medium-grained mafic schist; interlayered with felsic or sedimentary rocks or both locally

Albf Felsic to mafic rock, highly schistose and recrystallized; characterized by feldspar–quartz–amphibole schist

Albuf Strongly deformed and carbonatized, interleaved felsic volcaniclastic, ultramafic, and mafic volcanic rocks; mainly within Bardoc Tectonic Zone

Alc Massive carbonate rock; recrystallized

Ald Quartz–aluminosilicate rock within felsic volcanic sequences; highly poikilitic andalusite; minor kyanite locally

Alk Felsic schist with kyanite; locally andalusite or chloritoid or both present; quartz clasts preserved locally

Alld Quartz–chloritoid–aluminosilicate rock; with andalusite or kyanite or both; local quartz phenocrysts; within felsic volcanic and volcaniclastic rock

Allk Quartz–chloritoid–kyanite rock

Alqk Siliceous quartzofeldspathic schist containing kyanite

Alu Felsic quartz–fuchsite or andalusite–quartz–fuchsite rock; laminated, complexly veined, or massive; local chert or quartz–mica schist interlayers

Alum Fuchsite–quartz(–andalusite) rock with interlayered quartz–feldspar–muscovite schist and minor tremolite schist

Aly Phyllonite, fine-grained mafic cataclasite; resembles phyllite

Mafic intrusive rocks (metamorphosed)

Ao	Mafic intrusive rock, undivided
Aod	Dolerite
Aodp	Porphyritic dolerite, with feldspar phenocrysts
Aog	Gabbro, massive or undivided; minor pyroxenite or quartz gabbro components
Aogl	Leucogabbro; locally magnetite rich
Aogp	Porphyritic gabbro with plagioclase phenocrysts
Aogpg	Glomeroporphyritic gabbro
Aogx	Pyroxenitic gabbro
Aon	Gabbronorite and norite
Aox	Pyroxenite and pyroxenitic gabbro; feldspar phenocrysts locally

Layered mafic to ultramafic intrusive rocks (metamorphosed)

AaMEl	Leucogabbro and plagioclase-rich gabbronorite in Mount Ellis Intrusion
AaMEo	Gabbro in Mount Ellis Intrusion
AaMEqy	Iron-rich quartz gabbro with granophyric segregations in Mount Ellis Intrusion
AaMEx	Pyroxenite in Mount Ellis Intrusion
AaMIo	Gabbro in Mission Intrusion
AaMIp	Peridotite in Mission Intrusion
AaMIx	Pyroxenite in Mission Intrusion
AaMPd	Massive olivine orthocumulate at base of Mount Pleasant Intrusion
AaMPl	Leucogabbro and plagioclase-rich gabbronorite in Mount Pleasant Intrusion
AaMPn	Gabbronorite marker horizon in Mount Pleasant Intrusion
AaMPo	Gabbro in Mount Pleasant Intrusion
AaMPx	Pyroxenite in Mount Pleasant Intrusion
AaMPy	Iron-rich granophyre marker horizon in Mount Pleasant Intrusion
AaMTo	Gabbro in Mount Thirsty Intrusion; minor granophyric and quartz gabbro
AaMTp	Peridotite in Mount Thirsty Intrusion
AaMTqy	Quartz gabbroic and granophyric segregations in gabbro in Mount Thirsty Intrusion
AaMTx	Pyroxenite in Mount Thirsty Intrusion; includes dunite and olivine bronzitite layers, and minor peridotite
AaOBd	Massive olivine orthocumulate at base of Ora Banda Intrusion
AaOBn	Gabbronorite in Ora Banda Intrusion
AaOBqy	Quartz gabbro and granophyre in Ora Banda Intrusion; late differentiate
AaOBx	Bronzitite and norite in Ora Banda Intrusion
AaORo	Gabbro in Orinda Intrusion
AaORy	Iron-rich granophyre in Orinda Intrusion
AaPWl	Leucogabbro in Powder Intrusion
AaPWo	Gabbro in Powder Intrusion
AaTMo	Gabbro in Three Mile Intrusion

Sedimentary chemical rocks (metamorphosed)

Ac	Chert, banded chert; locally includes silicified (black) shale, slate, or exhalite
Aci	Banded iron-formation, oxide facies; finely interleaved magnetite- and quartz-rich chert or siliceous slate or both
Acis	Banded iron-formation, silicate facies; quartz–magnetite(–grunerite–hornblende) rock
Acs	Chert and fine-grained siliceous sedimentary rocks (shale and mudstone)
Acw	Grey-white banded chert, locally iron rich; includes siliceous grey-black shale, mylonite, and minor shale and slate
Acws	Ferruginous schist unit within banded cherts

Sedimentary clastic rocks (metamorphosed)

As	Sedimentary rock, undivided; includes sandstone, siltstone, shale, and chert; may have a volcaniclastic component
Asc	Conglomerate with subordinate sandstone; pebbles and boulders include granitoids, porphyritic felsite, basites, and chert; matrix or clast supported
Ascc	Conglomerate and breccia with chert clasts and fine-grained siliceous matrix
Ascf	Oligomictic conglomerate with clasts mainly of felsic volcanic rock; subordinate sandstone; matrix psammitic
Asckw	Conglomerate, sandy conglomerate, and pebbly sandstone of the lower KURRAWANG FORMATION
Asckwi	Banded iron-formation pebble horizon of the lower KURRAWANG FORMATION
Ascq	Oligomictic conglomerate with clasts mainly of quartz, quartzose sandstone, and minor shale
Asf	Volcaniclastic, tuffaceous, and other felsic sedimentary rocks; foliated; commonly deeply weathered and kaolinized
Asfc	Quartzofeldspathic pebbly sandstone; volcaniclastic derivation
Asfcc	Brown, fine-grained quartzofeldspathic rock associated with grey-white banded chert; includes local banded chert pebbles
Asfi	Intermediate sedimentary or volcaniclastic rocks; bedded, banded, foliated; amphibole-biotite–feldspar–quartz(–garnet) schist; local slate
Asfip	Conglomeratic intermediate sedimentary or volcaniclastic rocks; pebbles of amphibole–feldspar–quartz–garnet rock and feldspar-phyric felsic schist

Ash Shale–slate, in part chert; minor siltstone and sandstone; foliated; commonly silicified

Ashc Grey to black slate and interlayered quartzo-feldspathic schist with chert layers and lenses

Ashg Graphitic black shale or slate

Asm Biotite-bearing pebbly sandstone, sandstone, and siltstone of the Merougil beds

Asq Medium-grained quartzite; locally quartz siltstone and quartz–muscovite schist

Asqf Cream and brown, layered, foliated and mylonitic quartzite, and associated fine-grained siliceous rocks

Ass Sandstone to siltstone, locally partly conglomerate

Ast Sandstone; partly polymictic conglomerate, local volcaniclastic component with associated massive iron sulfide body; locally pelitic

Asti Ferruginous sandstone; includes green quartzite and mica schist

Astkw Sandstone and pebbly sandstone of the upper KURRAWANG FORMATION

Asw Poorly sorted wacke; local grading from wacke to pelite suggests deposition from turbidity currents or pyroclastic flows

Asx Sedimentary breccia

Felsic to intermediate igneous rocks (metamorphosed)

Af Felsic volcanic and volcaniclastic rocks, undivided; includes tuff; commonly deeply weathered and kaolinized

Afd Dacite; commonly tuffaceous; locally brecciated

Afdp Felsic intrusive porphyry (predominantly feldspar phenocrysts); porphyritic dacite (to rhyodacite)

Afi Intermediate rock, mainly dacite to andesite, includes minor rhyodacite, rhyolite, and basaltic andesite; amygdaloidal locally

Afih Hornblende–plagioclase porphyry; felsic to intermediate

Afil Layered intermediate rock

Afip Intermediate porphyritic volcanic or intrusive rock; numerous plagioclase phenocrysts; variably foliated

Afis Intermediate hornblende–biotite–quartz–feldspar(–garnet) schist; variable hornblende content; interlayered with felsic and mafic schists

Afisl Intermediate schist with feldspar clasts and chlorite aggregates; includes chlorite–carbonate, chlorite–sericite, epidote–chlorite schists

Afiv Intermediate volcanic rock; local fragmental textures; variably foliated and chloritized; local intermediate schist and greywacke interlayers

Afix Intermediate volcanic rock, with fragmental and tuffaceous textures; epidote and carbonate alteration

Afp Feldspar–quartz porphyry; dacite to rhyodacite; volcanic, subvolcanic, or intrusive; locally schistose

Afpa Felsic albite-rich, quartz-poor porphyry; variably foliated

Afpp Felsic intrusive porphyritic rock; plagioclase phenocrysts; locally schistose

Afpq Felsic to intermediate intrusive porphyry with quartz or feldspar phenocrysts or both; commonly foliated

Afpx Quartz–feldspar porphyry, with xenoliths

Afr Rhyolite lava flows, quartz-phyric, locally tuffaceous; weak to schistose foliation

Afs Schistose quartzofeldspathic micaceous rock derived from felsic volcanic or volcaniclastic protolith

Aft Felsic tuffaceous rock; finely banded; foliated; fine to medium grained; quartz and feldspar phenocrysts

Afv Felsic volcanic and volcaniclastic rocks; variably foliated; quartz or feldspar phenocrysts or both; includes fragmental rock and finely layered tuff

Afx Felsic fragmental rock, coarse grained; volcanic or volcaniclastic derivation

Mafic extrusive rocks (metamorphosed)

Ab Fine to very fine grained basite, undivided

Aba Amphibolite, fine to medium grained, undivided; commonly weakly foliated or massive

Abd Basalt–dolerite; fine-grained basalt with common dolerite-textured layers or zones

Abdo Basalt, dolerite, and gabbro; thin interleaved units (probably differentiated flows)

Abdp Blastoporphyritic basalt–dolerite with relict plagioclase phenocrysts

Abf Foliated, fine-grained basite; locally hornfelsed or epidotized

Abg Basite interleaved with minor foliated granitoid rock

Abi Basaltic andesite or andesite; amygdaloidal; locally feldspar-phyric

Abic Carbonatized (massive) basaltic andesite

Abip Basaltic andesite with plagioclase phenocrysts; variably foliated

Abiv Basaltic andesite; plagioclase and hornblende phenocrysts; locally fragmental; variably foliated; chlorite and carbonate alteration common

Abl Pillow basalt; flow-top breccia with varioles or spinifex locally; includes Kambalda Footwall Basalt

Abm Komatiitic basalt; pyroxene spinifex common; variolitic, pillowed locally

Abmo Variolitic komatiitic basalt

Abp Porphyritic basalt; medium- to coarse-grained plagioclase phenocrysts; local intense epidotization

Abpf Finely porphyritic basalt; plagioclase phenocrysts <1 mm

Abpg Glomeroporphyritic basalt

Abs Fine-grained schist derived from basalt; amphibole–chlorite assemblages locally strongly metasomatized, carbonatized

Abt Basaltic tuff (subsurface only)

Abtx Mafic to intermediate schist with small hornblende and feldspar fragments that suggest tuffaceous protolith, fine layering, locally lensoidal

Abu Mafic–ultramafic rock; commonly weathered; chloritic; protolith unknown

Abv Basalt, undivided; includes feldspar–hornblende or chlorite schist; locally porphyritic; doleritic in parts

Abvc Basalt, extensively carbonatized; includes massive carbonate lenses

Abve Epidotized basalt

Abx Basaltic fragmental rock; agglomerate, or hyaloclastite peperite or breccia

Aby Amygdaloidal basalt

Ultramafic rocks (metamorphosed)

Au Ultramafic rock, undivided; includes talc–chlorite(–carbonate) and tremolite–chlorite schists

Auc Talc–carbonate(–serpentine) rock; commonly schistose

Aud Dunite; massive serpentinite with preserved olivine cumulate microstructures

Auk Komatiite; olivine spinifex texture; tremolite–chlorite, serpentinite, carbonate assemblages; silicified or weathered

Aukc Komatiite, extensively carbonatized; includes carbonate–talc–chlorite schist and massive carbonate lenses

Aukl Komatiite (as for *Auk*); pillowed to massive

Aup Peridotite, commonly serpentinized; relict olivine-cumulate texture; locally rodingitized or silicified

Aupx Peridotite and pyroxenite

Aur Tremolite(–chlorite–talc–carbonate) schist; locally serpentinitic; derived from komatiitic basalt or pyroxenite

Aurp Tremolite schist, with relicts of amphibole after pyroxene phenocrysts ; locally massive

Aus Serpentinite, commonly massive

Aut Talc–chlorite(–carbonate) schist; minor tremolite–chlorite schist

Aux Pyroxenite; commonly associated with peridotite in layered sills; variably tremolitized, locally schistose

Auxo Orthopyroxenite

Appendix 2

MINEDEX commodity groups, mineralization types, and reference abbreviations

Commodity groups and minerals

Notes: Mineral order represents the sequence of relative importance within the specific commodity group. Contaminant or gangue minerals in potential products have an order of 500 or greater.

Commodity group	*Order*	*Mineral*	*Mineral abbrev.*
Alunite	10	Alunite	ALUM
	20	Potash	K_2O
	30	Gypsum	$CaSO_4$
Andalusite	10	Andalusite	AND
Antimony	10	Antimony	Sb
Arsenic	10	Arsenic	As
Asbestos	10	Asbestos	ASB
Barite	10	Barite	$BaSO_4$
Bauxite–alumina	10	Alumina (available)	ABEA
	20	Bauxite	BAUX
	500	Reactive silica	$RESIO_2$
Bismuth	10	Bismuth	Bi
Chromite–platinoids	10	Chromite	Cr_2O_3
	20	Platinum	Pt
	25	Palladium	Pd
	31	Rhodium	Rh
	40	PGE	PGE
	50	PGE + gold	PGEAu
	55	Gold	Au
	60	Nickel	Ni
	70	Copper	Cu
	100	Iron	Fe
Clays	10	Attapulgite	ATTAP
	20	Bentonite	BENT
	30	Kaolin	KAOLIN
	35	Saponite	SAPON
	40	Cement clay	C.CLAY
	60	White clay	W.CLAY
Coal	10	Coal	COAL
	20	Lignite	LIGN
Construction materials	10	Aggregate	AGGREG
	20	Gravel	GRAVEL
	30	Sand	SAND
	40	Rock	ROCK
	50	Soil	SOIL
	300	Vanadium	V_2O_5
	310	Titanium dioxide	TiO_2
	320	Iron	Fe
Copper–lead–zinc	10	Zinc	Zn
	20	Copper	Cu
	30	Lead	Pb
	40	Silver	Ag
	50	Gold	Au
	60	Molybdenum	Mo
	65	Cobalt	Co
	70	Barium	Ba
	80	Cadmium	Cd
	90	Tungsten	WO_3
Diamonds	10	Diamond	DIAM
Diatomite	10	Diatomite	DIATOM
Dimension stone	10	Dimension stone	DIM.ST
	20	Sandstone	SST
	30	Quartzite	QZTE
	40	Limestone	LST
	50	Black granite	B.GRAN
	55	Granite	GRAN
	60	Marble	MARBLE
	70	Dolerite	DOLER
	80	Slate	SLATE
	90	Spongolite	SPONG
Dolomite	10	Dolomite	DOLOM
Fluorite	10	Fluorite	CaF_2
Gem, semiprecious and ornamental stones	10	Amethyst	AMETH
	20	Emerald	EMER
	30	Opal	OPAL
	32	Tourmaline	TOURM
	35	Chrysoprase	CHRYSP
	37	Malachite	MALACH
	40	Tiger eye	T.EYE
	45	Jasper	JASPER
	50	Zebra rock	ZEBRA
	60	Chert (green)	CHERT
Gold	10	Gold	Au
	20	Silver	Ag
	30	Copper	Cu
	40	Nickel	Ni
	50	Cobalt	Co
	54	Lead	Pb
	55	Zinc	Zn
	60	Tungsten	WO_3
	70	Molybdenum	Mo
	500	Antimony	Sb
	510	Arsenic	As
Graphite	10	Graphite	GRAPH
	20	Carbon (fixed)	C
Gypsum	10	Gypsum	$CaSO_4$
	30	Alunite	ALUM
	500	Salt	SALT
Heavy mineral sands	10	Heavy minerals	HM
	20	Ilmenite	ILM
	30	Leucoxene	LEUCO
	50	Rutile	RUTILE
	60	Zircon	ZIRCON
	70	Monazite	MONAZ
	80	Xenotime	XENO
	90	Garnet	GARNET
	100	Kyanite	KYAN
	130	Synthetic rutile	SYN.R
	510	Slimes	SLIMES
	520	Titanium dioxide	TiO_2
	530	Zirconia	ZrO_2
Industrial pegmatite minerals	10	Mica	MICA
	20	Beryl	BERYL
	30	Feldspar	FELDS
	35	Alkalis	K+Na
	37	Alumina	Al_2O_3

Appendix 2 (continued)

Commodity group	Order	Mineral	Mineral abbrev.
	40	Quartz	QUARTZ
	510	Alumina	Al_2O_3
	520	Silica	SiO_2
	525	Sulfur	S
	530	Loss on ignition	LOI
Limestone – limesand	10	Calcium carbonate	$CaCO_3$
	20	Limestone – limesand	LIME
	50	Shell – grit	SHELL
	70	Chalk	CHALK
	100	Lime	CaO
	200	Magnesite	$MgCO_3$
	501	Silica	SiO_2
Magnesite	10	Magnesite	$MgCO_3$
	10	Manganese	Mn
	100	Iron	Fe
	510	Silica	SiO_2
	520	Alumina	Al_2O_3
	530	Phosphorus	P
Nickel	10	Nickel	Ni
	20	Copper	Cu
	25	Cobalt	Co
	30	Nickel + copper	Ni+Cu
	35	Nickel equivalent	Ni EQU
	40	Gold	Au
	50	Platinum	Pt
	55	Palladium	Pd
	70	Chromite	Cr O
	80	Silver	Ag^{2} ^{3}
	90	Magnesia	MgO
	500	Silica	SiO
Other	10	Gold	Au^{2}
Peat	10	Peat	PEAT
Phosphate	10	Phosphate	P O
Pigments	10	Ochre	$^{2}O^{5}$CHRE
	20	Hematite pigment	HEM
Potash	10	Potash	K O
	10	Sulfur	S^{2}
	20	Iron	Fe
	30	Zinc	Zn
	40	Copper	Cu
	50	Lead	Pb
Rare earths	10	Rare earth oxides	REO
	20	Yttrium	Y_2O_3
	25	Lanthanides	LnO
	30	Tantalite	Ta_2O_5
	40	Columbite	Nb_2O_5
	50	Tin (cassiterite)	SnO_2
	60	Xenotime	XENO
	70	Gallium	Ga
	80	Zirconia	ZrO_2
	90	Hafnium	HfO_2
	100	Beryl	BERYL
	510	Alumina	Al_2O_3
Salt	10	Salt	SALT
	20	Gypsum	$CaSO_4$
Silica – silica sand	10	Silica	SiO2
	20	Sand	SAND
	30	Quartzite	QZTE
	510	Ferric oxide	Fe_2O_3
	520	Titanium dioxide	TiO_2
	530	Alumina	Al_2O_3
	540	Heavy minerals	HM
Talc	10	Talc	TALC
Tin–tantalum–lithium	10	Tin (cassiterite)	SnO_2
	20	Tantalite	Ta_2O_5
	30	Columbite	Nb_2O_5
	40	Spodumene	Li_2O
	50	Kaolin	KAOLIN
	510	Ferric oxide	Fe_2O_3
Tungsten–molybdenum	10	Tungsten	WO_3
	20	Molybdenum	Mo
	30	Copper	Cu
	40	Antimony	Sb
	50	Vanadium	V_2O_5
	60	Gold	Au
Uranium	10	Uranium	U_3O_8
	20	Vanadium	V_2O_5
	30	Copper	Cu
Vanadium–titanium	10	Vanadium	V_2O_5
	20	Titanium dioxide	TiO_2
	30	Iron	Fe
	40	Gold	Au
Vermiculite	10	Vermiculite	VERMIC

Appendix 2 (continued)

Mineralization types

Abbreviation	Mineralization type
ALLAKE	Alunite in lake sediments
ANDSED	Andalusite in metasedimentary rocks
ASBAMP	Metasomatic asbestos deposits in amphibolites
ASBBIF	Asbestos deposits in banded iron-formations
ASBDLM	Asbestos deposits in dolomite intruded by dolerite
ASBSER	Asbestos deposits in serpentinites
ASBUM	Asbestos veins in ultramafic rocks
ASMASS	Stratiform massive arsenopyrite in metasediments
ASQTZV	Arsenic associated with auriferous quartz veins
AUALL	Alluvial–eluvial gold deposits
AUBIF	Gold in banded iron-formation and related sediments
AUCONG	Gold in conglomerate within greenstones
AUEPI	Epigenetic gold deposits in precambrian terrains
AUFVOL	Felsic volcanic rocks and volcanogenic sediments containing auriferous quartz veins or shear zones or both
AUGRAN	Gold deposits along granite–greenstone contacts and in granitoid rocks
AULAT	Lateritic gold deposits
AUPLAC	Precambrian placer gold deposits
AUPOR	Gold associated with felsic porphyry within greenstones
AUSHER	Basalt or dolerite or both containing auriferous quartz veins along faults or shear zones or both
AUSTOK	Dolerite or gabbro containing auriferous quartz stockworks or veins
AUSYN	Syngenetic gold deposits in precambrian terrains
AUUM	Gold deposits in ultramafic rocks
BABED	Stratabound bedded barite deposits
BACAV	Vein and cavity fill deposits
BAPEGM	Pegmatite-hosted barite deposits
BAUKAR	Karstic bauxite deposits
BAULAT	Lateritic bauxite deposits
BIPEGM	Bismuth in quartz-rich pegmatites
BIQTZV	Bismuth associated with gold mineralization
BMMASS	Volcanogenic Cu–Zn deposits
BMMISS	Mississippi valley-type Pb–Zn deposits
BMPOR	Porphyry Cu–Mo deposits
BMSED	Sedimentary Cu–Pb–Zn deposits
BMSHER	Base metal deposits in quartz veins and/or shear zones
CADUNE	Limesand in coastal dune sands
CALAKE	Calcareous material in lake sediments
CALIME	Limestone deposits
CASEA	Offshore limesand deposits
CLBED	Bedded sedimentary clay deposits
CLRES	Residual clay deposits
CLTRAN	Transported clay deposits
COJSBT	Jurassic sub-bituminous coal
COLIGN	Eocene lignite deposits
COPBIT	Permian bituminous coal
COPSBT	Permian sub-bituminous coal
CRLAT	Lateritic chromium deposits
CRPGLY	PGEs and chromium in layered mafic–ultramafic intrusions
CRPGUM	PGEs and chromium in metamorphosed mafic–ultramafic rocks
DIAALL	Alluvial–eluvial diamond deposits
DIALAM	Lamproitic diamond deposits
DLMBED	Dolomite deposits in sedimentary sequences
DLMKAN	Residual kankar (dolomite) deposits
DLMLAK	Dolomite deposits associated with lake sediments
DLMSOM	Metasomatic dolomite deposits
DTMLAK	Diatomaceous lake deposits
FEBIF	Primary banded iron-formation deposits
FEBR	Iron ore deposits in the Brockman iron-formation
FEGGT	Iron ore deposits in granite–greenstone terrains
FEMM	Iron ore deposits in the Marra Mamba iron-formation
FEPIS	Pisolitic iron ore deposit
FESCRE	Scree and detrital iron ore deposits
FESED	Sedimentary basin iron ore deposits
FGRAN	Fluorite deposits associated with granitic rocks
FPEGM	Pegmatite-hosted fluorite deposits
FVEIN	Vein fluorite deposits
GEMMET	Gem or semiprecious stones in high-grade metamorphic rocks
GEMPEG	Pegmatite-hosted gem or semiprecious stones
GEMSED	Sediment-hosted gem or semiprecious stones
GEMUM	Ultramafic-hosted gem or semiprecious stones
GEMVOL	Gem or semiprecious stones in volcanic rocks
GRMETA	Graphite deposits in metamorphic rocks
GRPEG	Pegmatite-hosted graphite deposits
GRQTZV	Graphite deposits quartz veins
GRUM	Graphite as segregations in ultramafic rocks
GYBBAS	Gypsum in coastal barred-basin deposits
GYDUNE	Dunal gypsum deposits
GYLAKE	Gypsum in lake sediments
HMSCAP	Heavy mineral deposits in the Capel shoreline
HMSDON	Heavy mineral deposits in the Donnelly shoreline
HMSDUN	Heavy mineral deposits in the Quindalup shoreline
HMSEN	Heavy mineral deposits in the Eneabba shoreline
HMSGIN	Heavy mineral deposits in the Gingin shoreline
HMSHV	Heavy mineral deposits in the Happy Valley shoreline
HMSMES	Heavy mineral deposits in mesozoic formations
HMSMIL	Heavy mineral deposits in the Milyeaanup shoreline
HMSMIS	Heavy mineral deposits — miscellaneous
HMSMUN	Heavy mineral deposits in the Munbinea shoreline
HMSWAR	Heavy mineral deposits in the Warren shoreline
HMSWRN	Heavy mineral deposits in the Waroona shoreline
HMSYOG	Heavy mineral deposits in the Yoganup shoreline
KBRINE	Potash deposits in brines and surface evaporites
KEVAP	Potash deposits in buried evaporite sequences
KGLAUC	Potash in glauconitic sediments
KLAKE	Potash associated with lake sediments
MGUM	Mafic–ultramafic rocks
MNCAV	Joint/cavity-fill manganese deposits
MNRES	Residual manganese deposits
MNSED	Sedimentary manganese deposits
MNSUPR	Precambrian supergene enrichment of manganiferous sediments
MOPOR	Porphyry Cu–Mo deposits
NABRIN	Salt in brines and surface evaporites
NAVAP	Salt deposits in buried evaporite sequences
NIINTR	Nickel in dunite phase of thick komatiite flows
NILAT	Lateritic nickel deposits
NISED	Nickel deposits in metasedimentary rocks
NITHOL	Nickel deposits in the gabbroic phase of layered tholeiites
NIVEIN	Vein-type nickel deposits
NIVOLC	Nickel associated with volcanic peridotites
PCARB	Carbonatite-hosted phosphate deposits
PEGPEG	Pegmatite-hosted industrial minerals
PGALL	Alluvial–eluvial platinoid deposits
PGUANO	Quaternary guano (phosphate) deposits
PIGHEM	Specular hematite pigment
PNOD	Seafloor (nodular) phosphate deposits
PSED	Phosphate deposits in phanerozoic sediments
PVEIN	Vein phosphate deposits

Appendix 2 (continued)

Mineralization types (cont.)

Abbreviation	*Mineralization type*
REALL	Alluvial–eluvial rare earth deposits
RECARB	Carbonatite-hosted rare earth deposits
REFELS	Felsic volcanic-hosted rare earth deposits
REHMS	Rare earths in heavy mineral sands
REPPEG	Pegmatite-hosted rare earth deposits
RESST	Xenotime in sandstones
SBQTZV	Antimony associated with auriferous quartz veins
SIDUNE	Mesozoic dune and bedded silica sands
SIQTZ	Silica in vein quartz
SIQZTE	Silica in quartzite or chert or both
SMASS	Sulfur in massive sulfides
SNALL	Alluvial–eluvial tin–tantalum deposits
SNGREI	Tin–tantalum deposits in greisen zones
SNPEGM	Pegmatite tin–tantalum–lithium deposits
SNVEIN	Vein tin–tantalum deposits
SSEDQZ	Sulfur in sediments or quartz veins or both
TALDLM	Talc deposits associated with dolomite
TALUM	Talc deposits in ultramafic rocks
UCALC	Calcrete-related uranium deposits
UCAV	Secondary (cavity-fill) vein-like uranium deposits
UCONG	Conglomerate-hosted deposits
ULIGN	Lignite-hosted uranium deposits
UPEG	Pegmatite-hosted uranium deposits
USST	Sandstone-hosted uranium deposits
UUNCF	Unconformity-related uranium deposits
UVEIN	Uranium in veins associated with base metals
VCALC	Calcrete-related vanadium deposits
VERUM	Vermiculite deposits associated with weathered mafic and ultramafic bodies
VTIALL	Alluvial–eluvial vanadium–titanium deposits
VTILAT	Lateritic vanadium–titanium deposits
VTIMAG	Titaniferous magnetite deposits
VTIVN	Vanadium–titanium vein deposits associated with base metals
WMOGRE	Tungsten–molybdenum deposits in greisen zones
WMOPEG	Pegmatite tungsten–molybdenum deposits
WSKARN	Tungsten–molybdenum skarn deposits

Abbreviations of source references

Source	*Full title*
02208/93	DME mines file number
?	Unknown source
A_____	M series Accession number
AIMM PRO	Australasian Institute of Mining and Metallurgy proceedings
AMH	Australian Mining Handbook
AMIQ	Australian Mineral Industries Quarterly
AR(CO)	Annual Report to Shareholders (abbreviated company name)
ASX(CO)	Report to Shareholders (abbreviated company name)
AUSIMM	Australasian Institute of Mining and Metallurgy report
AUSIMM14	Australasian Institute of Mining and Metallurgy bulletin and number
BHP	BHP correspondence
BMR	Bureau of Mineral Resources Report
BMR RR 1	Bureau of Mineral Resources Resource Report and number
BMR59/24	Bureau of Mineral Resources Record and number
BULL(NO)	GSWA Mineral Resource Bulletin (number)
CO CORR/REP	Company report to shareholders
CO(CO)	Company report to shareholders (abbreviated company name)
CSIROPUB	CSIRO publication
DN	Daily News newspaper
EMP (NO)	Environmental–management report (number)
ER	M series report
ERMP	Environmental Review and Management Program
F.NOTE	DME file note
FR	Financial Review newspaper
GG	Gold Gazette
GS BULL	GSWA Bulletin
GS REP	GSWA Report
GSWA AR	GSWA Annual Report
HI CORR/REP	Hamersley Iron correspondence/report
HOGAN	Hogan and Partners Investor's Sharewatch
HOMESWES	Homeswest report
HY (CO)	Half year report to shareholders (abbreviated company name)
I(NO)	M series open file Item (number)
IND MIN	Industrial Minerals
KAL MIN	Kalgoorlie Miner newspaper
M(NO)	M series M (number)
MB SYMP	Metals Bulletin Symposium
MEM 3	GSWA Memoir and number
MG	Metals Gazette
MINER	Miner
MINMET	MINMET report
MJ	Mining Journal
MM	Mining Monthly
MRR(NO)	GSWA Mineral Resources Report (number)
NOI(NO)	Notice of Intent to mine (number)
PAYD	Paydirt
PER	Public Environmental Review
PERS COM	Personal communication
PRO(CO)	Company prospectus (abbreviated company name)
QR(CO)	Quarterly report to shareholders (abbreviated company name)
REC(N0)	GSWA Record (number)
REP 33	GSWA Report (number)
ROY REP	DME Royalty Report
STAT DEC	Statutory Declaration submitted to DME
WEST A	West Australian newspaper